CHARACTERISATION OF PARTICULATE MATTER OF TRAFFIC ORIGIN IN SINGAPORE

YANG TZUO SERN

NATIONAL UNIVERSITY OF SINGAPORE

2004

CHARACTERISATION OF PARTICULATE MATTER OF TRAFFIC ORIGIN IN SINGAPORE

YANG TZUO SERN

(B. Eng. (Hons), RMIT)

A THESIS SUBMITTED

FOR THE DEGREE OF MASTER OF ENGINEERING

DEPARTMENT OF CHEMICAL AND BIOMOLECULAR ENGINEERING

NATIONAL UNIVERSITY OF SINGAPORE

2004

In memory of my beloved mother

Acknowledgements

This project would not be initiated and completed without the scholarship awarded by Department of Chemical and Biomolecular Engineering, National University of Singapore and the guidance and supervision of Dr. Rajasekhar BALASUBRAMANIAN. I wish to thank him for his opinions and the fruitful discussions that we have had throughout this research period. I also wish to extend my greatest appreciation to my team-mate cum best friend ER Show Lin for her courtesy helps and supports throughout the period of my research. Special thanks to Ellis SEE Siao Wei, Dr. Rajenara Kumar RATH and YAP Hui San for their assistance in this research. I like to extend my gratitude to LI Fengmei, Susan CHIA and LI Xiang for their helps in logistic procurement and handling as well as instrument operating in the laboratory. Their assistance and co-operation have made this project successful. I wish to extend my gratitude to *Instituto de Pesquisas Energéticas e Nucleares SP, Instituto de Química* of University of São Paulo, Brazil, especially Dr. Vasconcellos, for their help in analysing the samples. A special appreciation is extended to Land Transport Authority of Singapore for permitting us to conduct the sampling at the Boon Lay bus interchange. Lastly, I like to thank all my family members and friends who have been very supportive throughout the period.

Table of Contents

Acknowledgement i

Table of Contents ii

Summary v

Nomenclature viii

List of Figures x

List of Tables xiv

Chapter 1 Introduction 1

1.1 Objectives 4

Chapter 2 Literature Review 5

2.1 Sources of Atmospheric Particulate Matter 5

2.1.1 Natural sources 6

2.1.2 Anthropogenic sources 8

2.2 Measurement of Particulate Matter 12

2.2.1 Particle mass 12

2.2.2 Particle number 14

2.2.3 Particle surface area 14

2.2.4 Particle size classification 15

2.2.5 Particle Chemical Composition 16

2.3 Particulate Matter from Diesel Source 19

2.3.1 Nanoparticles 22

2.3.2 Diesel exhaust particle composition and structure 23

2.4 Particulate Matter Health and Environmental Impacts 24

2.4.1 Health impacts 24

2.4.2 Environmental impacts 27

Chapter 3 Sampling Site Description 31

3.1 NUS FoE Air Quality Monitoring Station 31

3.2 Punggol Multi-storey Car Park Rooftop 32

3.3 Boon Lay Bus Interchange 33

Chapter 4 Instruments and Analytical Procedures 36

4.1 On-site Sampling Instruments 36

4.1.1 Annular Denuder System (ADS) 36

4.1.2 MiniVol® Portable Air Sampler 39

4.1.3 Aethalometer™ 39

4.1.4 Micro-Orifice Uniform Deposit Impactor (MOUDI™ Model 110) 40

4.1.5 Hi-Vol Sampler HVP-3800AFC/230 41

4.1.6 Condensation Particles Counter (CPC) TSI 3007 41

4.1.7 Electrical Low Pressure Impactor (ELPI) (Dekati Ltd.) 42

4.1.8 Scanning Mobility Particle Sizer (SMPS) TSI 3034 42

4.2 Analytical Instruments and Methodology 43

4.2.1 Microbalance Sartorius MC-5 43

4.2.2 MLS-1200 MEGA Microwave Digestion System 44

4.2.3 ICP-MS Perkin Elmer Elan 6100 45

4.2.4 Ion Chromatography – Metrohm Ion Analyzer 45

4.2.5 Soxhlet Apparatus 47

Chapter 5 Results and Discussion 48

5.1 Mass Concentration 48

5.1.1 Background 48

5.1.2 Measurement of $PM_{2.5}$ mass concentration 50

5.1.3 PM Mass Size Distribution 53

5.1.4 Black Carbon Mass Concentration 58

5.2 Number Concentration 60

5.2.1 Background 60

5.2.2 Total Particle Number Concentration 63

5.2.3 PM Number Size Distribution 66

5.3 Chemical Characterization 70

5.3.1 Background 70

5.3.2 Chemical Composition of $PM_{2.5}$ 71

5.3.3 Mass Size Distribution of Ions and Trace Elements 93

Chapter 6 Conclusions 106

Appendix A 110

Appendix B 111

Appendix C 112

References 118

Summary

Among the major sources of air pollution in urban areas, emissions from on-road vehicles are of particular concern since they occur in close proximity to human beings. Particulate matter is one of the major pollutants derived from vehicular emissions, and has potential adverse effects on human health and the environment. The particulate matter (PM) in the urban atmosphere is mainly derived from the incomplete combustion of carbonaceous fuels, especially diesel.

Airborne particulate matter is a highly complex entity. It is a perfect carrier of non-airborne toxic and carcinogenic materials such as polyaromatic hydrocarbons (PAHs). In order to assess the health risk associated with particulate air pollution, an extensive field study was conducted to gather the information about the mass and number concentration of particulate matter, their respective size distributions and their chemical composition at three different locations in Singapore. These locations include the rooftop of a multi-storey car park at a residential area near an expressway, the rooftop of one of the tall buildings at the National University of Singapore campus, and a busy bus interchange with a majority of diesel-driven buses.

Gravimetric air samplers and sophisticated particulate analysers were deployed at strategic locations to collect PM samples and to measure particulate counts. MiniVol® and Hi-Vol air samplers were used to collect $PM_{2.5}$ (particle size smaller than 2.5μm in diameter) and Total Suspended Particles (TSP) samples, respectively. A Micro-orifice

Uniform Deposit Impactor (MOUDI^{TM}) was used to study PM mass size distribution at each of the sampling sites. Aethalometer^{TM} was deployed to measure real time black carbon (BC) diurnal emission profile. A portable Condensation Particles Counter (CPC) was used to count the total number of particles with diameters greater than 10 nm while Electrical Low Pressure Impactor (ELPI) and Scanning Mobility Particle Sizer (SMPS) measured real time particulate number size distribution. Weather conditions and surrounding human activities were closely monitored. The aerosol samples collected from the sites were carefully sealed and returned to the laboratory for the analysis of selected chemical components including water-soluble ionic species, microwave extractable trace elements and a range of organic compounds by gas chromatography.

The relationship among particle mass, number and size distribution was investigated. This study revealed that the PM concentration at the bus interchange was approximately 3 times the mass but over 10 times the number concentration measured at the university campus, which is considered to be an urban background location in this study. This suggests that the level of potential occupational health risk that an individual is exposed to in the bus interchange is probably higher than that in other urban microenvironments due to inhalation of ultrafine particles in large numbers. Black carbon accounted for 50% of the total $PM_{2.5}$ mass loading at the bus interchange, but was only 17% of that measured in the urban background location. A positive correlation between BC and particle number concentration strongly suggested that traffic emission is possibly the most important source of ultrafine particles in the urban air of Singapore. Water-soluble sulphate concentration measured at the bus interchange was not significantly different from the background concentration, indicating that

sulphuric acid formation was rather slow hence lower sulphate condensation taking place onto the particle. Concentration of particle-bound PAHs, Zn, Cu, Fe and Ti appeared to be much higher than that measured at the background location. The CPI, carbon preference index of n-alkane fractions identified fossil fuel combustion as the main source of n-alkanes at the bus interchange. Toxic Equivalent Factor evaluation suggested that B(a)P was one of the main carcinogens among the whole cluster of measured PAHs.

Nomenclature

Abbreviations

AYE	Ayer Rajah Expressway
BC	Black carbon
BKE	Bukit Timah Expressway
CCN	Cloud Condensation Nuclei
CPI	Carbon Preference Index
CTE	Central Expressway
DMS	Dimethylsulphide
EC	Elementary carbon
ECP	East Coast Expressway
ELPI	Electrical Low Pressure Impactor
FoE	Faculty of Engineering
HDB	Housing Development Board
KJE	Kranji Expressway
NUS	National University of Singapore
PIE	Pan-Island Expressway
PM	Particulate Matter
PM_{10}	Particulate matter smaller than 10 μm in aerodynamic diameter
$PM_{2.5}$	Particulate matter smaller than 2.5 μm in aerodynamic diameter
SLE	Seletar Expressway
SMPS	Scanning Mobility Particle Sizer
SOA	Secondary Organic Aerosol
SOF	Soluble Organic Fraction

TEF	Toxic Equivalency Factor
TPE	Tampines Expressway
TSP	Total Suspended Particle
UFP	Ultrafine Particle
VOCs	Volatile Organic Compounds

Symbols

C_c	Cunningham slip correction
d_{50}	Particle diameter with 50% cut point
d_a	Aerodynamic diameter
d_m	Mobility diameter
D_p	Particle diameter
DP_{50}	Particle diameter with 50% removal efficiency
$k_i(x)$	Kernel function
n	number of stages
s	MOUDI^{TM} manufacture-specified steepness
x_{max}	Upper size limit
x_{min}	Lower size limit
x_p	Particle diameter
σ	Standard deviation
Σ	Summation
λ	Mean free path of air
ρ_0	Unit density
ρ_e	Effective particle density

List of Figures

Figure 2.1 Saharan dust flows over the Mediterranean Sea towards Italy on July 16, 2003 captured by NASA/Seawifs Satellite. (Source: ESPERE http://www.espere.net/) 7

Figure 2.2 Volcano St. Helen erupted on May 18, 1980, injecting tons of ash and acidic gases into the atmosphere. (Photo courtesy: The Many Faces of Mt. St. Helens. Available: http://www.olywa.net/radu/valerie/StHelens.html [accessed 25 June 2004]. 8

Figure 2.3 Traffic emission is the major source of particulate matter in urban environment while industrial emission is another main contributor to atmospheric particulate matter in developed countries. (Photo source: http://www.freefoto.com) 9

Figure 2.4 Route of formation of SOA. (Source: Seinfeld and Pankow, 2003) 12

Figure 2.5 Typical diesel engine exhaust particle size distribution in number, mass and surface area weightings (Kittelson, 1998; Kittelson et al., 2002b). 21

Figure 2.6 Typical composition and structure of engine exhaust particles (Kittelson, 1998). 23

Figure 2.7 Typical particle composition for a heavy-duty diesel engine (Kittelson, 1998). 24

Figure 2.8 Fate of particles by normal clearance pathway (left) and those enter the interstitial compartment of the lung (right) (Donaldson et al., 1998). 27

Figure 2.9 Effect of particles on cloud droplet formation and properties (Source: ESPERE, 2004). 30

Figure 3.1 Field sampling locality map in this study (Note: AYE, BKE, CTE, ECP, KJE, PIE, SLE and TPE are expressways). 32

Figure 3.2 Boon Lay bus interchange layout plan (provided by Land Transport Authority of Singapore). 35

Figure 5.1 Average $PM_{2.5}$ mass concentration measured at Boon Lay bus interchange, Punggol and NUS. 51

Figure 5.2 Typical PM mass size distribution obtained from NUS FoE Air Quality Monitoring Station, Punggol multi-storey car park rooftop and Boon Lay bus interchange. 57

Figure 5.3 Black carbon (absorbing IR-880nm wavelength) mass concentration diurnal emission profile comparison at NUS, Boon Lay bus interchange and Punggol. 59

Figure 5.4 Total particle number concentration emission profile by ELPI at Boon Lay bus interchange (measured from 1st to 3rd Nov 03) and NUS FoE Air Quality Monitoring Station (measured from 7th to 8th Dec 03). 64

Figure 5.5 Particle number concentration and black carbon mass concentration 24-hour emission profile at Boon Lay bus interchange. 66

Figure 5.6 72 hours number concentration size distribution at the Boon Lay bus interchange measured by ELPI between 1st and 4th Nov 03 67

Figure 5.7 24 hours number concentration size distribution at the NUS FoE air quality monitoring station measured by ELPI from 6th to 7th Dec 03. 67

Figure 5.8 Number size distribution at the Boon Lay bus interchange measured on 7 Jan 04 from 12:00 to 14:45 with 15 minutes sampling interval. 68

Figure 5.9 Number size distribution at NUS FoE air quality monitoring station measured on 10 Jan 04 from 11:30 to 14:30 with 15 minutes up-scan time. 69

Figure 5.10 Correlation between total PAHs and Benzo(g,h,i)perylene. 88

Figure 5.11 Correlation between total PAH and Benzo(a)pyrene. 89

Figure 5.12 Major chemical components of $PM_{2.5}$ sampled at the NUS FoE air quality monitoring station, Punggol multi-storey car park rooftop and Boon Lay bus interchange. 92

Figure 5.13 Concentration of SO_2 and NO_x (NO & NO_2) at the each sampling sites measured by Annular Denuder System (ADS). 94

Figure 5.14 Comparison of sulphate mass concentration size distribution at Boon Lay bus interchange and NUS FoE air quality monitoring station. 95

Figure 5.15 Comparison of nitrate mass concentration size distribution at Boon Lay bus interchange and NUS FoE air quality monitoring station. 98

Figure 5.16 Comparison of chloride mass concentration size distribution at Boon Lay bus interchange and NUS FoE air quality monitoring station. 98

Figure 5.17 Comparison of sodium mass concentration size distribution at Boon Lay bus interchange and NUS FoE air quality monitoring station. 99

Figure 5.18 Comparison of ammonium mass concentration size distribution at Boon Lay bus interchange and NUS FoE air quality monitoring station. 101

Figure 5.19 Size distribution of Al, Cu, Fe, Mn, Pb, Zn, Ti and V at Boon Lay bus interchange. 102

Figure 5.20 Size distribution of Al, Cu, Fe, Mn, Pb, Zn, Ti and V at NUS FoE air quality monitoring station. 103

Figure A.1 48-hours Weatherlink® meteorology data from 11 to 12 December 2003 recorded at NUS FoE Air Quality Monitoring Station. 110

Figure A.2 48-hours Weatherlink® meteorology data from 9 to 10 January 2004 recorded at NUS FoE Air Quality Monitoring Station. 110

List of Tables

Table 2-1 Summary of main reaction mechanism of secondary aerosols formation. 11

Table 2-2 Particle number and surface area comparison of different sizes of spherical particles. 15

Table 4-1 ADS coating solution preparation, absorbing species identification, denuder coating and extraction procedures. 38

Table 4-2 Specification of aerosol number measuring capable instruments. 43

Table 4-3 Ion Chromatography Analysis Species 46

Table 4-4 Metrohm Ion Chromatography System Operating Parameters 46

Table 5-1 Spatial variability of $PM_{2.5}$ mass loading in Boon Lay bus interchange. ..52

Table 5-2 Mass median aerodynamic diameter of each mode reported elsewhere. 56

Table 5-3 Real times average BC mass concentration measured by Aethalometer™ at NUS, Punggol and Boon Lay bus interchange. 58

Table 5-4 Particle number concentration at three sampling sites, measured by CPC (24hours). 63

Table 5-5 Comparison of ultrafine particles number concentration (0.008 - 0.074 μm) to total particle number concentration (0.008 - 10 μm) at the University and the bus interchange measured by ELPI. 65

Table 5-6 Average concentration of ions in $PM_{2.5}$ collected by using MiniVol® at Punggol, NUS and Boon Lay bus interchange. 72

Table 5-7 Mean concentration of trace elements in $PM_{2.5}$ collected by using MiniVol® at Punggol, NUS and Boon Lay bus interchange. 79

Table 5-8 n-Alkanes identified and quantified in 24 hours TSP samples collected at Boon Lay bus interchange by Hi-Volume air sampler HVP-3800AFC/230. 84

Table 5-9 PAHs and nitro-PAHs mass concentration in 24 hours TSP samples collected at Boon Lay bus interchange by Hi-Volume air sampler HVP-3800AFC/230. 87

Table 5-10 B(a)P equivalent concentrations of individual PAHs concentrations: risk assessment for PAHs exposure at NUS and Boon Lay bus interchange. 90

Chapter 1 Introduction

Airborne particulate matter (PM) is a highly complex entity representing a mixture of primary emissions and secondary species formed in the atmosphere, and acts as a carrier of non-airborne toxic and carcinogenic materials such as PAHs due to its large surface area (Morawska and Thomas, 2000). In recent years, PM in urban cities has been under much scientific scrutiny because of its potential acute and chronic adverse health effects. An extensive epidemiological study carried out by Schwartz (1994) revealed that 578 more cases of deaths (25% of the deaths were due to chronic lung disease) occurred during high particulate air pollution days (TSP average mass concentration of 141 $\mu g/m^3$) in Philadelphia than normal. Based on this study, it was hypothesized that increased airborne PM exposure might elevate mortality and morbidity.

A number of toxicological studies have concluded that ultrafine particles (UFPs) are more toxic than larger particles with similar mass and chemical composition due to their efficient deposition in the pulmonary interstitial spaces (Ferin et al., 1992; Oberdörster, 1996, 2001; Donaldson et al., 1998, 2001), possibly triggering respiratory and cardiovascular complications (Schwartz, 1994; Samet et al., 2000). Recent animal studies demonstrated that UFPs could be translocated to interstitial sites in the respiratory tract and the liver (Oberdörster et al., 2002) via blood circulation (Nemmar et al., 2002). Recent studies by Oberdörster et al. (2004) revealed that UFPs deposited on the olfactory mucosa of the rat could be translocated to the olfactory bulb of the brain via the olfactory nerve. This means that inhaled UFPs may trigger a similar reaction in these organs like in cardio-pulmonary system.

In view of the adverse health implications associated with tiny airborne particles particularly UFPs, many studies have investigated the various possible sources of particles in the atmosphere so that effective air pollution control measures can be taken to mitigate their emission. Traffic emission, particularly of diesel origin, is a major source of airborne particles in urban air (Shi et al., 1999; Hitchins et al., 2000; Colvile et al., 2001; Zhu et al., 2002; Ashmore, 2001). Airborne particles derived from vehicular sources contain not only organic compounds, but also substantial amounts of ionic species, heavy metals, and trace elements (Park et al., 2003; Sakurai et al., 2003; Shi et al., 1999; USEPA, 2002). As a result of rapid urbanization and transportation demand, diesel engines are widely used in transportation, power generation, and other industrial applications (Lloyd and Cackette, 2001), contributing to high concentration of airborne particles in many urban cities (Nanzetta and Holmén, 2004; Weijers et al., 2004; Vignati et al., 1999) including Singapore.

The phenomenal economic growth in Singapore has led to rising automobile ownership and use, resulting in traffic congestion and air pollution issues (Chin, 1996). To address these problems, the government authority in Singapore had implemented vehicle quota scheme to control vehicles growth, and improved the infrastructure of public transport system by consolidating the public bus services and initiating the construction of the Mass Rapid Transit (MRT) system in 1982. Bus interchanges were built as a transit point to serve more than 2 million commuters daily (SBS Transit, 2004a) from the local bus routes to the well-established MRT network. Since the public buses are diesel-powered, the bus interchanges are potential pollution hot spots in Singapore due to emissions of particles and gaseous pollutants from idling buses.

Exposure of commuters and occupants of nearby buildings and residential houses to these diesel emissions is of considerable concern.

Exposure dosage plays an important role in determining the influence of PM on human health, which is related to the concentration of pollutants in exhaust fumes and the duration of an individual's actual exposure (Weijers et al., 2004; Ghio and Huang, 2004). Controlled emission studies were carried out by several research groups using chassis dynamometers to investigate the physical and chemical characteristic of particles emitted from diesel engines (Tanaka and Shimizu, 1999; Gonzalez Gomez et al., 2000; Miyamoto et al., 1997). However the results obtained from the controlled laboratory investigations may not reflect the actual particle concentration, size distribution and chemical composition of particles emitted from on-road vehicles. Stationary air quality monitoring stations have been established to routinely monitor urban air quality. However, the data obtained only reveal the daily average concentrations at fixed monitoring sites, and do not sufficiently represent pollution "hot-spots", which are characterized by higher-than-average pollution levels. Therefore, a range of emission and exposure studies have been conducted at specific hot-spots such as at road sides, street canyons, tunnels and highways (Unal et al., 2004; Abu-Allaban et al., 2004; Gouriou et al., 2004; Zhu et al., 2002; Molnár et al., 2002; Wehner et al., 2002; Wåhlin et al., 2001). Although these emission studies provided valuable information on the physical and chemical characteristics of particles derived from on-road vehicles, the exposure level of commuters in a confined bus interchange and that of the general public in urban microenvironments still remain poorly understood.

It is critically important to study the levels and characteristics of freshly emitted diesel particulate matter at the busy bus interchanges in Singapore in order to evaluate the risk associated with the exposure of commuters and sensitive members of the general population to UFPs. Since no such data are currently available in the published literature for countries with a high population density like Singapore, an extensive field study was undertaken in Singapore to fill the important knowledge gaps pertaining to diesel emissions and their impact on human health.

1.1 Objectives

This project was carried out to investigate and compare the air quality at a major pollution hot spot in Singapore (Boon Lay bus interchange) with that of an urban background location with the following specific objectives:

1) To investigate the physical characteristics of airborne PM at a major bus interchange;
2) To quantify the chemical contents of airborne PM of various sizes at the same location;
3) To assess the risk of toxicity exposure of individuals in the bus interchange.

Chapter 2 Literature Review

2.1 Sources of Atmospheric Particulate Matter

The category of air pollutants called "respirable particulate matter" includes liquids, hydrocarbons, soot, dusts and smoke particles that are smaller than 10 microns in diameter (USEPA, 1997). Invisible to our naked eyes, these respirable particles appear in various sizes and shapes with very complex make up. This makes them inherently more difficult to analyse and study than gas-phase aerosols in the atmosphere (Harrison and Grieken, 1998). Atmospheric particulate matter normally exists in very small size, which makes the particles airborne and capable of travelling over long distance due to their lightweight. The 1997 regional haze episode caused by the forest fires in Indonesia was an evidence of long-range transport of particulate matter derived from biomass burning which had contributed to trans-boundary air pollution in Singapore and other countries in the region (Koe et al., 2001).

Particulate matter comes from natural and anthropogenic sources. They can be directly emitted as primary aerosol, or they can be formed from chemical reaction in the atmosphere. Carbonaceous particles are the most commonly known primary aerosols emitted from motor vehicle. Sulphur dioxide (SO_2), an acidic gas, released from motor vehicles is oxidized in humid air to form sulphuric acid aerosols, which indirectly become one of the major constituents in the formation of secondary particles in the atmosphere. Such secondary aerosols will be further discussed in section 2.1.2.

2.1.1 Natural sources

Particles are generally either emitted directly into the atmosphere or produced in the atmosphere from the physical and chemical transformation of other vapour or gaseous pollutants. Marine agitation, volcanic eruption, forest fires ignited by lightning, winds and soil erosion (producing fugitive dust) and photochemical reactions (complex chain reactions between sunlight and gaseous pollutants) are some of the natural sources of particulate matter in the ambient air.

Marine Aerosol

Aerosols emitted from the sea are known as sea salt aerosols. They are formed from sea spray coming from waves at high wind speeds and by the bursting of entrained air bubbles during whitecap formation. These processes produce coarse mode aerosol of larger than 10 μm in diameter. Such aerosols are commonly enriched in sodium chloride, potassium chloride, calcium sulphate and sodium sulphate.

Mineral Aerosol

Wind is one of the natural forces that are responsible for the formation of mineral aerosol by picking up the particles from land surface, especially when the soil is dry and desiccated. These mineral aerosols may contain materials derived from the Earth's crust which usually are rich in iron, aluminium oxides and calcium carbonate. Deserts are the main origin of mineral aerosols. Satellite picture as shown in Figure 2.1 illustrates that the Saharan dust was transported by wind over the Mediterranean Sea heading towards Italy.

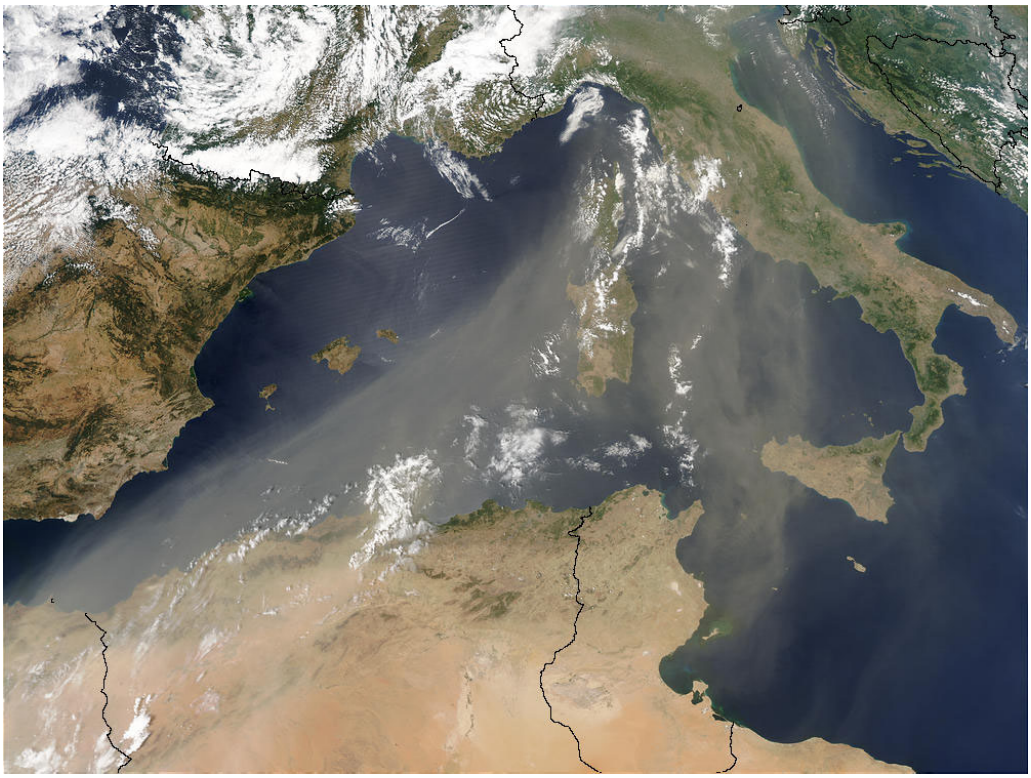

Figure 2.1 Saharan dust flows over the Mediterranean Sea towards Italy on July 16, 2003 captured by NASA/Seawifs Satellite. (Source: ESPERE http://www.espere.net/)

Volcanic Aerosol

Volcanic eruption is one of the most dynamic natural forces that inject huge amounts of gases and aerosols into the atmosphere. The eruption is so strong that it infuses tons of acidic gases and particles high into the stratosphere. The acidic gases tend to be oxidized and condensed to form fine secondary aerosols. The primary and secondary aerosols can remain in the upper atmosphere for a long period of time before settling to the ground. It is believed that stratospheric particles have a significant impact on climate change and global warming (ESPERE, 2004).

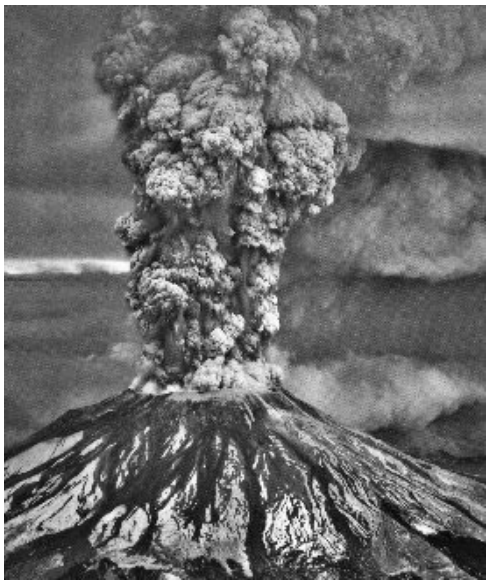

Figure 2.2 Volcano St. Helen erupted on May 18, 1980, injecting tons of ash and acidic gases into the atmosphere. (Photo courtesy: The Many Faces of Mt. St. Helens. Available: http://www.olywa.net/radu/valerie/StHelens.html [accessed 25 June 2004].

Biogenic Aerosol

Some particles can be produced from living organisms or plants. These particles are called biogenic aerosols. Some examples include primary aerosols such as pollens, fungi spores, bacteria and viruses. Biomass burning due to land clearance and burning of agricultural waste is also regarded as one of the sources of biogenic aerosol.

2.1.2 Anthropogenic sources

Primary carbonaceous PM

The major anthropogenic source of atmospheric particles is through fossil-fuel combustion (which produces ash and soot) in industrial processes (involving refinery, metals smelting, incineration) and transportation (exhaust emission, particles from wear on road, tyres and brakes, resuspension from road surface), which emits PM directly into the atmosphere. Internal combustion engine exhaust emission is regarded as one of

the main contributors of ambient PM in the urban environment. Field investigations in the Netherlands revealed that concentrations of number and mass of PM increase along with the degree of urbanization due to contribution of vehicular emissions (Weijers et al., 2004). In the United Kingdom, emission inventories of sources revealed that most of the particulates in urban air arise from road traffic (APEG, 1999). Air pollution associated with transport sector has been partly responsible for acid rain formation and also climate change (Colvile et al., 2001). Nevertheless, traffic emitted PM is of concern due to its close proximity to human beings and its potential adverse impacts on human health and urban air quality. Other than traffic and industrial emissions, particles are also produced at home through activities including residential wood fire and indoor cooking activities (Lee et al., 2001; Morawska et al., 2003; Wallace et al., 2004).

Figure 2.3 Traffic emission is the major source of particulate matter in urban environment while industrial emission is another main contributor to atmospheric particulate matter in developed countries. (Photo source: http://www.freefoto.com)

In urban atmosphere, airborne particles are mostly derived from automobiles emissions (APEG, 1999). Motor vehicles emit not only primary particles, but also reactive gases such as NO, SO_2, NH_3, and hydrocarbon vapours that react chemically in the atmosphere to form secondary aerosol mass (Allen et al., 2000).

Secondary aerosols from in situ nucleation

Gaseous pollutants such as SO_2 and NO_x may condense on pre-existing particulate matter to form bigger and denser aerosols. These gases, alternatively, may go through a gas-to-particle homogeneous nucleation forming new particles in the atmosphere. Both natural and human activities in combination release significant amount of secondary aerosols precursors into the atmosphere continuously, periodically or intermittently. Combustion of fossil fuels in power plants and in vehicles is considered to be the two major contributors to the formation of secondary particles with the abundant emission of SO_2, NO_x and VOCs. The oxidation of SO_2 and NO_x are the main atmospheric reactions that produce significant amounts of secondary aerosols in the atmosphere. It is estimated that about 50% of the acidic gases are oxidized prior to deposition (Denterner and Crutzen, 1998). Sulphate particle formation is the best-known example. As shown in Table 2-1, SO_2 reacts with OH radicals forming H_2SO_4 vapour, which will either condense on pre-existing particles or homogeneously nucleate to form sulphate particles. Under the favourable conditions of high H_2SO_4 production rate, high relative humidity, low temperature and low pre-existing PM concentration, nucleated particles can be formed in huge numbers within a short period of time (Seinfeld, 2004). However, these particles are mostly found in nanometre size range. Hence, their mass is generally negligible compared to the rest of the particle mass distribution. However, their number is dominating the total number concentration of particles in the atmosphere. These nanoparticles may coagulate via collision and adherence to form larger particles.

Table 2-1 Summary of main reaction mechanism of secondary aerosols formation.

Aerosol Species	Precursors/Reactants	Source	Reactions
Sulphate Aerosol	¤ SO_2 ¤ Dimethyl Sulphide ¤ H_2S ¤ $OH\cdot$ (radical) ¤ O_3	¤ Automobile ¤Volcanic activities ¤ Marine phytoplankton ¤ Power plant ¤ Vegetation & animal decay	1) $O_3 + uv \rightarrow O_2+O\cdot$ 2) $H_2O+O\cdot \rightarrow H\cdot+OH\cdot$ 3) $SO_2+OH\cdot \rightarrow HSO_3$ 4) $HSO_3+O_2 \rightarrow SO_3+HO_2$ 5) $SO_3+H_2O \rightarrow H_2SO_4$ 6) $H_2SO_4+2NH_3 \rightarrow NH_4SO_4$
Nitrate Aerosol	¤ NO_2 ¤ NH_3 ¤ $OH\cdot$ (radical) ¤ O_3	¤ Automobile ¤ Fertilizer ¤ Power plant	1) $NO_2+OH\cdot \rightarrow HNO_3$ or 2) $NO_2+O_3 \rightarrow NO_3+O_2$ 3) $NO_3+NO_2 \rightarrow N_2O_5$ 4) $N_2O_5+H_2O \rightarrow 2HNO_3$ 5) $HNO_3+NaCl \rightarrow NaNO_3+HCl$ or 6) $HNO_3+NH_3 \rightarrow NH_4NO_3$
Organic Aerosol	¤ VOCs i.e. Toluene ¤ NO_x ¤ O_3	¤ Automobile ¤ Refinery	Most of the VOCs go through photo-oxidation with O_3, OH or NO_x reaction.

Reference: Seinfeld, 2004; Seinfeld and Pankow, 2003; ten Brink, 2003.

Secondary organic aerosol (SOA) is formed when higher polarity and lower volatility oxidation products of certain VOCs condense on pre-existing aerosols (Seinfeld and Pankow, 2003). However, only organic molecules of six or more carbon atoms are capable of producing oxidized products, which condense to form SOA. This is because high carbon atom number organic compounds will produce oxidized products of low vapour pressure. Figure 2.4 illustrates the route of formation of secondary organic PM.

The low volatility or "semi-volatile" products will either condense on pre-existing particles or nucleate homogeneously to form new mass of particles.

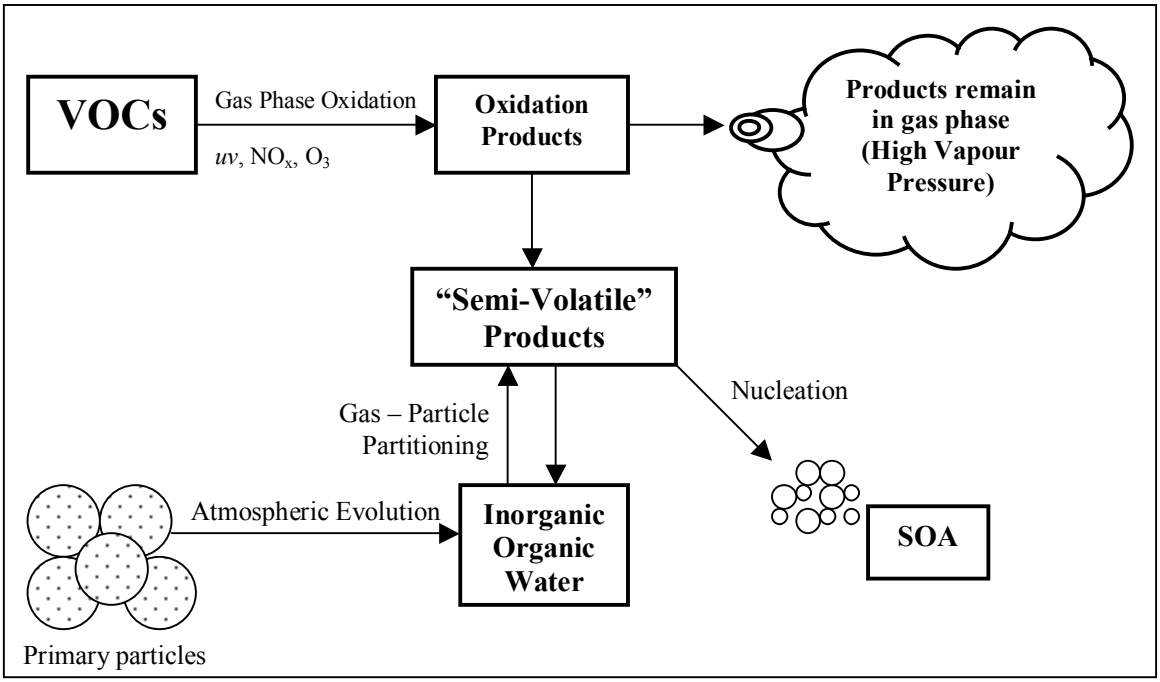

Figure 2.4 Route of formation of SOA. (Source: Seinfeld and Pankow, 2003)

2.2 Measurement of Particulate Matter

In this study, only atmospheric PM concentration measurements are discussed. Measurement of PM from direct vehicular exhaust emission involving a dilution tunnel has a different approach of measuring the PM mass, number, surface and size distribution.

2.2.1 Particle mass

Particle mass is determined by collecting airborne particles simply by drawing atmospheric air through a filter element of specific porosity with the assumption that all particles that are smaller than the filter pore size would be trapped. The filter is weighed before and after particle collection. The weighed mass is then divided by the

total volume of air that passed through the filter, which yields mass concentration of particles in a known volume of air. Particle mass concentration of various restricted size range, such as PM_{10}, $PM_{2.5}$ or $PM_{1.0}$, is measured by replacing size selective inlets, which only allow selected particle size to reach the filter. Size selectivity is achieved by impaction or inertial collection using a cyclone at a designated airflow rate.

Particle mass concentration is measured by two common methodologies: 1) tapered element oscillating microbalance (TEOM) sampler and 2) gravimetric sampler. TEOM measures the particle mass by collecting the particles on a small filter located on a tip of a tapered glass element, which forms part of an oscillation microbalance. The oscillation frequency of the microbalance will change with the mass of particles collected on the filter. In TEOM sampling, inlet air stream is pre-heated to about 50^{o}C, inadvertently removing all of semi-volatile particles, which may represent a significant portion of particle mass in certain area (Harrison et al., 2000). On the other hand, gravimetric sampler i.e. MiniVol® collects the particle mass without any pre-heating involved. Hence, the aerosol samples collected gravimetrically may reveal more hidden information about the sampling field air quality and aerosol apportionment.

Currently, the mass of particles smaller than 100 nm in diameter is measured by means of collecting particles in size-fractionated cascade impactors. However, no instrument with an inlet of 100 nm selectivity has been designed to specifically determine the ultrafine particle mass.

2.2.2 Particle number

The number of particles in a specific volume of air can be measured by the use of condensation nucleus counters (CNCs) or condensation particulate counters (CPC). Continuous CNCs draw particles through a zone saturated with alcohol vapour, mainly n-butanol or isopronanol, which is cooled subsequently to condense the vapour on the particles (Stolzenburg and McMurry, 1991). The condensation will cause the particle to grow to the order of 10 μm in diameter. These particles then become very effective in light scattering, which are then monitored through counting the signals from particles by passing through a light beam or a photometric mode that determines 90^o scattered intensity of incident light. The cut size of the CNCs is dependent on the design and degree of supersaturation achieved. Most of the particle counters have a lower cut size of about 3 nm to 20 nm in less sophisticated devices. The upper size limit is determined by the inlet aspiration efficiency, which is likely to be around 5 μm.

2.2.3 Particle surface area

When particles decrease in size, for an equal mass of particles, the surface area exposed increases. Traffic emitted particles are always less than 1 μm in diameter by both number and mass measuring methodology. As a result, PM_{10} and $PM_{2.5}$ are neither suitable nor effective to measure the impact of vehicle emissions. In a strongly traffic-influenced urban environment, PM_1 makes up only a few percent by mass measurement, but would provide in excess of 95% of the surface area and number concentration. As shown in Table 2-2, assuming spherical particles of equal mass, $PM_{0.01}$ has a surface area of 1000 times larger than that of PM_{10}. Therefore, it is reasonable that health impacts are best correlated to surface area - the area available to carry toxins into the lungs (Morawska and Thomas, 2000). There are limited methods and devices to

measure surface area. Hence, it is rarely measured from any direct device except one called an epiphaniometer which determine the *Fuchs* surface area of particles (Gaggeler et al., 1989), by attaching a gaseous radionuclide to the particle surface and counting collected radioactivity. Nevertheless, surface area can be estimated by measuring the particle size distribution with known or assumed particle geometry.

Table 2-2 Particle number and surface area comparison of different sizes of spherical particles.

PARTICLE size	**PM_{10}**	**$PM_{2.5}$**	**$PM_{1.0}$**	**$PM_{0.1}$**	**$PM_{0.01}$**
Number for equal mass	1	64	1000	1000,000	1,000,000,000
Surface area for equal mass	1	4	10	100	1000
Functional classification	Coarse mode		Accumulation mode		Nuclei mode

Source: Morawska and Thomas (2000).

2.2.4 Particle size classification

Airborne particles are generated in different sizes, shapes, density and composition from different sources. Generally, it is widely accepted that in atmospheric studies, ambient PM is divided into the following categories based on their aerodynamic diameter:

- *PM_{10}* - particulates of an aerodynamic diameter of less than 10 μm
- *$PM_{2.5}$* - fine particles of diameters below 2.5 μm
- *Ultrafine particles* of diameters below 0.1 μm or 100 nm
- *Nanoparticles*, characterized by diameters of less than 50 nm.

Aerodynamic diameter is the diameter of a 1 g/cm^3 density sphere of the same settling velocity in air as the measured particle. Due to the association of the fine particles and adverse health effect, the United States Environmental Protection Agency (USEPA) has

imposed strict air quality standards (National Ambient Air Quality Standards-NAAQS) to regulate ambient level of PM_{10} and $PM_{2.5}$ of not exceeding 50 $\mu g/m^3$ and 15 $\mu g/m^3$ in terms of annual average concentration, respectively (USEPA, 1997). However, air quality standard is yet to be imposed on ambient level of ultrafine particle (<100 nm), although it is hypothesized to have strong correlation to adverse health effects.

2.2.5 Particle Chemical Composition

Chemical components found in PM are very diverse, ranging from neutral and soluble substances such as ammonium sulphate, ammonium nitrate and sodium chloride, through organic compounds and elemental carbon, and insoluble minerals such as particles of clay and soil. It is believed that water-soluble components, probably metal ions, are responsible for pulmonary toxicity (Adamson et al., 1999) as they can rapidly dissolve in the lining fluids of the respiratory system, which can exert significant physiological effect. Trace metals are also believed to have significant influence on the toxicity of airborne particles (Harrison and Yin, 2000). The evidences were mostly derived from toxicological instead of epidemiological studies based on the idea that metals are redox-active and can induce chemical changes leading to production of free radicals such as hydroxyl radical that can cause tissue inflammation (Harrison and Yin, 2000).

Airborne particle are made up of several major components, each representing several percent of the total mass of the particles. The typical chemical components found in airborne particles are sulphate, nitrate, ammonium, chloride, elemental and organic carbon, trace elements and crustal materials.

Sulphate

Sulphate is predominantly derived from sulphur dioxide oxidation in the atmosphere. Sulphur dioxide is oxidized to form sulphuric acid. As sulphuric acid is not volatile, once formed the acid will immediately condensed into airborne particles to form a strong acid content.

Nitrate

Nitrate is formed mainly from the oxidation of atmospheric nitrogen dioxide. The oxidation will produce nitric acid vapour, which can only be incorporated into airborne particles by loss of its acidity either through displacing hydrochloric acid from sea salt particles forming sodium nitrate, or by ammonia neutralization to form ammonium nitrate (Harrison and Allen, 1990). Ammonium nitrate is believed to be in equilibrium in the atmosphere with ammonia and nitric acid vapour. (Harrison and Msibi, 1994).

Ammonium and Chloride

Ammonium salt is formed when ammonia neutralizes sulphuric acid and nitric acid in the atmosphere (Harrison and Kitto, 1992). Ammonia is abundant in most but not all urban locations, often exceeding and reacting with the hydrogen ions in the neutralization process. Chloride found in the airborne particle is mainly contributed from two major sources: (1) sea spray, even at locations hundreds of miles from the coast, and (2) neutralization of ammonia and hydrochloric acid vapour. The latter is emitted from incinerators and power stations (Harrison and Yin, 2000).

Elemental and Organic Carbon

Elemental carbon and organic carbon are produced in most combustion processes. Road traffic emission is the major source of particle soot which contains solid black elemental carbon often coated with semi-volatile organic compounds which apparently condense from the vehicular exhaust gases (Amann and Siegla, 1982).

Trace Elements

Most of the trace metals arise predominantly from industrial sources, with the exception of lead, which is still primarily contributed by road traffic. Trace elements such as lead, cadmium and mercury are highly toxic in sizeable doses. However, exposures through inhalations of urban airborne particles are insufficient to cause toxic effect through classical mechanisms of toxicity (Department of Health, 1995; Harrison and Yin 2000). Gilmour et al. (1996) suggested that transition metals particularly iron might have adverse effects through non-classical mechanisms such as contributing to the production of hydroxyl radicals through the Fenton reaction. Nevertheless, simple measurements of the total airborne concentrations of a trace metal may not be representative of its potential health impacts as the chemical speciation and its potential reactivity to certain chemicals reaction varies significantly with the source.

Crustal Materials

Crustal materials are mostly wind-blown soil dusts and rock minerals, which reflect local geological and surface conditions. Crustal materials are often emitted into the atmosphere in harsh weather conditions with dry and strong wind turbulence. These materials are mostly found in the coarse particle fraction.

2.3 Particulate Matter from Diesel Source

Most of the emitted particles from diesel engines are less than 1 μm in diameter (Kittelson, 1998) with a large number of them distributed in nano-size ranging from 20 nm to 130 nm (Kittelson, 1998; Shi et al., 1999; Zhu et al., 2002). As such, they represent a mixture of fine, ultrafine, and nanoparticles. A typical size distribution of diesel engine exhaust PM is shown in Figure 2.5 (note that a logarithmic scale is used for particle aerodynamic diameter). PM emitted from diesel engines includes both solids, such as elemental carbon and ash, and liquids, such as condensed hydrocarbons, water, and sulphuric acid. Formation of particulates starts with nucleation, which is followed by subsequent agglomeration of the nuclei particles. Nucleation occurs in the engine cylinder (carbon, ash) and the exhaust system (hydrocarbons, sulphuric acid, water), through homogeneous and heterogeneous nucleation mechanisms.

Diesel engine exhaust particle size distribution conforms to a tri-modal lognormal form as shown in Figure 2.5. Most of the diesel particle mass is contained in the accumulation mode while nuclei mode particle dominates the majority of the particle number (Kittelson, 1998). Coarse mode usually consists of re-entrained particles such as crankcase fumes. Agglomeration of carbonaceous particles that have been generated from incomplete combustion usually takes place in accumulation mode, dominating the majority of mass and surface area of the particles. Nuclei mode normally consists of particles formed from volatiles precursors when freshly emitted exhaust mixes with denser air. Sometimes, this mode may consist of particles with size smaller than 10 nm. Although the exact composition of diesel nuclei mode nanoparticles is not known, it is

believed that they are composed primarily of condensates (hydrocarbons, water, and sulphuric acid) (Kittelson, 1998; Tanaka and Shimizu, 1999).

(a) Coarse particle mode

These particles fall in the particle size range of 10 μm – 2.5 μm in aerodynamic diameter, contribute 5 – 20% of the total PM mass, but minority or almost none of the particle numbers (Kittelson, 1998). Coarse particles in the atmosphere mostly originate from resuspension of road dust or soil. In the instance of exhaust emission from a diesel vehicle, these visible coarse particles (black smoke) are not generated in the diesel combustion process. Rather, they are formed through agglomeration process or deposition and subsequent re-entrainment of particulate material from walls of the engine cylinder, exhaust system, or the particulate sampling system (Kittelson et al., 2002a).

(b) Accumulation mode

The accumulation mode consists of sub-micron particles of diameters ranging most often from 30 – 1000 nm (0.03 – 1.0 μm) with a maximum mass concentration falling between size ranges of 100 – 300 nm (0.1 – 0.3 μm). Accumulation mode particles are mostly derived from solids agglomerated particles (carbon, metallic ash) intermixed with condensates and adsorbed material such as hydrocarbons and sulphur species. As shown in Figure 2.5, the accumulation mode extends through the fine, ultrafine and the upper end of the nanoparticle range.

(c) Nuclei mode

This mode typically consists of particles in the 5 – 50 nm (0.005 – 0.05 μm) size range, usually containing volatile organic, sulphur species and, sometimes, carbon and metal compounds. The nuclei mode particles contribute 1 - 20% of the total PM mass, while more than 90% of the PM number concentration. The diameters of nuclei mode particles are generally less than 50 nm (0.05 μm). Based on particle size research in the 1990's-technology heavy-duty diesel engines, it has been postulated that the nuclei mode extends through sizes from 3 – 30 nm (0.003 – 0.03 μm) (Kittelson et al., 2002a; Hall et al., 2001). All of the above size ranges place nuclei mode particles entirely within the nanoparticle range. As shown in Figure 2.5, the maximum concentration of nuclei mode particles occurs at 10 nm – 20 nm size range.

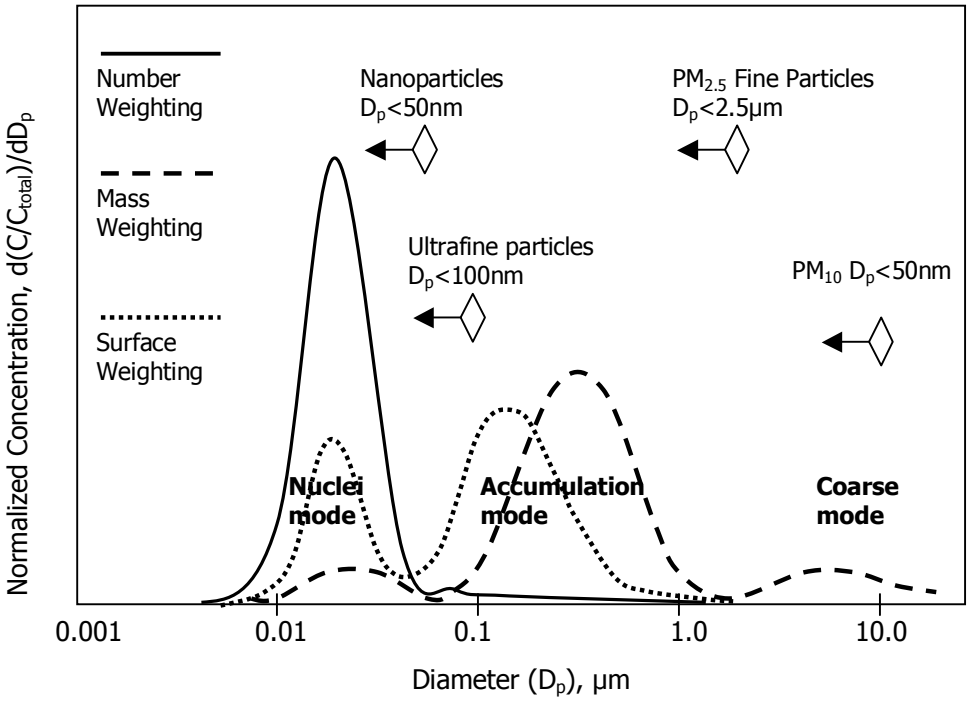

Figure 2.5 Typical diesel engine exhaust particle size distribution in number, mass and surface area weightings (Kittelson, 1998; Kittelson et al., 2002b).

2.3.1 Nanoparticles

The increased interest in diesel nanoparticles has been sparked primarily by a number of health and environmental concerns:

1) They are suspected to be able to penetrate deep into human lungs, based on a recent evidence obtained from animal studies and it is believed that nanoparticles may be more harmful than larger particles (Harrison et al., 2000; Oberdörster, 2001);
2) Almost weightless, these nanoparticles are so buoyant that they may even reach the stratosphere and may affect global climate in direct mechanisms related to absorption and scattering of solar and terrestrial radiation, or indirect mechanisms as cloud condensation nuclei (Harrison et al., 2000);

Exhaust emissions from diesel engines are believed to be one of the major sources of ultrafine PM in the urban atmospheres (Harrison et al., 2001). Kittelson (1998) reported that the majority of the PM number concentration emitted from a diesel engine was in the nano-size range, $D_p < 50$ nm. Findings of medical research indicate that nano-size particles are possibly more harmful to humans than the larger ones (Ferin et al., 1992; Oberdörster, 1996, 2001; Donaldson et al., 1998, 2001) as these nanoparticles may penetrate deeper into human lung. Moreover, these particles have a large surface area, which makes them an excellent medium for adsorbing condensates, and organics compounds where some are mutagenic or carcinogenic. Most recent animal tests by Oberdörster (2004) revealed that nanoparticles could travel to the brain after being inhaled. The finding was confirmed after an experiment was performed on a rat by exposing the whole rat to 20 nm ultrafine particles. Translocation of the ultrafine

particles was detected 24 hours after inhalation at the olfactory bulb, the part of brain that deals with smell.

2.3.2 Diesel exhaust particle composition and structure

Diesel engine emits a significant amount of highly agglomerated solid carbonaceous material and ash, volatile organic, and sulphur compounds. Solid carbon is the product of incomplete combustion in rich burning state (low air-fuel ratio). The structure is illustrated in Figure 2.6. Most of the carbon particles are oxidized and exhausted with the residues, which form solid agglomerates (Kittelson, 1998). Some fraction of the unburned fuel and lube oil that escape oxidation are exhausted as volatile or soluble organic compounds (soluble organic fraction, SOF). The SOF contains polycyclic aromatic compounds containing oxygen, nitrogen, and sulphur. Sulphur is commonly found in diesel fuel. In the combustion, sulphur is mostly oxidized to SO_2 and SO_3, which lead to the formation of sulphuric acid and sulphates in the exhaust particles. Metal compounds are also commonly found in diesel fuels and lubricating oil, which contribute to the emission of inorganic ash. Figure 2.7 illustrates the typical composition of particle from a heavy-duty diesel engine tested in a transient cycle (Kittelson, 1998).

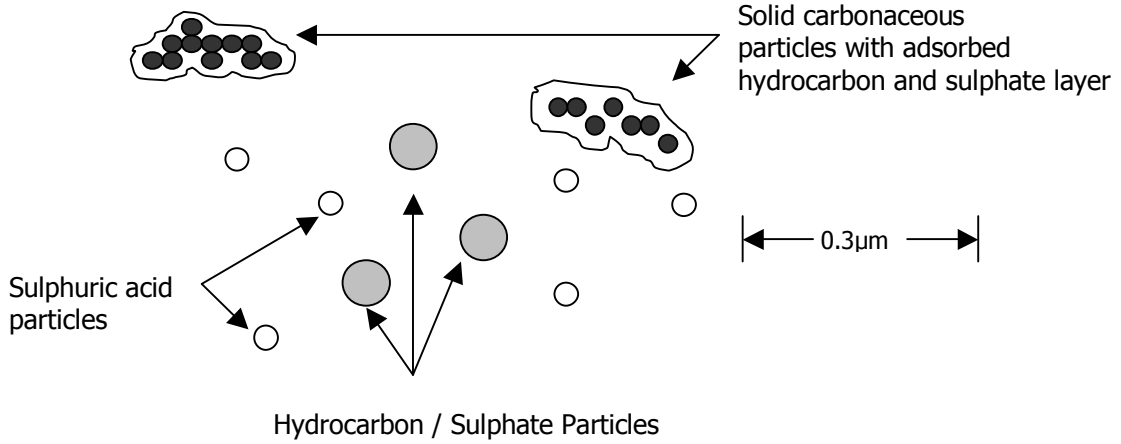

Figure 2.6 Typical composition and structure of engine exhaust particles (Kittelson, 1998).

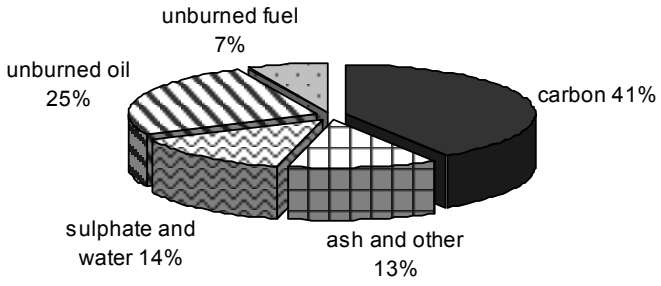

Figure 2.7 Typical particle composition for a heavy-duty diesel engine (Kittelson, 1998).

2.4 Particulate Matter Health and Environmental Impacts

2.4.1 Health impacts

Vehicular emission produces fine particles with most of them smaller than 2.5 μm in diameter. Fine and ultrafine particles were linked to adverse health effect including shorter life expectancy, premature mortality and morbidity (Schwartz, 1994; Hall, 1996; Künzli at al., 2000). Episodes of high pollution days have been postulated as the main reason leading to increase morbidity and death cases particularly among elderly and those with pre-existing cardiovascular and respiratory illnesses (Anderson, 1999; Nemery et al., 2001; Nemmar et al., 2004; Chalupa et al., 2004). Experimental studies found that exposure to ultrafine particles in animals could sustain more lung injury and pathology than those breathing in fine respirable particles in the same deposited mass of the same compositions (Donaldson et al., 1998). Dockery et al. (1993) and Pope et al. (1995) realized that the correlation between particle concentration and health effect

increases with decreasing particle diameter. Inhalation is the most common PM exposure pathway to enter a human body. The likelihood of an adverse response to particles is influenced by the degree of exposure at a specified concentration through the outer (e.g., skin) or inner (e.g., respiratory tract epithelium) surface of the human body. Changes in the degree of exposure are influenced by the duration, magnitude and frequency of exposure.

There are several hypotheses used to explain the correlation between PM and observed adverse health effects. Some believe that the intrinsic toxicity of the particulate itself and its surface contaminants such as the transition metals may exert adverse health effects on human beings (Fubini et al., 1995; Gilmour et al., 1996). The particles are believed to act as transmitters, which mean that they carry the contaminants into the lung causing epithelial damages. Another hypothesis is that physical characteristics such as number, size, shape and aggregation properties are responsible for negative health effects. For instance, the shape of a particle is regarded as a factor of toxicity in the case of asbestos, which is toxic in a long fibre shape but its toxicity is significantly reduced when it becomes a short fibre (Donaldson et al., 1989). Some particles are clearly pathogenic to the lungs, such as quartz and asbestos, whilst others are seen as non-toxic or nuisance dusts. However, researchers began to pay attention to these nuisance particles when they found them to be harmful to the lung especially when they are in very small size (Donaldson et al., 1998). A key study by Ferin et al. (1992) brought this issue to the attention of inhalation toxicologists. In the study, rats were exposed to same mass concentration of both ultrafine TiO_2 and fine TiO_2. Those exposed to ultrafine TiO_2 developed inflammatory response, but little effect was observed on those exposed to fine TiO_2. It is believed that the ultrafine particles may

induce acute and chronic respiratory discomforts such as throat and bronchial irritation, neurophysiological symptoms (nausea, lightheadedness), persistent cough and some long-term exposure effect such as inflammation and carcinogenic complications (USEPA, 2002).

The macrophages and the epithelial cells natural response will determine the pulmonary effects when the particles first deposited in the lung (Donaldson et al., 1998). The natural clearing system will be activated when an alien object is detected within the lung. Macrophages will engulf the particles to minimize the particle interaction with the epithelium as a protective measure. During this process, the macrophages will release minimal amounts of inflammatory mediators and migrate to the mucociliary escalator and leave the lung with their particle burden (Donaldson et al., 1998). However, there are two possibilities that will lead to the failure of the clearance process: 1) particle-mediated macrophage toxicity or impairment of motility; 2) particle overload. Either of these events will allow the direct interaction to take place between the particles and epithelium, which will induce *interstitialization*, an adverse outcome where interstitial particles will either remain in the interstitium or transfer to the lymph nodes (Donaldson et al., 1998) as shown in Figure 2.8. Some particles are intrinsically toxic due to their surface reactivity such as quartz. At high dose, for example, quartz can cause damage to cells (Allison et al., 1966; Donaldson et al., 1998). At lower doses, it may stimulate the release of inflammatory mediators, which will lead to inflammation (Driscoll et al., 1990; Donaldson et al., 1998). Long-term exposure in high particle concentration microenvironments may increase the number of particles deposited in the lungs causing particle overload phenomenon. Even the least toxic carbon or titanium dioxide may pose a serious threat to human health when present in

large number. Macrophages with a large volume of particles will affect their clearance functions (Morrow, 1998), which ultimately fail to transport large number of particles out of the lungs. Particles deposited in the lungs will then interact with epithelial cells. They will transfer across the epithelium and eventually settle or accumulate in the interstitium (Ferin et al., 1992), leading to inflammation, increased epithelial permeability, proliferation and retardation of clearance, culminating in fibrosis and cancer in the long term if exposure to a high concentration environment continues (Donaldson et al., 1998).

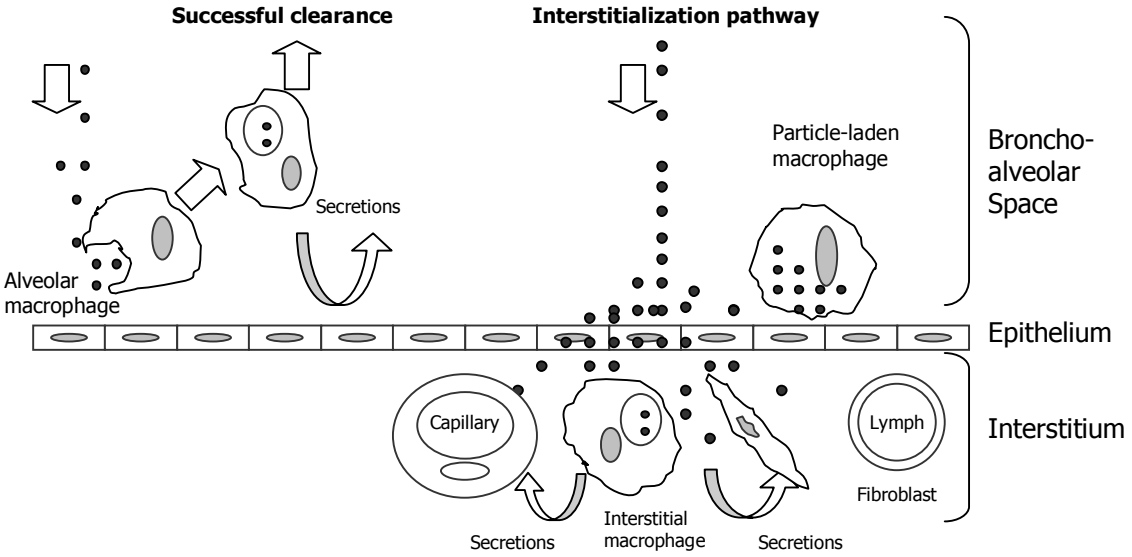

Figure 2.8 Fate of particles by normal clearance pathway (left) and those enter the interstitial compartment of the lung (right) (Donaldson et al., 1998).

2.4.2 Environmental impacts

Visibility

Light is a form of energy that travels in waves. Light waves travel in straight lines and will only change the course of travelling when it hits an obstacle such as a particle or a gas molecule. When light hits gas molecules or particles, the light may be absorbed or

scattered in the atmosphere, resulting in poor visual quality, which is commonly perceived as a sign of atmospheric pollution. Light scattering by particles is the most important phenomenon responsible for impairment of visibility. Nevertheless, light can also be absorbed by the atmospheric constituents, for example, elemental carbon otherwise known as "soot", and NO_2, are both particularly effective at absorbing light (ESPERE, 2004). Size, concentration and chemical characteristics of particles are some of the factors that affect visibility. The finest particles (and particularly those between 0.1 and 1 μm) are most efficient at reducing visibility. These small particles are mostly of human origin such as motor vehicle emission and biomass burning (Kittelson, 1998). Humidity can significantly increase the effect of pollution on visibility. Water soluble components of the fine aerosol can grow to seven times their dry radius, dramatically increasing scattering efficiency and thus causing greater visibility impairment (ESPERE, 2004). Poor visibility may pose serious threat to land, sea, and air transportation.

Impacts on climate

Airborne particles may scatter or absorb light and have a significant impact on visibility. At the same time, this process may also have a significant influence on climate. Particles are believed to have similar function as cloud does to reflect partial of the solar energy reaching our planet back to the outer space and trap infrared radiations coming from Earth's surface, keeping our planet warm. However, an opposite hypothesis about the impact of particles on the Earth's climate is that blanket of airborne particles may reduce the amount of solar energy that reaches the ground, inevitably cooling down the planet, as has been widely suggested as the cause to the extinction of dinosaurs.

In addition to the direct effects discussed previously, particles may also have indirect effects on global climate. Indirect forcing by aerosols is defined as the overall process by which aerosols perturb the atmosphere radiation balance by changing the cloud albedo and volume. Indirect climate effects of aerosols are more difficult to assess than direct effects, which involve the correlation between aerosols properties and cloud characteristics. A change in number and size of particles may lead to a change in Cloud Condensation Nuclei (CCN) concentrations, which affect the volume and size of cloud droplets (ESPERE, 2004).

Fine airborne particles in the atmosphere are believed to have two major effects on cloud properties: 1) the increased number of CCN results in a larger number of smaller cloud droplets hence enhance the scattering of light within the clouds, thus increasing the cloud albedo, and 2) as cloud droplets become smaller, frequency of precipitation is reduced, thus prolongs cloud lifetime that cover the Earth surface. As illustrated in Figure 2.9, both effects may reduce the amount of sunlight absorbed by Earth and thus may cause global cooling (ESPERE, 2004). However, NASA scientists observed that sunlight absorbed by soot might cause global warming instead (Sato et al., 2003). Regardless global warming or cooling effect, airborne particles are indeed having the properties that play an important role in the change of climate, in both local and global scale.

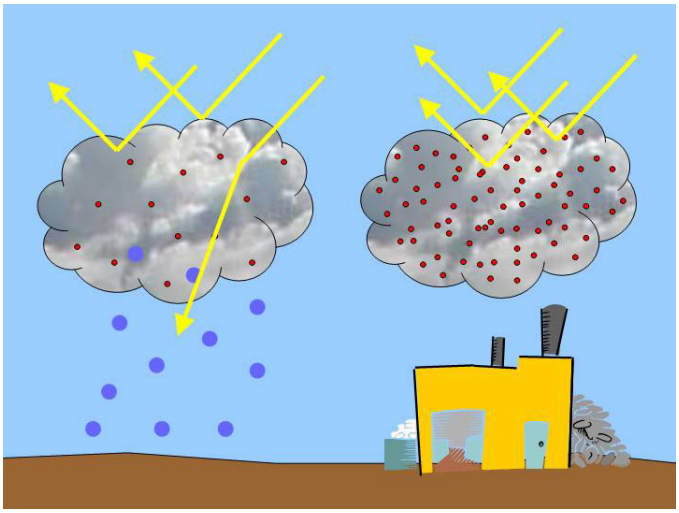

Figure 2.9 Effect of particles on cloud droplet formation and properties (Source: ESPERE, 2004).

Impacts on vegetation and materials

As discussed before, airborne particles may reduce the amount of solar energy from reaching the Earth's surface, affecting the photosynthesis process of vegetations, hence deterring crops growth and productivity. In a more direct way, particulate matter may have phytotoxic impacts on vegetation (HECS, 2003). The mechanisms of action are through smothering of the leaf; physical blocking of the stomata, bio-chemical interactions and indirect effects through the soil. Particles make contact with vegetation surfaces in three ways: sedimentation, impaction and deposition. The relative efficiency of these methods will depend upon the plant or soil surface, the microclimate and ambient (temperature and humidity) conditions. The deposition of PM on materials can reduce their aesthetic appeal as well as increase their physical and chemical degradation. The primary effects of PM on materials are on the rates of corrosion and erosion, followed by soiling and discolouration. Particles may act as catalysts for the conversion of SO_2 and NO_x to sulphuric acid and nitric acid respectively which accelerate the chemical degradation of susceptible material surfaces.

Chapter 3 Sampling Site Description

Three sampling sites representing different conditions were chosen in this study. The three sampling sites are as follows: 1) Air Quality Monitoring Station (67 m above sea level) at the NUS Faculty of Engineering (FoE), 2) rooftop of a multi-storey car park at Block 119 Edgefield Plains, Punggol (north eastern part of Singapore, approximately 20 km from NUS), and 3) a bus interchange (Boon Lay bus interchange) in the western industrial region of Singapore (approximately 8 km from NUS).

Residents and commuters who spend a significant amount of time at their homes, schools or in the bus interchange are exposed to varying levels of traffic emitted particulate air pollution. Therefore, aerosol measurements at the three sites, especially the bus interchange, are deemed to be important for health risk and exposure assessments. Aerosol measurements at the NUS FoE air quality monitoring station and the multi-storey car park rooftop at Punggol are necessary in order to evaluate the variation of PM loadings from residential area (low PM concentration) to the university campus (moderate PM concentration) followed by a bus interchange (high PM concentration). Figure 3.1 illustrates the locality map of field samplings conducted in this study.

3.1 NUS FoE Air Quality Monitoring Station

Field measurements were conducted at the NUS FoE air quality monitoring station which is located 67 m above sea level, approximately 10 km northeast of Jurong Island, the largest refinery hub in Singapore. An expressway (AYE) is located approximately

500 m north of the university campus. Relatively heavy traffic volume was observed in the campus as well as in the expressway during morning (7 – 9 am) and evening (5 – 8 pm) peak hours.

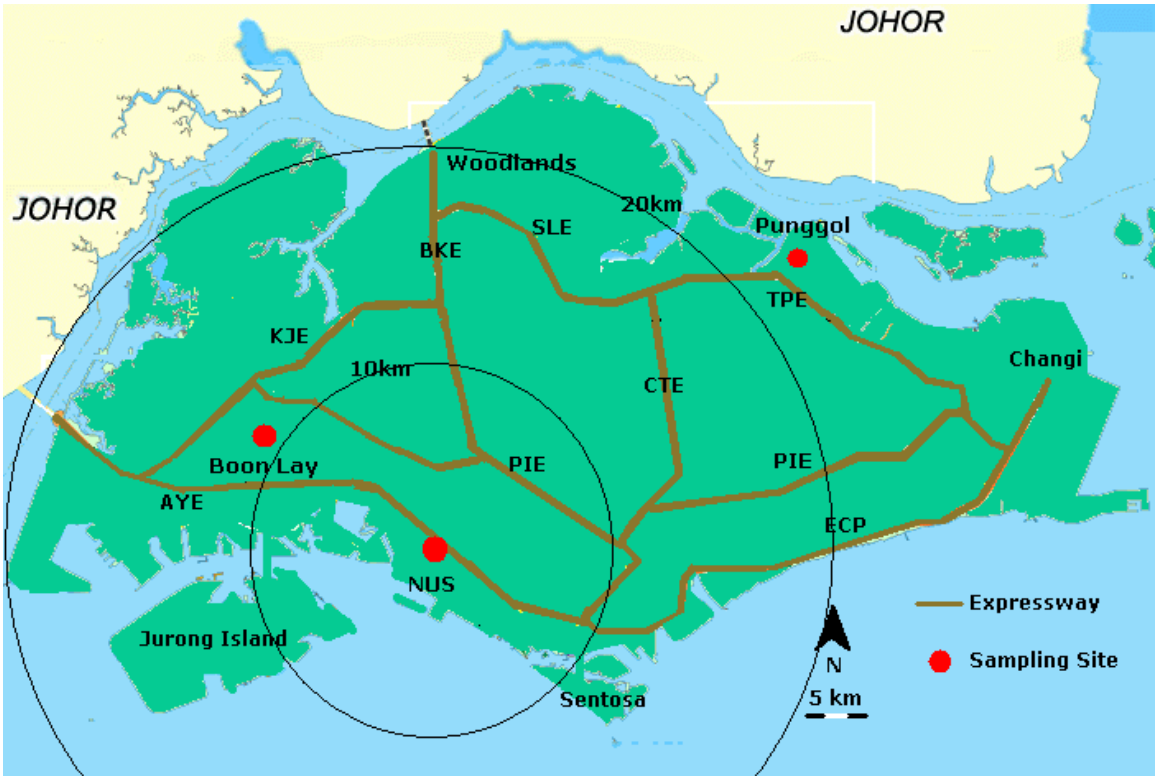

Figure 3.1 Field sampling locality map in this study (Note: AYE, BKE, CTE, ECP, KJE, PIE, SLE and TPE are expressways).

3.2 Punggol Multi-storey Car Park Rooftop

With the completion of the first HDB flats in the year 2000, the Punggol new town, located at the north-eastern corner of Singapore, is well-known for high quality HDB flats, executive condominium and private housing with efficient and convenient public transportation network comprising of public bus, Light Rail Transit (LRT) and Mass Rapid Transit (MRT). Tampines Expressway (TPE) divides the town of Punggol from Sengkang, which is located approximately 1.5 km to the south. Punggol has a

relatively low residential occupancy and local traffic volume among the sampling sites. Without major industrial emission within 10 km radius except the Senoko Power Plant that is located approximately 15 km northwest of Punggol, Punggol is one of the urban background air sampling sites in Singapore with minimum traffic emission influences. Field sampling was conducted on the rooftop of a 5-storey car park, approximately 50 m above ground, located at Block 119 Edgefield Plains. The car park was under-utilized due to low resident occupancy in the surrounding HDB flats at the time of sampling. However, the car park is located approximately 300 m away from the TPE, which had a traffic volume of approximately 3000 vehicles per hour during peak hours at the time of sampling.

3.3 Boon Lay Bus Interchange

There are 16 major bus interchanges throughout Singapore (SBS, 2004b). Boon Lay bus interchange is located at the west point of Singapore. It is one of the busiest interchanges with at least 24 bus service routes serving the Jurong industrial areas, as well as the western residential zone. The bus interchange is operating from 0500 to 2400 daily. With the estimation of one bus trip per 20 minutes per route service, a total of 72 bus trips were made every hour, or 1296 bus trips per 18 hours operating day.

Boon Lay along with Jurong East and Jurong West region is housed to more than 284,800 residents in the nearby HDB flats (HDB, 2003). The town also serves as a transit point to the nearby Jurong – Tuas Industrial Estate, which is well known for the establishment of electrical, electronic, metal fabrication, pharmaceuticals and petrol-chemical companies. The country's major power and incineration plants were also

established in the industrial zone. As the result, a complete and efficient public transport network is necessary to support and ensure smooth flow of workers and residents in the areas. Boon Lay Bus Interchange was built with such purpose to converge buses in west region of Singapore that serve the Jurong-Tuas Industrial Estate and the surrounding residential areas, connecting to Boon Lay Mass Rapid Transit (MRT) station which is linked to the island-wide public transport network. Figure 3.2 demonstrates the layout plan of the bus interchange and the sampling points where the instruments were positioned.

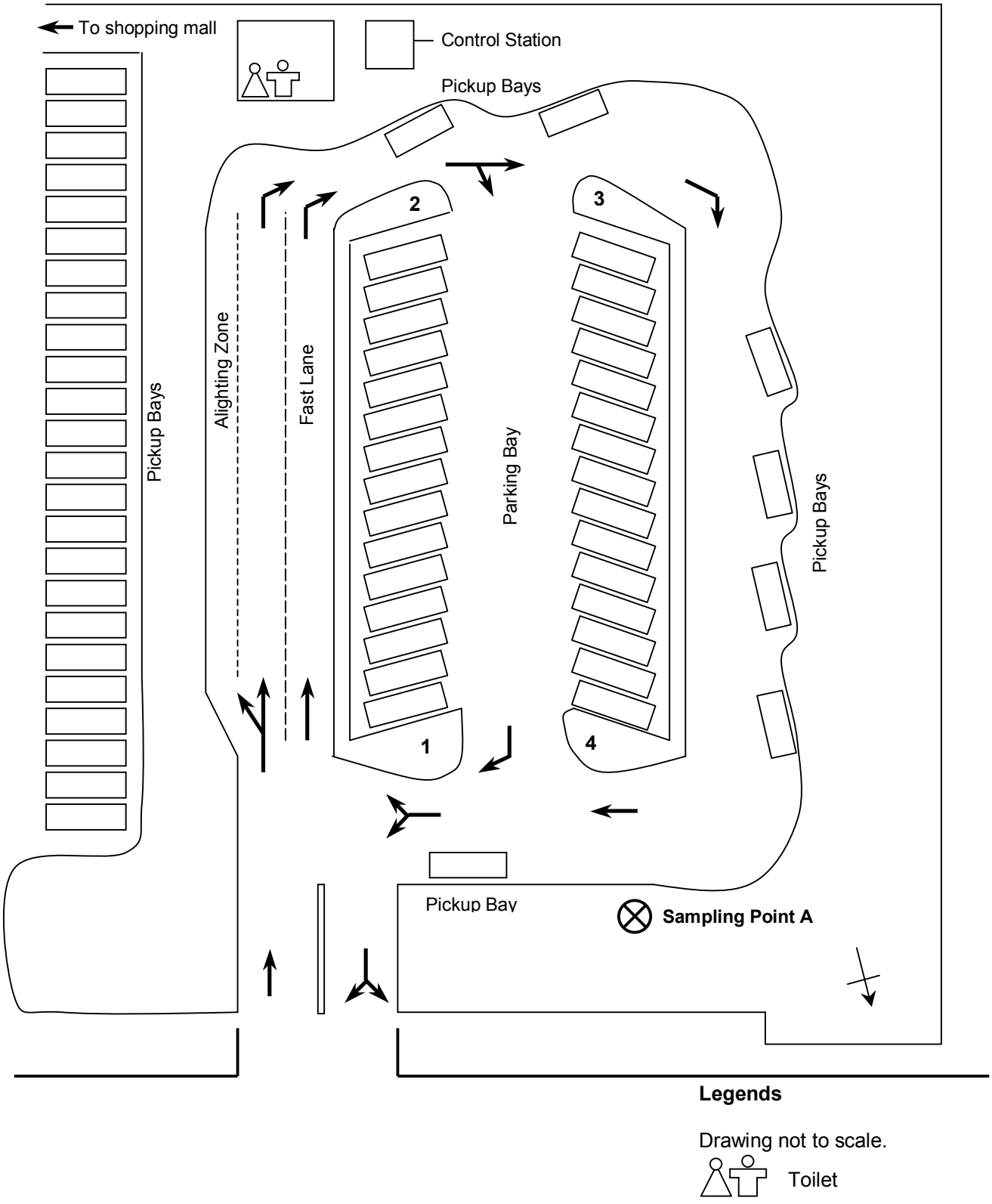

Figure 3.2 Boon Lay bus interchange layout plan (provided by Land Transport Authority of Singapore).

Chapter 4 Instruments and Analytical Procedures

Instrumentation used in this research is classified into two categories: 1) On-site Sampling Instruments and 2) Laboratory Analytical Instruments. On-site sampling instruments are the instruments used during field sampling to collect samples or to conduct real time measurements. Laboratory analytical instruments are the instruments used in the laboratory to analyse collected samples from the sampling sites.

4.1 On-site Sampling Instruments

Instruments used during the field sampling include Annular Denuder System (ADS), MiniVol®, Aethalometer™, Micro-Orifice Uniform Deposit Impactor (MOUDI™), Condensation Particle Counter (CPC, TSI-3007), Electrical Low Pressure Impactor (ELPI, Dekati) and Scanning Mobility Particle Sizer (SMPS, TSI-3034). ADS was utilised to measure atmospheric NH_3, SO_2 and NO_x levels. MiniVol® was designed to collect aerosol samples and to measure airborne particle mass loading at all proposed sites. Aethalometer™ was used to measure black carbon (BC) mass loading in the atmosphere. MOUDI™ was useful to obtain the total mass of total suspended particles and mass size distribution. CPC, ELPI and SMPS were repeatedly used in this study to measure the number concentration of airborne particles at the proposed sites. Table 4-2 illustrates the operating conditions and detection limits of CPC, ELPI and SMPS.

4.1.1 Annular Denuder System (ADS)

ADS (URG Corp., USA) is designed to measure acidic and basic gaseous pollutants such as sulphur dioxide and ammonia as well as particulate matter suspended in

ambient air. The system consists of 1) an inlet with a cyclone pre-separator designed to remove all particles with a DP_{50} of 2.5 μm and above, 2) annular denuders to quantify acidic and basic gases and 3) a filter pack for atmospheric acidity and particles. Details about ADS coating solutions preparation, absorbing properties, denuders coating and extraction procedures are shown in Table 4-1.

While the ADS was in operation, ambient air was drawn through the cyclone pre-separator and flew past the denuder walls that had been coated with chemicals that absorb gaseous species of interest. The remaining air stream was then filtered through 47 mm 2.0 μm Teflon® and Nylabsorb® membrane filters. Teflon® and nylon membrane filters were used to capture ammonium and nitrate aerosol and sulphate particulate matter. The nylon filter also collected nitric acid and sulphur dioxide, but these measurements were treated as interference. Following each run, the ADS assembly was removed from the field housing and the denuders were capped and transported back to the laboratory for extraction as described in Table 4-1. The extracted solution was then analysed for ions corresponding to the collected gaseous species. The filters were placed into a 50 mL conical flask with cap, facing downward. All Teflon® filters were wetted with 0.1 mL of isopropanol as the Teflon® filters were hydrophobic. The filters were then completely covered by 15 mL of ultra pure water. The conical flasks were capped and sonicated for 1 hour. The extracts were then transferred into a labelled 25 mL vial. Additional 5 mL of ultra pure water was added to wash off the residue in the conical flask and poured into the same vial. The vials were sealed and stored in a refrigerator until analysis. Calculation method of gaseous aerosols concentration such as SO_2 and NO_x is shown in Appendix B.

Table 4-1 ADS coating solution preparation, absorbing species identification, denuder coating and extraction procedures.

Coating Solution	Coating solutions preparation procedures	Absorbing Species	Coating procedure	Extraction procedure
Citric acid	Add 0.5 g of citric acid into 50 mL methanol; mix thoroughly, cover and store at room temperature.	NH_3	Cap one end of the denuders. Add 10 mL of the coating solution into respective denuders. Cap and rotate the denuders to wet every surface within. Pour out the excessive coating solution and proceed to drying process on a drying manifold by using pure Nitrogen gas.	Cap one end of the denuders. Add 5 mL of ultra pure water into each denuder. Cap and rotate the denuders to wet every surface within. Remove the cap and pour the liquid into a clean 25 mL well-labeled vial. Repeat this procedure with a second 5 mL ultra pure water (total extract volume is 10 mL, which is placed into a single vial). Seal and label the vial with denuder ID number and sampling details.
Sodium Chloride (NaCl)	Weight 0.1 g of reagent grade NaCl, add 90 mL of ultra pure water and 10 mL of methanol; mix thoroughly, cover and store at room temperature.	HNO_3		
Sodium Carbonate (Na_2CO_3)	Mix 50 mL of equal volume methanol and ultra pure water with 1 g of equal weight glycerol and Na_2CO_3; Mix thoroughly, solution may fizz; wait for fizzing to stop before sealing the vial; cover and store in room temperature.	HONO, SO_2		

4.1.2 MiniVol® Portable Air Sampler

MiniVol® (Airmetrics™ Inc.) portable air sampler is a gravimetric time integrated ambient air sampler for particulate matter. MiniVol® is designed to operate from either AC line power or DC battery pact power sources. This makes the sampler portable for use in many sampling fields that have no access to line power. Air is drawn through a 2.5 μm cut size impactor and a 47 mm 2 μm porosity Teflon® (PALL, R2PJ047) filter. The Teflon® filters were pre-conditioned at least 24 hours in a controlled temperature and humidity dry box (25 ^{o}C, 40 %RH) and weighted before and after each measurement using a micro-balance (Sartorius MC-5) (1 μg resolution, ±3 μg). Air flow rate is to be maintained at a pre-determined value to ensure consistent collection efficiency of the correct particle size through the impactor. Hence, the samplers used in the research were calibrated at 5 L/min before and after each sampling.

4.1.3 Aethalometer™

BC is one of the major pollutants of diesel fuel combustion process, and is considered as one of the indicators of incomplete combustion process. Aethalometer™ (Magee Sci. Co.) is the most commonly used equipment to collect the daily emission profile of black carbon (BC). The Aethalometer™ is easy to use and is relatively lightweight to be transported. The Aethalometer™ uses optical attenuation method to project the value of BC in a known volume of air. The equipment is equipped with an internal air pump and air flow rate calibrator, where known amount of air will be drawn through the particle filter tape. A specific frequency of light will be applied on the aerosols collected on the web-reinforced quartz fibre filter tape. The light will be detected on the opposite site of the filter tape by a photodiode. The quantity of BC in the sampled

air can then be calculated with the information on the light attenuation and air flow rate. BC is the only commonly found species that has a strong light absorption, which is quantitative and can be calibrated as a mass concentration of BC.

4.1.4 Micro-Orifice Uniform Deposit Impactor (MOUDI^{TM} Model 110)

MOUDI^{TM} (MSP Corp.) (Marple et al., 1991) was used to study the TSP mass and size distribution at the proposed sites. MOUDI^{TM} model 110 is a cascade impactor equipped with 10 cut sizes of 18 μm, 5.6 μm, 3.2 μm, 1.8 μm, 1.0 μm, 0.56 μm, 0.32 μm, 0.18 μm, 0.1 μm and 0.056 μm. At each stage jets of particle-laden air impinge upon the impaction plate, particles larger than the cut-size of that stage cross the air streamlines and are collected upon the impaction plate. The smaller particles with less inertia do not cross the streamlines and proceed on to the next stage where the nozzles are smaller, the air velocity through the nozzles is higher and finer particles are collected. This continues on through the cascade impactor until the smallest particles are collected at the after-filter. Aluminium foils or Teflon® (Pall, R2PJ047) filters of 47 mm diameter were placed on top of each cascade impactor in order to collect and measure the mass of particles at each stage. The aluminium foil and Teflon® filters were preconditioned and weighted by Sartorius MC-5 (1 μg resolution, ±3 μg) microbalance before and after use to obtain the particles mass collected on it. The flow rate for optimum collection efficiency of particles is 30 litre of air per minute. MOUDI^{TM} was operated at a 24-hour or 48-hour interval at various sites, depending on the local PM mass loading.

4.1.5 Hi-Vol Sampler HVP-3800AFC/230

In order to analyse organic compounds in trace amounts, a large mass of particles need to be collected. Hi-Vol (Hi-Q Co.) sampler is designed to collect large amount of particles within a limited period of time at high airflow rate of about 39 scfm (approximately 1.1 m^3/min). Particles were collected on Whatman® Quartz microfibre filter (filter size: 20.3 cm x 25.4 cm). The filters were pre-conditioned at least 24 hours in a controlled temperature and humidity dry box (25 ^oC, 40 %RH) and weighed before and after each sampling.

4.1.6 Condensation Particles Counter (CPC) TSI 3007

Airborne particle counters are sophisticated instruments that measure airborne particles in all size ranges, some are far too small to be seen, but may have a serious impact on air quality, personal health and safety. Designed by TSI Inc., CPC measures particle size ranging from 0.01 to >1 μm to a maximum concentration of 4 x 10^5 particles per cm^3 of air in real time. For particle concentration up to 100,000 particles per cm^3 of air, coincidence is low and no correction is necessary. The CPC runs with pure alcohol (99.5% pure isopropyl alcohol), which is used to grow microscopic particles in the air into larger droplets that are easier to detect and count. The CPC is equipped with internal data memory device, which can store all the collected data. The data can be transferred to a computer for further statistical analysis.

4.1.7 Electrical Low Pressure Impactor (ELPI) (Dekati Ltd.)

The ELPI (Keskinen et al., 1992) is a real-time particle size spectrometer designed to measure aerosol particle mass and number size distribution. The ELPI was developed to measures airborne particle size distribution in the size range 0.03 – 10 μm with 12 channels (size range 0.008 – 10 μm with filter stage), based on the principle on charging, inertial classification, and electrical detection of the aerosol particles. The instrument consists primarily of a corona charger, low-pressure cascade impactor and multi-channel electrometer. The nominal air flow rate for ELPI is 30 litres per minute. The ELPI charges the particles prior to entering the impaction section, and each impaction is connected to an electrometer, which detects the current produced by the impacting particles. This current is converted into a particle concentration for that size range, hence allowing the instrument to measure real time particle size distribution of mass and number concentration.

4.1.8 Scanning Mobility Particle Sizer (SMPS) TSI 3034

The SMPS (TSI Inc.) measures the real time airborne particle size distribution over the range of 10 to 487 nm within 54 channels. A maximum of 10^7 particles/cm^3 of the total aerosol concentration can be determined by means of its mechanical subsystems, including a built-in Differential Mobility Size Analyser (DMA) and a Condensation Particle Counter (CPC). The DMA is responsible for separating the particles based on their unique electro-mobility. DMA functions in the manner where the sampled particles are charged to a known charge distribution using a radioactive Kr-85 neutralizer. The charged particles will pass through an electrical field where the particles of different sizes are separated. Subsequently, the particle number

concentration is determined by the CPC, which employs a condensing butyl alcohol (butanol) vapour to "grow" the small separated particles to enhance visibility and sensitivity of the measurement of ultra fine particles. The particles are then passed through a focal point of a laser light source. The PM number and mass concentration is then determined by measuring the scattered light intensities, which is detected using a photo-detector. The operational specification and detection limit are shown in Table 4-2.

Table 4-2 Specification of aerosol number measuring capable instruments.

Instrument	Number Conc.	Mass Conc.	Concentration Range (pt/cm^3)	Particle Size Range (µm)	Flow Rate L/min
CPC	Yes	No	0 ~ 4x10^5	0.01 ~ 1	0.1
ELPI	Yes	Yes	0 ~ 9x10^6	0.03 ~ 10 0.008 ~ 10 (with filter stage)	30
SMPS	Yes	Yes	0 ~ 1x10^7	0.01 ~ 0.487	1

4.2 Analytical Instruments and Methodology

4.2.1 Microbalance Sartorius MC-5

The microbalance is an essential piece of sophisticated instrument necessary to determine PM mass collected on the filters. A Sartorius MC-5 (1 µg resolution, ± 3 µg) microbalance was used throughout the study. The microbalance was calibrated according to the manufacturer's recommendations and procedures.

4.2.2 MLS-1200 MEGA Microwave Digestion System

The filter samples collected were cut into two halves by ceramic scissor C-124 (Kyocera Corp.): one half was used for trace element analysis and the other half was used for water soluble ion chromatographic analysis. Microwave digestion is commonly used to extract trace elements from airborne particles (Yang et al., 2002). The microwave oven used in this study was a MLS-1200 MEGA Microwave Digestion System (MDS) following the procedures described by Swami et al. (2001) and Yang et al. (2002) with some minor modifications. During the extraction process, 5 mL of concentrated HNO_3, 4 mL of H_2O_2 and 0.5 mL of HF was added into each extraction vessel. The vessels were capped, fastened on the rack and placed in the microwave oven to undergo the digestion procedure below.

Step 1. The temperature was gradually ramped to 110 ^oC in 25 minutes by applying 600W of power, followed by a dwell time of 5 minutes. The vessels were removed from the oven and cooled to about 35 ^oC. The vessels were vented, recapped and placed in the microwave oven.

Step 2. The temperature was gradually increased to 170 ^oC in 20 minutes with the application of 600W of power, followed by a dwell time of 2.5 minutes. The temperature was then increased to 180 ^oC in 13 minutes at 600W of power, followed by a dwell time of 5 minutes. The vessels were removed from the oven and cooled. The vessels were vented and opened.

Step 3. A 5 mL of 5% boric acid was added to each vessel. The vessels were recapped and placed in the microwave oven and heated to 110 ^oC in 15 minutes at 500W of

power, followed by a dwell time of 5 minutes. The vessels were cooled and the samples were transferred to graduated polypropylene centrifuge tubes and diluted with ultra pure deionised water to a final volume of 50 mL.

4.2.3 ICP-MS Perkin Elmer Elan 6100

Inductively coupled plasma mass spectrometry (ICP-MS) of Perkin Elmer Elan 6100 was used to analyse trace elements including Al, As, Cr, Co, Cu, Fe, Mn, Ph, Zn, Cd, Ni, Sb, Ti and V. The instrument and sample analysis procedure have been discussed in detail by Swami et al. (2001). The samples were diluted 10 times by adding ultra pure water prior to the ICP-MS analysis, as the upper concentration limit was only 200 ppb (µg/L). A baseline concentration of the trace elements was determined by performing the extraction on a fresh Teflon® filter. The actual concentration of trace element was obtained by deducting the baseline concentration.

4.2.4 Ion Chromatography – Metrohm Ion Analyser

The other half of the filter underwent a straightforward extraction process in ultra pure water. About 0.1 mL of iso-propanol was added onto the Teflon® filter to wet the surface totally as the PTFE filters are hydrophobic. The Teflon® filter was then submerged in 15 mL ultra pure water in a 50 mL screw cap conical flask. The samples were then sonicated for about 1 hour at 60 ^{o}C. The sonicated solution was poured into the clean 25 mL PE bottle. Another 5 mL of ultra pure water was added into the conical flask to wash out the residue and poured into the same PE bottle. The sonicated solution was then filtered with Whatman® Syringeless Filter Device PTFE Autovial® 0.45 µm pore size before being injected into the IC system. Metrosep Anion Dual 2

column was used for the anion analysis with chemical suppression while Metrosep C2–100 was used for the cation detection. The anions and cations analysed are listed in Table 4-3. The operating parameters are given in Table 4-4.

Table 4-3 Ion Chromatography Analysis Species

Anion	Cation
Fluoride, F^-	Lithium, Li^+
Chloride, Cl^-	Sodium, Na^+
Nitrite, NO_2^-	Ammonium, NH_4^+
Nitrate, NO_3^-	Calcium, Ca^{2+}
Phosphate, PO_4^{3-}	Magnesium, Mg^{2+}
Sulphate, SO_4^{2-}	Potassium, K^+

Table 4-4 Metrohm Ion Chromatography System Operating Parameters

Analysis	***Anion***	***Cation***
Column	Metrosep Anion Dual 2	Metrosep C2-100
Eluent	Sodium hydrogen carbonate 336 mg/2L Sodium carbonate 276 mg/2L	Tartaric acid 1200 mg/2L Dipicolinic acid 250 mg/2L
Eluent Flow rate	0.8 mL/min	1.0 mL/min
Suppressor	Yes	No
Detector	Metrohm 732 IC Detector	Metrohm 732 IC Detector
Sample Loop Volume	20 µL	20 µL
System Operating Pressure	6~9 MPa	5~7 MPa
Total Elution Time	Approx. 16 minutes	Approx. 14 minutes

4.2.5 Soxhlet Apparatus

Analysis of organic compound was conducted by *Instituto de Pesquisas Energéticas e Nucleares SP, Instituto de Química, Brazil*, under the bilateral collaboration program between the University of São Paulo and the National University of Singapore. A Soxhlet apparatus filled with methylene chloride was used for extracting the organic compounds including n-alkanes, PAHs and nitro-PAHs as described by Vasconcellos et al. (2003) and Ciccioli et al. (1996). The samples were extracted for approximately 20 hours and a fractionation was used to obtain n-alkanes, PAHs and nitro-PAHs. The compounds were identified by using a gas chromatograph coupled to a mass spectrometry detector (Shimadzu model GCMS-QP5000). The detection mode used for identification was the single ion monitoring (SIM). A 30-m fused-silica capillary column, DB-5 (0.2 mm ID, 0.25 μm film thickness), was used for separation.

Chapter 5 Results and Discussion

Physical and chemical characteristics of airborne particles may vary from location to location and from time to time at the same location depending on the intensity of human activities and the prevailing meteorological conditions. This study was conducted with the motivation to assess the contribution of traffic emissions to the localised PM loading in the air. Field sampling was conducted at three different sites, as described in Chapter 3, from March 2002 through July 2004. Sampling instruments and real-time particle analysers used at the sampling sites include those described in Chapter 4. A detailed analysis was conducted to investigate the physical and chemical characteristics of PM collected at each microenvironment. This determination includes the mass and number concentration of PM of various sizes and their corresponding chemical composition including trace elements, organic compounds, and water-soluble ionic species. The concentration of sulphur dioxide (SO_2) was measured in an attempt to establish the possible relationship between particulate sulphate concentration and SO_2 in the atmosphere. Since black carbon (BC) is commonly known as the precursor of incomplete combustion source particularly from diesel engines exhaust emission, its mass concentration was measured in order to track the traffic emission profile.

5.1 Mass Concentration

5.1.1 Background

Particle concentrations in the atmosphere are generally measured by determining the total mass of particles per volume of air (i.e. micrograms of particle per cubic meter of ambient air, $\mu g/m^3$). The amount of particulates, suspended in the air, is commonly

referred to as TSP (Total Suspended Particles) (Vesilind et al., 1994). Particles with aerodynamic diameter less than 10 μm (denoted as PM_{10}) are of major concern as they pose a higher health risk than the coarse particles. The annual average PM_{10} level measured in Singapore was 31 $\mu g/m^3$ in the year 2002 (NEA, 2003), well below the US National Ambient Air Quality Standards (NAAQS) annual mean of 50 $\mu g/m^3$ (USEPA, 1997). Particles less than 2.5 micrometers in diameter ($PM_{2.5}$) are referred to as "fine" particles and are believed to pose larger health risks than PM_{10} because of their small size which allows them to penetrate deeply into the lungs. In 1997, the USEPA established annual and 24-hour NAAQS for $PM_{2.5}$ for the first time and mass loading of $PM_{2.5}$ was closely monitored in the US. However, such systematic field studies are yet to be conducted here in Singapore (NEA, 2003). As a result, the current study is important in highlighting and assessing the $PM_{2.5}$ mass concentration levels in urban Singapore and in certain "hot-spots". Urban traffic emission is believed to be an important source of $PM_{2.5}$ in Singapore (Chin, 1996).

MOUDI™ and MiniVol® were used to determine the mass loading of PM at the three sampling sites. The portable MiniVol® air samplers were installed with a 2.5 μm cut size impactor to remove all particles larger than 2.5 μm in diameter in order to determine the $PM_{2.5}$ mass concentration. MOUDI™, which has the capability of fractionating airborne particles to 10 different sizes, was used to determine the mass loading of size-fractionated particles. Mass size distribution was established from the MOUDI™ data to identify the modal size(s) of particles. The chemical composition of particles collected on each impactor was also determined, and is reported in this section. Ambient particulate matter generally appears in black when collected on a filter due to the presence of black carbon (BC). BC is emitted by virtually every combustion

process involving carbonaceous material; it is produced only by combustion processes and not generated by any known atmospheric reactions (Hansen et al., 1988; Hansen et al., 1984; Andreae et al., 1984). Therefore, almost all BC aerosols are smaller than 1 μm in size and have a long atmospheric lifetime. Ambient data indicates that long-range transport becomes important with such long lifetimes (Hansen et al., 1988; Andreae et al., 1984). Although BC can be regional in nature (especially in remote areas) local sources are usually dominant (Hansen et al., 1988) due to localised traffic emissions. Particulate BC has been the subject of interest in recent years for a variety of reasons. It is known that BC plays an important role in atmospheric chemistry because of its catalytic properties (Cadle and Mulawa, 1990; Hansen et al., 1988) and also affects visibility by light-extinction (Cadle and Mulawa. 1990). Because BC absorbs light, it may be potentially climate altering (Cadle and Mulawa, 1990). Hence, Aethalometer™ was deployed to measure the concentration of BC in order to verify the significance of traffic emissions at each sampling site.

5.1.2 Measurement of $PM_{2.5}$ mass concentration

The average $PM_{2.5}$ mass concentration measured at the rooftop of a multi-storey car park at Punggol was 18.8 $\mu g/m^3$ with the recorded minimum and maximum mass concentrations of 11.2 $\mu g/m^3$ and 27.4 $\mu g/m^3$ respectively. At NUS FoE Air Quality Monitoring Station, an average of 19.2 $\mu g/m^3$ of $PM_{2.5}$ mass concentration was obtained with the lowest and highest concentrations of 13.5 $\mu g/m^3$ and 24.7 $\mu g/m^3$ were recorded respectively. The average $PM_{2.5}$ mass concentration measured at the Boon Lay bus interchange was 46.4 $\mu g/m^3$ with maximum and minimum concentration of 101.2 $\mu g/m^3$ and 22.5 $\mu g/m^3$ respectively. Figure 5.1 illustrates the $PM_{2.5}$ mass

concentration at the three distinctive sampling sites. The $PM_{2.5}$ mass loading at all the three sampling sites was found to have exceeded the NAAQS legislative allowance of 15 $\mu g/m^3$.

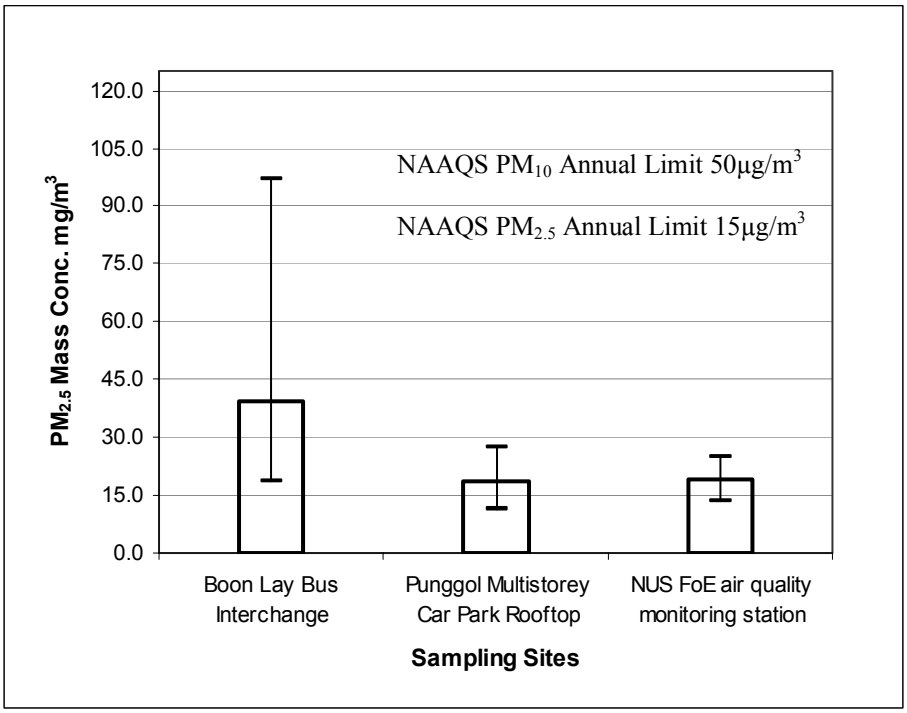

Figure 5.1 Average $PM_{2.5}$ mass concentration measured at Boon Lay bus interchange, Punggol and NUS.

At the bus interchange, 4 units of portable MiniVol® air sampler were deployed simultaneously at the 4 traffic islands labelled as 1, 2, 3 and 4 as shown in Figure 3.2. The intention was to establish the spatial variation of $PM_{2.5}$ mass concentration at the site. The results are shown in Table 5-1, indicating that $PM_{2.5}$ mass loading was highest at location 2, followed by 3, 1 and 4. This is probably due to the structural design of the bus interchange, which may obstruct airflow and dispersion at location 2. In addition, the traffic flow in the bus interchange is believed to have caused the accumulation of PM at location 2, which is also situated within the alighting zone. Buses that enter from the only entry point of the bus interchange have to stop at the

alighting zone to alight commuters. The longer the buses stop at the alighting zone, the more PM is emitted. Buses without commuters will take the fast lane and enter the parking bay. Overall, MiniVol® positioned at location 2 collects PM emitted from both stationary and passing-by buses under poor air circulation/dispersion conditions, resulting in high yield of PM mass. As one moves away from location 2 (the source), $PM_{2.5}$ mass concentration dropped dramatically with increasing distance. At the two nearest sampling locations (1 and 3), the mass concentration was 32.6 $\mu g/m^3$ and 39.9 $\mu g/m^3$ respectively. However, the $PM_{2.5}$ mass loading decreased to 27.3 $\mu g/m^3$ at location 4. The dramatic decrease of $PM_{2.5}$ mass concentration was likely due to atmospheric dilution with better dispersion of air pollutants at location 4.

Table 5-1 Spatial variability of $PM_{2.5}$ mass loading in Boon Lay bus interchange.

Date \ Location	1	2	3	4	Average
10/Dec/03	47.5	101.2	43.7	39.5	58.0
11/Dec/03	27.5	79.7	48.2	22.5	44.5
12/Dec/03	28.2	96.9	33.3	22.7	45.3
13/Dec/03	27.1	65.0	34.3	24.5	37.7
Average	**32.6**	**80.7**	**39.9**	**27.3**	**46.4**

All values are in $\mu g/m^3$

Industrial emissions from Jurong Islands and traffic emissions from the nearby Clementi Road and AYE were believed to be the main sources of fine aerosol in the NUS campus. Zhang (2001) actually found that PM mass concentration increased as concentration of combustion source pollutants (BC, CO and NO_x) increased,

concluding that urban traffic had a significant impact on PM mass loading in the campus and other parts of Singapore. Similarly, local traffic emission and landscaping activity were believed to be the two main contributors of fine and coarse particles, respectively at Punggol. TPE traffic emission was believed to be the main source of $PM_{2.5}$ at Punggol. At Boon Lay bus interchange there was a mix of industrial and traffic emissions that contribute to the fine particle mass loading. In order to identify the source of PM at the sampling sites, the black carbon analyser, Aethalometer™, was used to study the 24-hour black carbon emission profile at all sampling sites, which will be discussed in section 5.1.4. Black carbon (soot) is the by-product of incomplete combustion and mainly emitted from diesel combustion source. In conclusion, the maximum $PM_{2.5}$ mass concentration that was observed at location 2 (the most crowded location) in the bus interchange was about 4 times greater than that for the background location. This suggests that people who work or spend a substantial amount of time in the bus interchange will have a much higher fine particle exposure than those who do not.

5.1.3 PM Mass Size Distribution

As discussed in the previous section, it is essential to study the mass size distribution at the sampling sites in order to verify the PM mass concentration and chemical composition of various particle sizes. MOUDI™ were deployed at the NUS FoE Air Quality Monitoring Station, the Punggol multi-storey car park rooftop and the Boon Lay bus interchange to study the mass size distribution at each sampling site. Due to restrictions on electric power accessibility and space (to avoid inconvenience to the

commuters), the MOUDI^{TM} was deployed at point A in the bus interchange, as shown in Figure 3.2.

In order to identify the modal diameter of the particle size distribution, the MOUDI^{TM} data has to be inverted by applying a non-linear iterative algorithm as illustrated by Twomey and Zalabsky (1981). This involves solving the *Fredholm equation* for each impaction stage in order to recover the actual size distribution *f(x)* where y_i is the responded mass concentration on each size selective impactor.

$$y_i = \int_{x_{\min}}^{x_{\max}} k_i(x) f(x) dx \qquad \textbf{Eq. (1)}$$

The *Kernel functions* $k_i(x)$ are instrument-specific response functions, which gives the probability of a particle with size x deposited on stage i within the upper size limit x_{max} and lower size limit x_{min} of the impactor. A mathematical inversion computer program (as shown in Appendix C) was used to facilitate the calculation of the mass concentration size distribution from experimental results obtained by MOUDI^{TM}. In this program, the measured results from each impactor stage of MOUDI^{TM} were used as an initial guess for function $f_0(x)$, which will give the mass concentration y_i when integration was performed in Eq. (1). In the subsequent integrations the initial guess distribution was modified by applying the Kernel function $k_i(x)$, which was derived in the following equations:

$$k_n(x_p) = E_n(x_p) \qquad \textbf{Eq. (2)}$$

$$k_i(x_p) = E_i(x_p)[1 - E_{i+1}(x_p)]...[1 - E_n(x_p)] \qquad \textbf{Eq. (3)}$$

$$E(x_p) = [1 + (d_{50} / x_p)^{2s}]^{-1} \qquad \textbf{Eq. (4)}$$

where, i = n-1, n-2, … , 1;

n = number of stages;

x_p = particle diameter;

d_{50} = particle diameter with 50% cut point;

s = manufacture-specified steepness which varies in each stage and impactor.

The MOUDI^{TM} inversion routine was performed based on this procedure with the MOUDI^{TM} stage transmission *Kernel function* derived from the manufacturer's calibration. The measured data of mass loading on each stage was then loaded into the inversion program, which is illustrated in Appendix C. All data collected from the three sampling locations were loaded into the program. The size distributions of mass concentration at all three sampling sites were obtained and plotted in Figure 5.2. A bimodal log-normal distribution was obtained at all the three sampling sites in this study, which was in line with the results obtained 3 years ago by Zhang (2001) in Singapore. Other similar studies conducted at Seoul (Baik et al., 1996), Leeds (Clarke et al., 1999), central Vienna (Horvath et al., 1996), central Jakarta (Zou and Hooper, 1997) and north-western region of Taiwan (Lee et al., 1999) also showed bimodal distributions. Table 5-2 illustrates the mass median aerodynamic diameter of each mode conducted at different sampling sites in Europe and other parts of Asia in comparison to that conducted in this study.

Particles in the coarse mode are generally less affected by chemical reaction and gas-to-particle conversion. Hence, there was very little variation on coarse modal diameter (4 – 7 μm) at the three sampling sites. However, the mass loading of coarse particles at Boon Lay bus interchange was highest among the three sites. At Boon Lay bus interchange, resuspension of road dust was believed to be the main cause for the higher mass loading of coarse mode particle, as the sampling point A is only a few meters away from the busy internal bus lane. In Punggol, there were some construction and

landscaping activities in progress during the sampling period, which possibly caused an increase in coarse particle uptake. There was relatively lower uptake of coarse particle mass loading in NUS as there was no major coarse particle generating activities within the close proximity except some controlled renovation works and wind-blown dust or sea salt.

Table 5-2 Mass median aerodynamic diameter of each mode reported elsewhere.

Sampling Site	Reference	Fine Mode (μm)	Coarse Mode (μm)
Singapore (NUS)	This study	0.25 – 1	4.0 – 7.0
Singapore (Punggol)	This study	0.4 – 1	4.0 – 7.0
Singapore (Boon Lay)	This study	0.15 – 0.7	4.0 – 7.0
Singapore (NUS)	Zhang, 2001	0.25 – 0.63	5.01 – 5.62
Seoul	Baik et al., 1996	0.8	5.0
Central Jakarta	Zou and Hooper, 1997	0.6	6.3
Central Vienna	Horvath et al., 1996	0.5	>3.0
Leeds, U. K.	Clarke et al., 1999	1.0	5.0
North-western Taiwan	Lee et al., 1999	0.32	3.2

Fine particle formation is rather complicated as it involves not only chemical reactions, but also physical agglomeration mechanisms. Wind speed, humidity and ambient temperature have significant effects on fine particle formation, resulting in variation of fine mode distribution. When the particle size distributions are compared among the three sampling sites, there is an obvious variation of particle diameter in fine mode as shown in Figure 5.2. At Punggol, the fine particle modal diameter ranged between 0.5

and 1.0 µm. This range was wider at NUS, ranging from 0.3 to 1.0 µm, and in Boon Lay bus interchange where fine particle modal diameter shifted towards even finer region ranging from 0.15 to 0.7 µm. Obviously, the peak of fine mode distribution in the bus interchange had shifted towards finer modal diameter, indicating that there were more particles in smaller size than the other two sampling sites. However, as submicron-sized particles are less dense and smaller in size, even in high numbers, the mass-measuring instrument like MOUDI™ may have possibly underestimated the fine and ultrafine particles loading at the site. Besides, MOUDI™ is unable to gain information on transient particles. Therefore more sophisticated equipment was used to study the PM concentration at the bus interchange and the other sites, this time from a number concentration perspective.

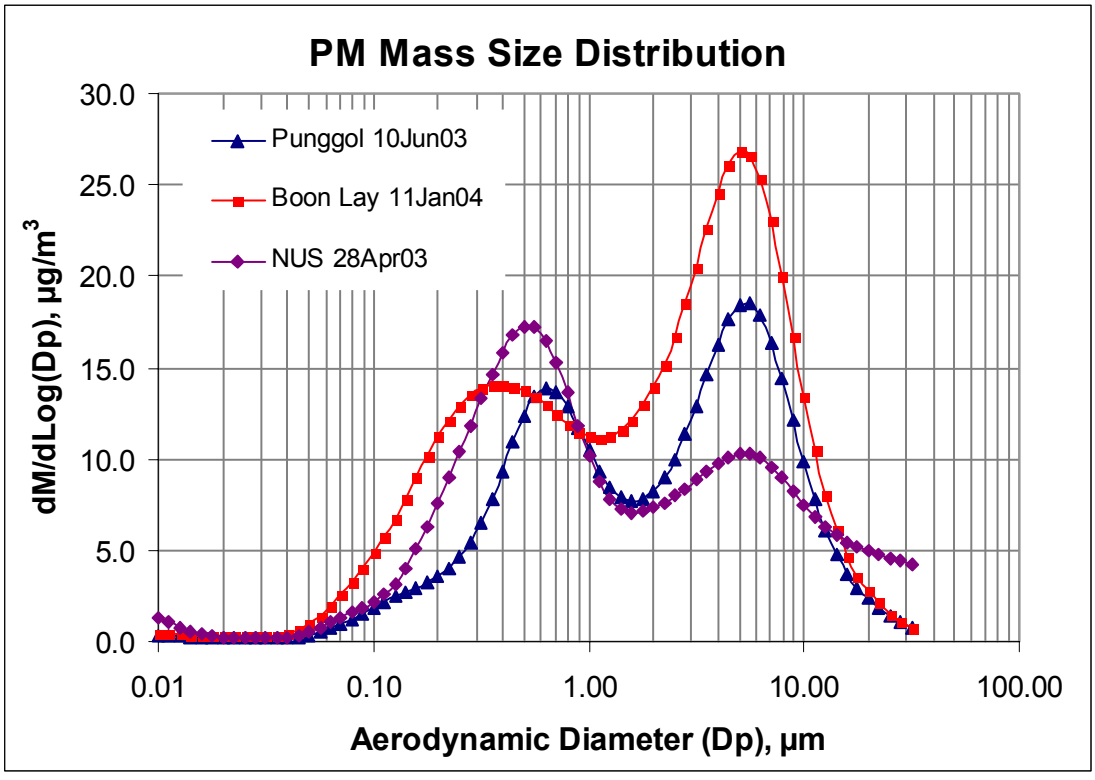

Figure 5.2 Typical PM mass size distribution obtained from NUS FoE Air Quality Monitoring Station, Punggol multi-storey car park rooftop and Boon Lay bus interchange.

5.1.4 Black Carbon Mass Concentration

Aethalometer™ 5-minute interval datasets were analysed to identify daily temporal patterns of BC mass concentration in ambient air at the three sampling sites. At Punggol and NUS, a strong diurnal BC pattern was observed, with peaks occurring between 7 am and 9 am local time as shown in Figure 5.3. This is consistent with the increase in traffic emissions from nearby freeway and roads in the morning rush hours, coupled with poor dispersion of air before daytime vertical mixing is established. The temporal patterns of BC mass concentration at Boon Lay bus interchange were found to very different from what was observed at NUS and Punggol. Multiple peaks were observed throughout the day with elevated BC concentration when the public bus service was in operation. The peak was detected when the first bus started to operate from the bus interchange at about 6am in the morning. Subsequently, with more buses in operation on road, BC concentration remained high throughout the operating hours from 6am to 12-midnight. The appearance of peaks as shown in Figure 5.3 indicates that the Aethalometer™ actually intermediately detected freshly emitted BC from the buses that randomly passed by the sampling point. Average BC mass concentrations at the three sampling locations are summarized in Table 5-3.

Table 5-3 Real times average BC mass concentration measured by Aethalometer™ at NUS, Punggol and Boon Lay bus interchange.

Locations	BC mass concentration (ng/m^3)		
	Minimum	Maximum	Mean ± σ
NUS FoE air quality monitoring station	952	11309	3210±1775
Punggol multi-storey car park rooftop	865	16074	2668±1410
Boon Lay bus interchange	1769	45378	11622±6838

σ = standard deviation

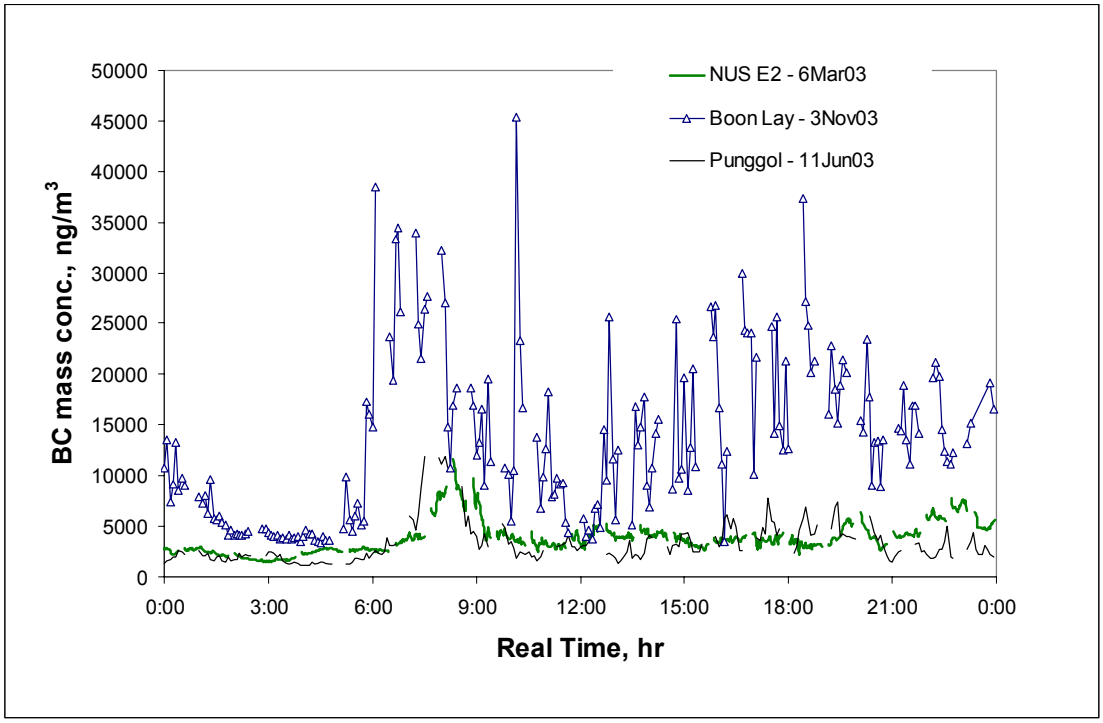

Figure 5.3 Black carbon (absorbing IR-880 nm wavelength) mass concentration diurnal emission profile comparison at NUS, Boon Lay bus interchange and Punggol.

During peak hours (0600-2400), BC concentration at the bus interchange was over 10 times higher than the background concentrations measured at NUS and Punggol. During off-peak hours (0000-0600), the BC mass loading was about 2 times that measured at an urban background location although it is much lower compared to the peak hour concentrations. This clearly indicates that heavy-duty diesel buses are likely to be the main contributor of the BC detected at the bus interchange. Inevitably, there was probably a very high proportion of fine and ultrafine particles at the bus interchange as most BC are less than 1 μm in diameter, which contributed very minimal mass in relation to the TSP mass. Therefore, PM mass measuring instruments such as MOUDI™ and MiniVol® are not useful for demonstrating the existence of the ultrafine particles in the bus interchange.

5.2 Number Concentration

5.2.1 Background

From a regulatory point of view, the ambient PM standards are regulated in terms of PM mass concentration. Although it is convenient for regulatory purposes, the mass concentration measurement is only one of the many methods to assess PM emissions. As the research community begins to recognize the impact of particle size and composition on human health, the particle number concentration has become another subject of active research with considerable interest. More than 90% of the particles emitted from diesel engines are nanoparticles (d_a < 50 nm) in the nucleation mode although they only contribute to 1 – 20% of the total particle mass (Kittelson, 1998). Molnar et al. (2002) studied the roadside measurement of fine and ultra fine particles at a major road north of Gothenburg in June 2000 and found that $PM_{2.5}$ and the mass of accumulation mode particles do not sufficiently represent ultrafine particles.

To date, no study has been conducted to measure the number concentration of particles and their size distribution in a bus interchange in order to assess the exposure of commuters to particulate pollution derived from diesel-powered buses. Furthermore, as discussed in a previous section, gravimetric mass measuring instruments do not reflect the actual presence of particles, especially those smaller than 100 nm. As a result, this study is important to determine the concentration of tiny particles that the general public is exposed to.

A series of particle counting instruments were used to measure the PM number concentration at each sampling site. Portable CPC (TSI-3007) was first used to count the total number of airborne particles larger than 10 nm up to 2 x 10^5 particles per cubic

centimetre of air. The CPC is reliable in obtaining total number concentration of airborne particles. However, it is unable to establish number size distribution, which is important in the effort to determine what particle sizes dominate the largest concentration at the sampling sites particularly in the bus interchange where mass concentration did not sufficiently represent the actual level of particulate pollution.

Consequently, particulate-counting instruments with size differentiation capability such as ELPI and SMPS were used in this study. These instruments have the internal conversion function to develop the size distribution of not only the number concentration but also the surface area and the mass concentration. ELPI equipped with an additional filter stage allows the detection of particle size ranging from as small as 8 nm to 10 μm (50% cut size) in aerodynamic diameter over a 12-stage impactor cascade.

ELPI measures electrical current, which is internally calibrated to show the correct number concentration. As in other similar instruments, the number distribution results are converted into mass results by assuming some physical properties of the sample aerosol. However, some uncertainties arise regarding estimated mass concentration derived from the current measurement. According to Dekati Limited, the manufacturer of ELPI in Finland, the mass in the upper stages of the ELPI can be overestimated if there are a lot of particles below the lowest stage cut-off diameter. The phenomenon is probably caused by diffusion of particles from the lowest stage cut-off diameter to the upper stages. On a gravimetric impactor, this is not a significant problem as the mass of these diffused particles is negligible compared to the actual impacted mass. However, when the particles are detected by their electrical charges, the effect can be

significant due to high sensitivity of the charge measurement. Even a small current signal can have big influence on mass results on the upper stages. Therefore, we report no ELPI mass concentration data. This problem will have to be resolved by revisions to the analysis software and/or instrument modification. However, this has little impact on the number concentration determination of the equipment.

SMPS, on the other hand, is a complete particle sizing and counting instrument measuring airborne particles size ranging from 0.01 μm to 0.487 μm (electrical mobility diameter) over 54 channels and determining the aerosol number concentrations up to 10^7 particles per cubic centimetre of air. SMPS particle size is determined by using a well-recognized state-of–the-art scanning electro-mobility particle sizing technology. The SMPS measures the electrical mobility diameter whereas the ELPI measure the aerodynamic diameter. As a result, there is a need to convert one form of diameter to the other in order to establish a common diameter for comparison. Since the size of particles is generally described by their aerodynamic diameter which is the diameter of a 1 g/cm^3 sphere having the same gravitational settling velocity as the particle being measured, the electrical mobility diameter (d_m) was changed to the aerodynamic diameter (d_a) based on the following relationship (Shi et al., 2001):

$$d_m = d_a \left[\frac{\rho_0 C_c(d_a)}{\rho_e C_c(d_m)} \right]^{0.5} \qquad \textbf{Eq. (5)}$$

where ρ_0 is unit density, ρ_e is the effective particle density, $C_c(d) = 1 + 2.284\lambda/d + 1.116\lambda/d \exp(-0.500d/\lambda)$ is the *Cunningham slip correction* and λ is the mean free path of air which is 6.63×10^{-8} m (Perry et al., 1997). The default particle density is set at

1.2 g/cm^3 for the SMPS, typical of airborne aerosols, and this value was used in the conversion of d_m to d_a.

5.2.2 Total Particle Number Concentration

The portable CPC was first used to measure particle number concentration at all sampling locations. It measured real time particle concentration in 1-minute interval. The results are tabulated and included in Table 5-4. Average number concentration of particles measured at Boon Lay bus interchange was 5.32 x 10^4 per cm^3, over 90% higher than that measured at Punggol. A maximum count of 1.70 x 10^5 per cm^3 was detected in the bus interchange, compared to 8.87 x 10^4 per cm^3 and 8.37 x 10^4 per cm^3 that were measured in the NUS and Punggol, respectively. All peaks were detected during the day, with minimum values detected in the night hours.

Table 5-4 Particle number concentration at three sampling sites, measured by CPC (24hours).

Number Conc. [cm^{-3}]	NUS FoE Air Quality Monitoring Station	Punggol multi-storey car park rooftop	Boon Lay bus interchange [a]
Minimum	5.3 x 10^3	1.11 x 10^4	1.32 x 10^4
Maximum	8.87 x 10^4	8.37 x 10^4	1.70 x 10^5
Average	1.05 x 10^4	2.78 x 10^4	5.32 x 10^4
Std. Deviation	9.85 x 10^3	1.21 x 10^4	2.54 x 10^4

Real time particle number concentrations at NUS and Boon Lay (not at Punggol due to unavailability of the instrument) measured by ELPI for every 5 minutes interval are shown in Figure 5.4, which reveals clearly that the temporal variation in total number concentration was indicative of traffic emission at both locations. The 48-hour plot

indicates that the concentration of airborne particles within the bus interchange remained high throughout the operating hours (0600-2400). The number of particles in the air at the University campus increased significantly as the ELPI began to detect traffic emitted airborne particles when the traffic volume was steadily increasing during the morning rush hours from 0600 to 0900 in the expressway and nearby road networks. The particle concentration declined and stabilized as the traffic volume was decreased. A build up in the particle number concentration was observed again during the evening rush hours from 1700 to 2000.

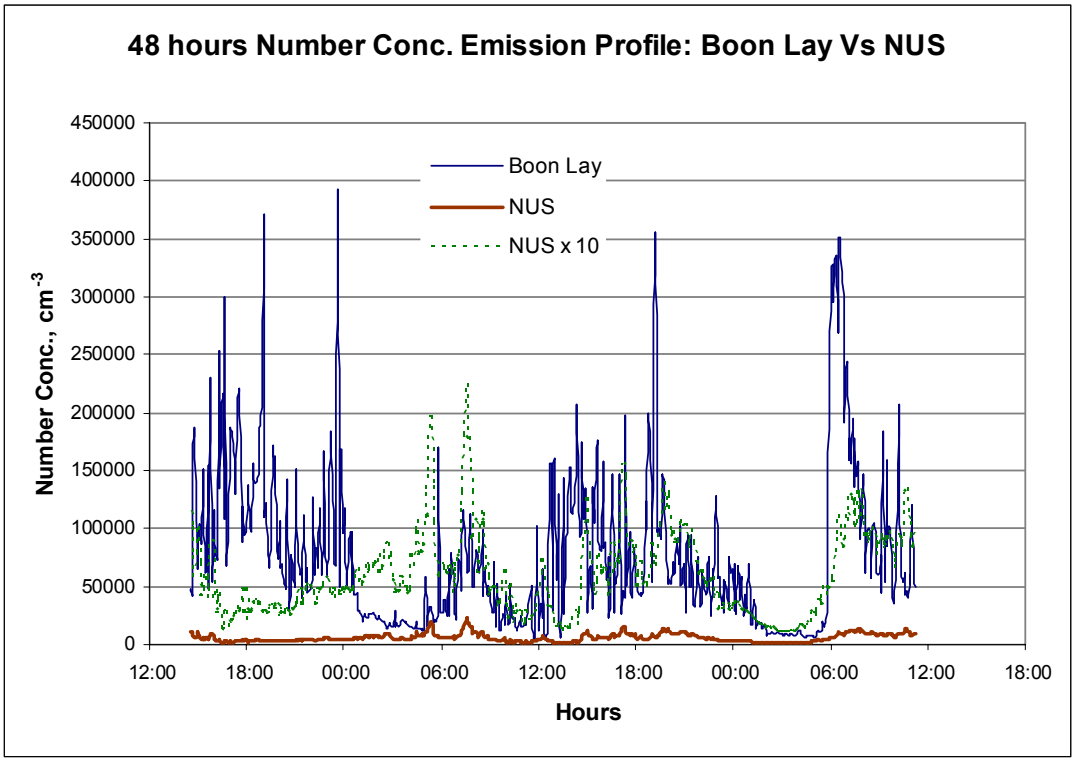

Figure 5.4 Total particle number concentration emission profile by ELPI at Boon Lay bus interchange (measured from 1st to 3rd Nov 03) and NUS FoE Air Quality Monitoring Station (measured from 7th to 8th Dec 03).

Airborne particle number concentration in the bus interchange was higher compared to the urban background concentration as shown in Figure 5.4. Although the maximum number concentration of 3.9 x 10^5 per cm^3 was recorded at the bus interchange just

before midnight, most of the peaks were detected during the day, indicative of higher risk of personal exposure as more commuters patronize the bus interchange during the day rather than at the night hours. Moreover, almost 90% of total number of airborne particles detected by ELPI at the bus interchange fell within the ultrafine particle size range (d_a < 100 nm) as indicated in Table 5-5, inline with findings by Kittelson (1998), Shi et al. (1999) and Zhu et al. (2002). This proves that airborne particles, especially ultrafine particles, exist at the bus interchange with high number concentrations.

Table 5-5 Comparison of ultrafine particles number concentration (0.008 - 0.074 µm) to total particle number concentration (0.008 - 10 µm) at the University and the bus interchange measured by ELPI.

Total Number Concentration measured by ELPI	NUS FoE Air Quality Monitoring Station	Boon Lay bus interchange
$N_{0.008\ \mu m - 0.074\ \mu m}$	3.65 x 10^3 cm^{-3}	6.23 x 10^4 cm^{-3}
$N_{0.008\ \mu m - 10\ \mu m}$	6.56 x 10^3 cm^{-3}	6.99 x 10^4 cm^{-3}
$N_{0.008\mu m-0.074\mu m} / N_{0.008\mu m-10\mu m}$	0.56	0.89

In order to identify the main source of airborne particles at the bus interchange, Aethalometer™ and ELPI were deployed concurrently. Figure 5.5 illustrates that the emission profile of black carbon correlates reasonably well with particles number emission profile at the Boon Lay bus interchange, suggesting that the local traffic diesel exhaust emission is the major airborne PM source at the bus interchange. Although ELPI measures particle size range up to 8 nm, it has a relatively low size differentiation resolution particularly at the ultrafine size range. Hence, SMPS was used to analyse the

particle size distribution focusing at the nuclei mode at Boon Lay bus interchange and NUS FoE Air Quality Monitoring Station, which will be discussed in next section.

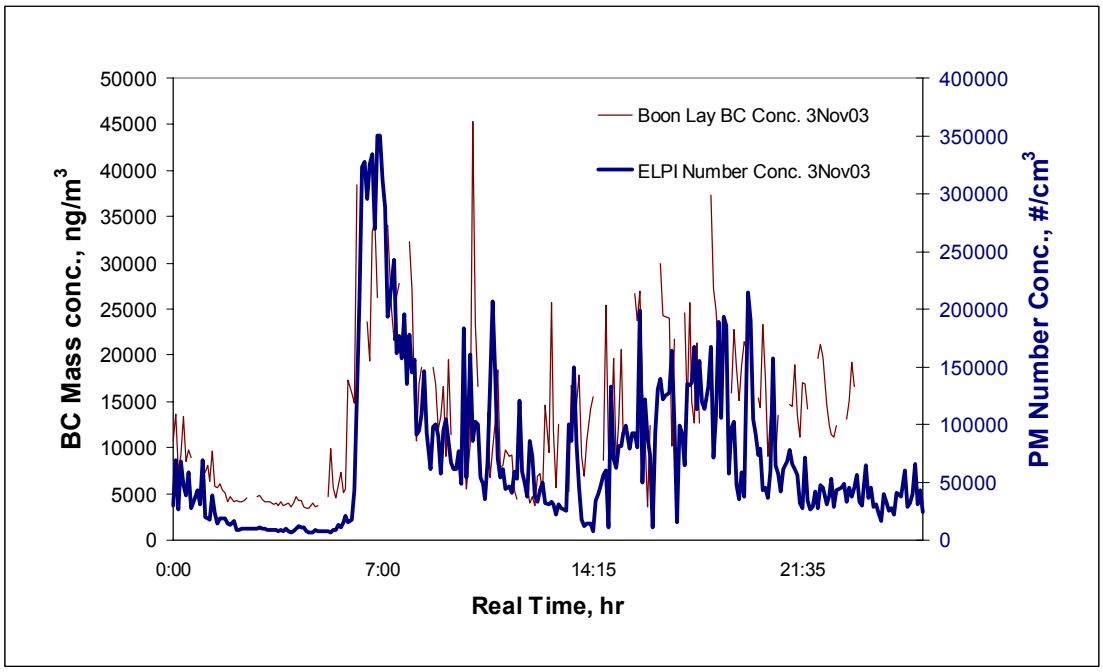

Figure 5.5 Particle number concentration and black carbon mass concentration 24-hour emission profile at Boon Lay bus interchange.

5.2.3 PM Number Size Distribution

ELPI is designed to measure number size distributions in real-time. The instrument sizes particles by their aerodynamic diameter in the range from 8 nm to 10 µm when a filter stage was used (30 nm to 10 µm without filter stage). The airborne particle size distributions of number concentration obtained at the Boon Lay bus interchange and the NUS FoE Air Quality Monitoring Station are shown in Figure 5.6 and Figure 5.7, respectively. We observed mono-modal size distribution with an extremely high number of particles in the nuclei mode of modal diameter ranging from 8 nm to 30 nm in the bus interchange, while a bimodal distribution were observed at the air quality monitoring station in NUS. Two peaks were observed here one with the nuclei modal

diameter of 8 to 30 nm and the other at the accumulation mode with a modal diameter between 0.1 to 0.2 μm.

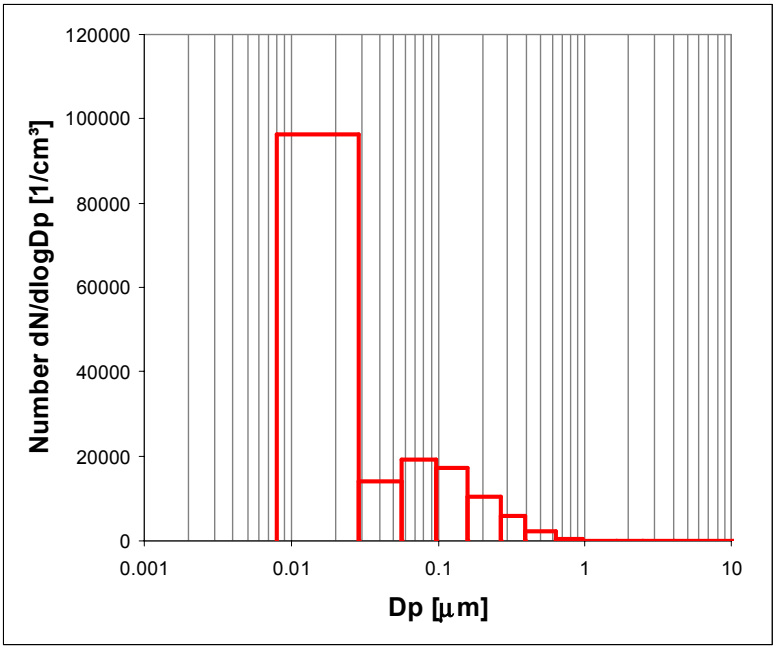

Figure 5.6 72 hours number concentration size distribution at the Boon Lay bus interchange measured by ELPI between 1st and 4th Nov 03

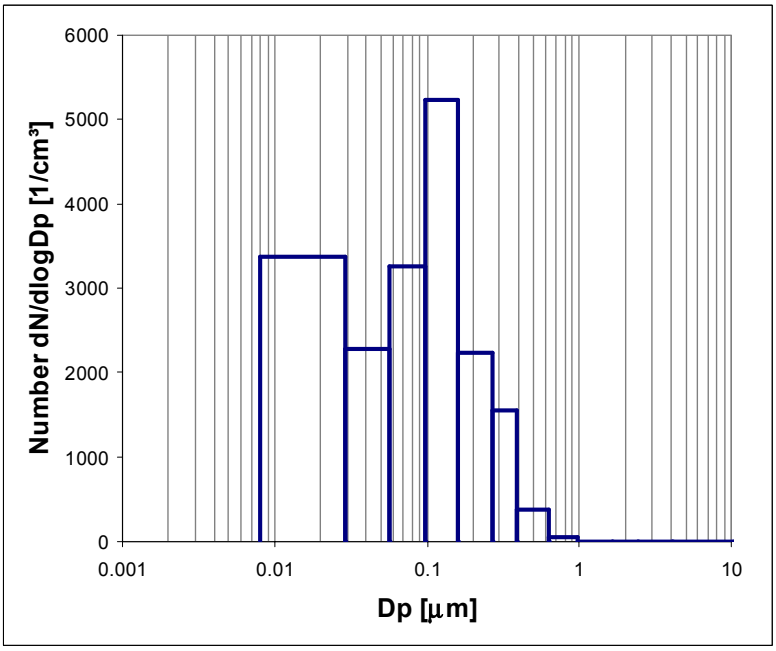

Figure 5.7 24 hours number concentration size distribution at the NUS FoE air quality monitoring station measured by ELPI from 6th to 7th Dec 03.

SMPS was deployed to study the particle number size distribution at a higher resolution within the ultrafine range. Since the public bus schedule and operation hours at the bus interchange are hardly altered, the number size distributions measured here have minimum variations. The SMPS number size distribution obtained at the bus interchange is shown in Figure 5.8. On an average, the bus interchange had a single mode number size distribution. The average peak measured by the SMPS falls in the particle size range of 20 to 30 nm, consistent with that measured by ELPI. From the plots, one could observe a series of fluctuations occurring throughout the sampling period, indicating that the SMPS was sensitive enough to pick up variations in freshly emitted particle counts as buses passed by the sampling point. Within the 15 minutes sampling time (i.e. the time interval between scans), more than 10 buses passed by the sampling point, which explains the multiple spikes that are observed in Figure 5.8.

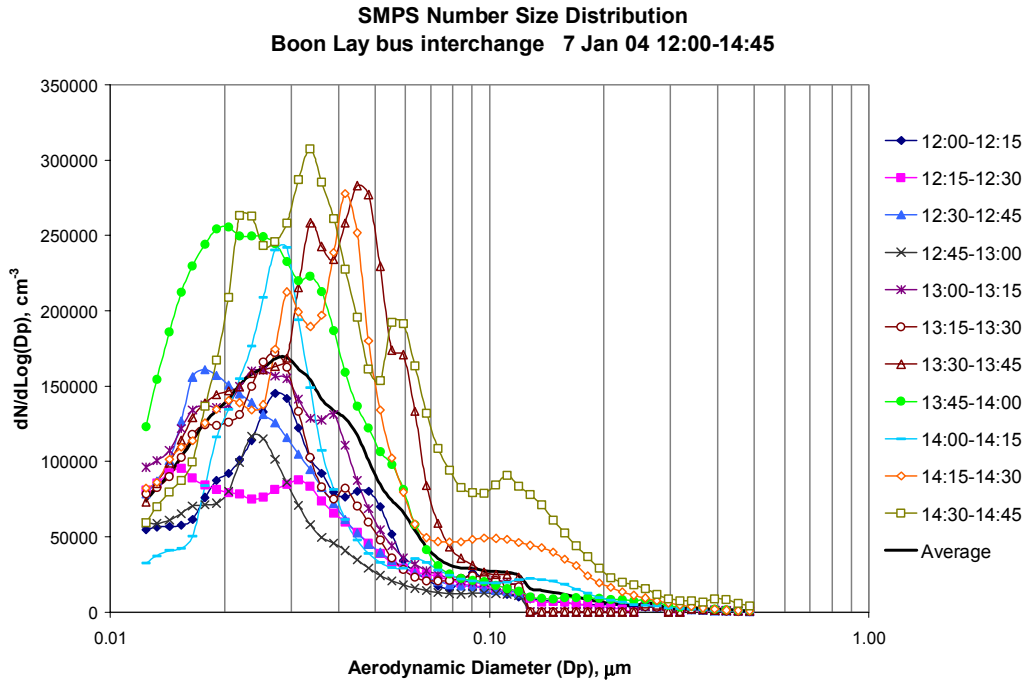

Figure 5.8 Number size distribution at the Boon Lay bus interchange measured on 7 Jan 04 from 12:00 to 14:45 with 15 minutes sampling interval.

Unlike the number size distribution profile observed in the bus interchange, SMPS measured relatively flatter and uniform size distribution in the campus except that some significant peaks were observed after a tropical rain around mid-day between 1345 and 1430. It is believed that gas-to-particle conversion was taking place right after the afternoon rains as discussed in section 2.1.2. Nucleation events (i.e. the formation of particles in the nuclei mode) are believed to have produced significant amounts of nuclei mode particles which contributed to the spikes in the number of particles particularly within 20 to 30 nm particle size range as shown in Figure 5.9.

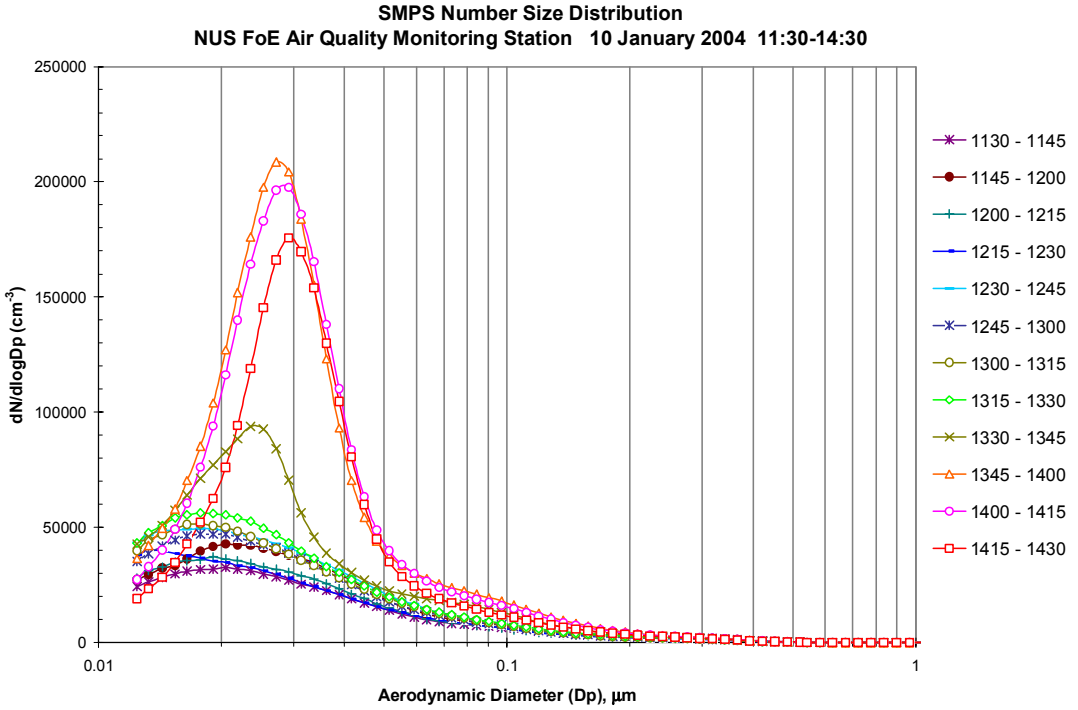

Figure 5.9 Number size distribution at NUS FoE air quality monitoring station measured on 10 Jan 04 from 11:30 to 14:30 with 15 minutes up-scan time.

5.3 Chemical Characterization

5.3.1 Background

Other than particle physical size and shape, the chemical composition of particles is also playing an important role in a series of adverse effects on human health. The influence of PM on individual's well being is very dependent on the actual exposure, which determines the doses that organs receive when an individual comes in contact with the particle with various chemical constituents (Weijers et al., 2004). The actual exposure requires detailed knowledge of the concentration variability of certain major chemical components that are known to be harmful to human health. As reported by Department of Health Committee in United Kingdom on the Medical Effects of Air Pollution, no chemical substance is of sufficient toxicity given the current levels of exposure to PM to explain the observed magnitude of health effects (Department of Health, 1995; Harrison and Yin, 2000). Therefore, it is important to establish the chemical composition of particles by determining as many chemical constituents as possible so that their potential health effects can be better assessed. However, it is difficult to rule out that the chemical composition of a particle has little effects on human health.

In this study, the chemical analysis of the $PM_{2.5}$ particles and the size-fractionated particles (from MOUDI^{TM}) collected from the sampling sites were determined to identify and quantify water-soluble ions (anion and cation) species and trace elements. The size distribution of some major ionic constituents and trace elements is also established. The correlation among ionic species and gaseous pollutants is further discussed in this section. Limited organic compounds including n-alkanes, PAHs and

nitro-PAHs were also identified and quantified from the samples collected by the Hi-Vol sampler. The risk associated with the inhalation of carcinogenic PAHs at the bus interchange was also examined.

5.3.2 Chemical Composition of $PM_{2.5}$

Water-soluble Ionic Species

In the previous section, the BC mass concentration determined at all sampling sites was presented with the results included in Table 5-3. According to Garg (2000), about 40% of the total suspended particle mass concentration collected at the NUS FoE Air Quality Monitoring Station was due to carbonaceous aerosols, approximately 10% of which was contributed by BC and the balance by organic matter (OM). In this study, BC was found to have contributed approximately 13% of the TSP mass concentration at the same site in the campus, followed by about 10% and 42% at the rooftop of the multi-storey car park at Punggol and at the Boon Lay bus interchange, respectively. TSP mass concentrations at NUS, Punggol and the Boon Lay bus interchange (location A) were 25.5 $\mu g/m^3$, 27.3 $\mu g/m^3$ and 27.5 $\mu g/m^3$, respectively.

In order to obtain a more comprehensive information about the chemical composition of PM at each sampling site, aerosol samples collected on Teflon® filters by MiniVol® were extracted and analysed for the ionic species and trace elements in the airborne particles. The average concentrations of both anion and cation species found in the airborne particles at the three sampling sites are given in Table 5-6.

Table 5-6 Average concentration of ions in $PM_{2.5}$ collected by using MiniVol® at Punggol, NUS and Boon Lay bus interchange.

Ions Species	NUS			Punggol			Boon Lay		
Anions (ng/m^3)	Min	Max	Mean±σ	Min	Max	Mean±σ	Min	Max	Mean±σ
F^-	28	67	47±27	5	50	22±16	16	183	51±53
Cl^-	144	150	147±4	172	1527	638±405	106	606	286±186
NO_2^-	39	50	44±8	6	233	54±66	22	433	86±142
NO_3^-	561	844	703±200	244	1505	678±260	211	4888	1479±1688
PO_4^{2-}	ND	ND	ND	ND	ND	ND	ND	ND	ND
SO_4^{2-}	4533	5117	4825±412	1228	4900	3640±898	961	11585	4319±3475
		Sub-total	5766±651		Sub-total	5032±1645		Sub-total	6221±5544
Cations (ng/m^3)	Min	Max	Mean±σ	Min	Max	Mean±σ	Min	Max	Mean±σ
Li^+	ND	ND	ND	ND	ND	ND	ND	ND	ND
Na^+	200	261	231±43	189	883	459±223	89	239	172±82
NH_4^+	1089	1444	1267±251	194	1661	1031±370	89	3298	1105±950
K^+	ND	ND	ND	ND	ND	ND	ND	ND	ND
Ca^{2+}	ND	ND	ND	ND	ND	ND	ND	ND	ND
Mg^{2+}	ND	ND	ND	ND	ND	ND	ND	ND	ND
	Sub-total		1498±294	Sub-total		1490±593	Sub-total		1277±1032
	Total Ions		7264±945	Total Ions		6522±2238	Total Ions		7498±6576
	PM Mass (ng/m^3)		19200	PM Mass (ng/m^3)		18800	PM Mass (ng/m^3)		46400
	Total Ions %		38%	Ions Mass %		35%	Ions Mass %		16%

ND = Not detectable; σ = standard deviation

Among the three distinctive sites, aerosols collected at the Boon Lay bus interchange contained highest concentration of water-soluble ionic species than the other two

locations. This is mainly due to the relatively high amounts of sulphate, nitrate and ammonium ions, principally contributed by the diesel engine emission within the bus interchange. The water-soluble ion species accounted for 38%, 35% and 16% of the $PM_{2.5}$ total airborne particles mass concentration at the NUS FoE Air Quality Monitoring Station, the rooftop of the Punggol multi-storey car park and the Boon Lay bus interchange, respectively.

The samples collected from the Punggol new town contained the lowest amount of ions compared to the University and the bus interchange samples. At the rooftop of the multi-storey car park at Punggol, sulphate was the most abundant ionic species available in $PM_{2.5}$ samples, contributing about 56% of the total dissolved ions mass concentration. Ammonium and nitrate were the two next abundant ions found here, each took up 16% and 10% of the total ions mass concentration, respectively.

Particulate samples collected at Punggol were found to contain a significant amount of sulphate. This was probably due to the emission of SO_2 from off-road stationery equipment such as the diesel-driven power generators and construction equipment at the construction sites around the area as many sites around the new town were still under construction at the time of sampling. Distant power plant emission and the nearby TPE freeway traffic emissions could also have contributed to the high concentration of sulphate at the residential site. The Senoko Power Plant, located approximately 15 km northwest of the sampling site, was likely to be one of the sulphate contributors detected here in Punggol. However, sea-spray could be another possible source of sulphate as the site is located close to the coast of Johor Strait. This

source is highly possible as sodium and chloride were detected here in significant proportions compared to that in NUS and Boon Lay bus interchange.

Out of the total dissolved ion concentration of $PM_{2.5}$ collected at the University, sulphate dominated 66% with the balance contributed by ammonium (17%), nitrate (10%), sodium (3%), chloride (2%), nitrite (1.5%) and fluoride (0.5%). The relatively higher contribution of sulphate at NUS compared to the other two sites is probably due to the migration of SO_2 from the distant source, the Jurong Island refinery hub, which is located approximately 10 km southwest of the university sampling site. During the transportation from the refinery emission, SO_2 gas-to-particle nucleation process could have taken place in the atmosphere especially after an afternoon rain as revealed by SMPS measurement in the campus, which was discussed in section 5.2.3. Alternatively, photochemical oxidation of SO_2 could have taken place to form sulphuric acid in the humid atmosphere. Unlike nitric acid, sulphuric acid is non-volatile and once formed it is immediately incorporated into airborne particles in the atmosphere. The sulphuric acid molecules may nucleate to form submicron secondary particles (Harrison and Yin, 2000).

Boon Lay bus interchange appears to be a site where an enormous amount of SO_2 gas is freshly emitted from the diesel buses. The ground-level SO_2 gas could have possibly overshadowed the SO_2 emitted from industrial sources, which generally remain in the upper troposphere once emitted from the smoke stacks before settling down to the ground level. Within the bus interchange, a substantial amount of freshly emitted SO_2 is believed to remain in gas phase for a longer period before being oxidized to form sulphuric acid (Harrison and Yin, 2000). This is because the oxidation rate of sulphur

dioxide is rather slow (Harrison and Yin, 2000). This explains why the sulphate concentration in the particles collected at the bus interchange was lower than that collected at the air quality monitoring station in NUS despite the fact that overall sulphur mass loading (both gas-phase SO_2 and particulate-bound SO_4^{2-}) was about 16 $\mu g/m^3$, almost triple of that in NUS. Aerosol samples collected at Boon Lay bus interchange were found to contain more nitrate than that collected at Punggol and at NUS. Nitrogen dioxide and other forms of oxides of nitrogen (NO_x) are the precursor of nitrate found in the airborne particles. These oxides are more readily oxidized in the gas-phase leading to HNO_3, which being semi-volatile is incorporated into the particulate-phase. So, it is not surprising that the nitrate concentration in the particulates sampled in the bus interchange was high as heavy-duty trucks and buses are known as the major contributors of NO_x among the vehicles on-road (Schwela and Zali, 1999).

Sulphate and nitrate were the two most abundant ions found in the particles, followed by ammonium in this study. Other ionic species including chloride, nitrite, fluoride and sodium were also detected at a lower concentration at all locations. Overall, anions outweigh cations by over 2/3 of the total ion contents in $PM_{2.5}$ particulate samples collected at all sites. Sulphate was the most abundant ionic species, which had contributed as high as 66%, 56% and 58% of the total dissolved ion contents in $PM_{2.5}$ aerosol samples collected at the University, the rooftop of the multi-storey car park and the bus interchange, respectively. Nitrate was the second most commonly available ionic species at all sites. It contributed about 10% of the total ions measured at Punggol new town and at NUS, but about 20% of the total ions or approximately 1.5 $\mu g/m^3$ of nitrate was found in $PM_{2.5}$ aerosols collected at the bus interchange.

Sulphate and nitrate are predominantly derived from the oxidation of sulphur dioxide (SO_2) and nitrogen dioxide (NO_2) in the atmosphere (Harrison and Yin, 2000). Sulphur dioxide and nitrogen dioxide are some of the most abundant gaseous pollutants to be found in refineries and power plant emission. Diesel-powered vehicles are responsible for the emission of urban sulphur dioxide and nitrogen dioxide in Singapore (Chin, 1996). Nitric acid is formed when nitrogen dioxide is oxidized in the atmosphere in a much faster rate than SO_2. Nitric acid is in vapour form in the atmosphere. Nitric acid vapour may condense into airborne particles, which cause the particles to be acidic. However, the particle may loss its acidity via displacement of hydrochloric acid from sea-salt to form sodium nitrate or by ammonia neutralization to form ammonium nitrate (Harrison and Yin, 2000).

In addition to anthropogenic emission sources, sea-spray is another major contributor to atmospheric sulphate (non-sea salt sulphate and methanesulphonate) via the formation of gaseous SO_2, H_2SO_4 and methanesulphonic acid by the oxidation of DMS (Dimethylsulphide) emitted from sea water (Cheng et al., 1999; Zhang et al., 2000; Brasseur et al., 2003). Changes in the regional climate with the increased frequency of forest fires in the region have also contributed to sulphur burden in the region (Zhang, 2001), which become worse when a thermal inversion develops (i.e. limited dispersion of air). Sea-sprayed particles which can be detected almost everywhere around Singapore are also believed to be the major source of sodium and chloride in the atmospheric particles measured in this study.

Among the six cations analysed, ammonium and sodium were the two species readily available at all locations. Other cation species such as lithium, potassium, calcium and magnesium were rather very low or below detection limits, hence no values are reported in this study. These positive ionic species are commonly found in wind-blown dust, which was ultimately removed by the MiniVol® 2.5 μm cut size impactor during sampling as most of the dust particles are in coarse size range.

Ammonium was the most abundant cation detected at the three sampling sites. The IC analysis revealed that particulates collected from the three sampling sites contained similar concentration of ammonium ranging between 1031 ng/m^3 and 1267 ng/m^3 on average. Atmospheric ammonia is readily available in urban atmospheres, which can progressively react or condense on an acidic particle surface of anthropogenic origin. The neutralization process of ammonia gas with sulphuric acid, nitric acid and hydrochloric acid forms ammonium salts (ammonium sulphate, ammonium nitrate and ammonium chloride). The stability and preference of the ammonium salts is highly dependent on local ambient temperature and relative humidity. In this study, average ammonium concentration was 1.3 μg/m^3 in NUS, consistent with 1.24 μg/m^3 of that measured by Zhang (2001) at the same location, and marginally higher than that measured at Punggol and at the Boon Lay bus interchange with a concentration of 1 μg/m^3 and 1.1 μg/m^3, respectively. There was an immediate source of ammonia (sewage pipe vent) within the close proximity of the sampling site in the university, which should explain the higher ammonium concentration in the NUS campus.

In order to identify the possible sources of major ionic species at the bus interchange and the campus, ion analysis was conducted on particles collected by size-proportionate

PM sampler MOUDI™. Particles in various cut sizes were collected on the Teflon® filters at each stage and analysed for ion concentration. This will help us to determine the sources of each ion, which could have originated from local traffic emission, distant industrial emission or any other human activities. The results will be further discussed in a later section.

Trace Elements

Some of the trace elements such as Pb and Cd are chemically toxic to humans (Goyer and Cherian, 1995). A microwave digestion method followed by inductively coupled plasma mass spectrometric (ICP-MS) analysis was performed to determine trace metal concentrations in atmospheric aerosol samples collected in this study, which include Al, As, Cd, Co, Cr, Cu, Fe, Mn, Ni, Pb, Sb, Ti, V and Zn. The statistical data related to the measurement of trace elements at NUS, Punggol and the Boon Lay bus interchange throughout the sampling period are summarized and shown in Table 5-7.

$PM_{2.5}$ samples collected from the bus interchange contained 2.23 $\mu g/m^3$ of trace elements on average or about 5% of the total $PM_{2.5}$ mass concentration measured at the site, which is twice the amount measured at the University and Punggol. Average mass loading of trace elements at NUS and Punggol was 0.83 $\mu g/m^3$ and 0.93 $\mu g/m^3$ respectively, each representing 4% and 5% of the total $PM_{2.5}$ mass loading at each site.

Table 5-7 Mean concentration of trace elements in $PM_{2.5}$ collected by using MiniVol® at Punggol, NUS and Boon Lay bus interchange.

	NUS (ngm^{-3})			Punggol (ngm^{-3})			Boon Lay (ngm^{-3})		
	Min	Max	Mean±σ	Min	Max	Mean±σ	Min	Max	Mean±σ
Al	30.8	55.6	43.2±17.6	15.3	216.1	104.9±56.3	59.4	1024.2	153.6±63.7
Co	0.8	0.9	0.9±0.1	0.1	5.8	0.8±1.3	0.5	3.1	0.7±0.9
Cr	40.6	43.5	42.0±2.0	3.6	101.9	48.4±33.7	14.8	85.4	43.2±25.3
Cu	185.6	221.6	203.6±25.4	21.5	167.1	68.5±47.0	30.0	1893.1	649.2±702.9
Fe	125.9	198.1	162.0±51.1	59.0	312.7	151.4±73.6	87.4	569.9	310.4±167.6
Mn	2.6	7.4	5.0±3.3	1.5	20.4	7.2±6.2	0.3	56.4	27.5±19.5
Pb	17.0	44.2	30.6±19.2	0.4	51.7	18.3±11.7	28.9	151.5	68.2±46.6
Zn	42.2	79.7	61.0±26.5	8.2	415.8	165.9±108.1	42.9	900.7	564.5±282.5
Cd	1.6	1.9	1.8±0.3	0.1	1.7	0.1±0.4	0.1	1.1	0.4±0.4
Ni	38.3	41.3	39.8±2.1	18.4	47.9	28.1±5.8	25.8	44.0	31.7±5.6
Ti	159.9	298.8	229.3±98.2	79.7	636.3	303.6±173.6	42.9	808.1	333.5±251.2
V	8.1	14.2	11.2±4.3	1.3	17.7	6.3±4.7	11.3	28.2	19.3±5.2
Sb	NA	NA	NA	1.1	41.5	20.9±11.1	9.6	37.4	23.6±9.4
As	NA	NA	NA	0.1	0.6	0.2±0.2	0.1	0.6	0.4±0.3
		Sub-total	830.4±250.1		Sub-total	924.6±533.7		Sub-total	2226.2±1581.1
		PM Mass (ngm^{-3})	19200		PM Mass (ngm^{-3})	18800		PM Mass (ngm^{-3})	46400
		Trace Element Mass %	4%		Trace Element Mass %	5%		Trace Element Mass %	5%

NA = Not Available; σ = standard deviation

At Boon Lay bus interchange, the concentration of Cu was 0.65 $\mu g/m^3$ on average, approximately 9 times higher than the Cu concentration detected at Punggol. Zn of anthropogenic origin contributed about 25% or 0.56 $\mu g/m^3$ of the total trace element concentration detected in the bus interchange, about 3.4 and 9 times higher than that obtained at Punggol and NUS, respectively. Lead was measured with a mean concentration of 0.068 $\mu g/m^3$, 0.018 $\mu g/m^3$ and 0.031 $\mu g/m^3$ in the bus interchange,

Punggol and NUS respectively, well below the 3-month average USEPA primary ambient air quality standards of 1.5 μg/m^3 (NEA, 2003). Unleaded petrol was introduced in Singapore in January 1991 and leaded petrol was phased out on 1 July 1998 (NEA, 2003), hence limiting the possible atmospheric sources of Pb to industrial origin such as incineration or smelting plant. Our study shows that the concentrations of Cu, Zn and Pb at the bus interchange were significantly higher than that measured elsewhere, showing strong correlations indicative of a traffic source contribution as reported by Harrison et al. (2003). Concentrations of Cu, Zn, Fe, Ti, Al and Pb were among the highest in the bus interchange whilst low concentrations of Mn, Cd, Ni, V, Sb and As were also detected in this study. Due to their low concentrations, the impacts of Mn, Cd, Ni, V, Sb and As are of less concern, hence they are not discussed here.

Inert titanium (Ti) was found to be one of the most abundant trace metals at all three sampling points. A higher concentration of Ti was recorded at the bus interchange with an average of 0.33 μg/m^3, marginally higher than that in Punggol with a mean concentration of 0.23 μg/m^3. Titanium has historically maintained the reputation of being an inert and relatively biocompatible metal. However, there was scientific evidence that titanium might cause harmful reactions after travelling through the circulatory or lymphatic systems. These by-products of Ti could cause reactions in the blood, fibrotic tissue, and in the osteogenic cells (Wang et al., 2003; Bermudez et al., 2002; Rehn et al., 2003). Watanabe (2002) placed macrophages in both a fibrous environment of titanium oxide and particulate environment. The fibrous TiO_2 macrophages exhibited an increase in LDH (lactate dehydrogenase) release, causing a significant change in cellular vacuolar and cell surface damage. LDH is most often

measured to evaluate the presence of tissue damage. The enzyme LDH can be found in many body tissues, especially the heart, liver, kidney, skeletal muscle, brain, blood cells, and lungs (MedlinePlus, 2004). Another conclusion of the study was that titanium oxide toxicity was dependant on the shape and size of the material. These results were in accord with the work done by Kumazawa (2002) who showed that cytotoxicity was dependant on the titanium particle size, and that the smaller the size, the more toxic it is (USEPA, 2002). As a result, the size distribution analysis of Ti was initiated and will be discussed in the next section.

Aluminium (Al) and iron (Fe) are trace metals largely found in earth crust (Harrison et al., 2003). Al was accumulated with an average of 0.15 $\mu g/m^3$ in the bus interchange, 2.5 times higher than the Al mass loading measured at Punggol. Trace Fe concentration on the other hand was double the Al concentration measured in the bus interchange with a mean concentration of 0.31 $\mu g/m^3$, almost double the Fe concentration measured at Punggol. The higher concentrations of Al and Fe at the bus interchange were probably due to the resuspension of road dust. Manganese (Mn) and vanadium (V) mass concentrations were also found larger at the bus interchange than those measured at NUS and Punggol. In summary, mass concentration of Al, Cu, Fe, Mn, Pb, Zn, Ti and V shows strong correlation with anthropogenic combustion emission and/or resuspension of road dust due to on-road traffic. In order to determine and verify the possible origin of the trace elements at the bus interchange and the University, PM samples were collected on Teflon® filters in the 10-stage MOUDI™ cascade impactor. The size-apportioned samples were then analysed for the size distribution of Al, Cu, Fe, Mn, Pb, Zn, Ti and V, which will be discussed in section 5.3.3.

n-Alkanes

Particulate organic carbon (OC) is produced from both human and natural activities (Rogge et al., 1993a, 1998). Combustion of fossil fuels, wood and agricultural debris are typical sources of OC i.e. n-alkanes. OC contributes not only to visibility reduction but also may contain compounds, which are detrimental to human health (Cadle and Mulawa, 1990). In California, samples collected from 10 different sites were analysed and found to contain the total carbon constituting 40 – 60% and 25 – 35% of the $PM_{2.5}$ and PM_{10} masses respectively (Chow et al., 1996). In Hong Kong, automotive combustion sources were estimated to have contributed 39 – 63% of OC in the TSP samples (Zheng et al., 1997). Garg (2000) studied the concentrations of BC and PAHs in Singapore but no data on n-alkanes was reported. This is the first study in Singapore that attempts to explore and verify the traffic originated PM chemical composition inclusive of organic compounds in order to gain a better understanding about the potential health and environmental implications particularly of diesel emitted aerosols.

The concentration of n-alkanes ranging from C_{15} to C_{35} was analysed from the TSP samples collected from the Boon Lay bus interchange. The results are listed in Table 5-8. The concentration of n-alkanes at the bus interchange ranged between 22.19 ng/m^3 and 84.53 ng/m^3 with the mean concentration of 44.55 ng/m^3, almost two times that detected on the rooftop of a 25 m tall residential building on the campus of Hong Kong University of Science and Technology which had the concentrations of total n-alkanes ranging between 6.5 and 41.1 ng/m^3 with an average of 23.5 ng/m^3 (Zheng et al., 2000). During the 4-day sampling at the bus interchange, meteorological conditions played an important role in determining the mass of organic compounds recovered from the

particles at the site. On the first day of sampling (11th December 2003), ambient temperature was at its peak temperature of 31 ^{o}C, but declined to just below 25 ^{o}C when tropical rain washed out the region at about 4pm and continued to rain throughout the night hours as shown in Figure A.1 in Appendix A. The air was stagnant when the rain began and a lower ambient temperature was recorded. Poor dispersion of air, a low ambient temperature with higher relative humidity are believed to be the major factors that resulted in higher total n-alkanes concentration of 84.53 ng/m^3 in the TSP sample compared to those recorded at the later dates. Lower ambient temperature, stronger wind dispersion, and a short rain on the following day (12th December 2003) were observed when the TSP mass loading and n-alkanes concentration significantly declined to 21.9 μg/m^3 and 22.19 ng/m^3 respectively, indicative of possible meteorological disturbance.

Air sampling was resumed on 9th and 10th January 2004 when the weather was hotter and drier with no rains recorded, as illustrated in Figure A.2 of Appendix A which indicates that a very mild north-easterly wind in the morning hours of the 9th day of January. The wind began to gain momentum after mid-noon, causing a minor stir of the ambient air. However, the ambient temperature was higher compared to that was recorded on 11th December 2003. Lighter molecular weight organic compounds tend to evaporate or sublime at higher ambient temperature. As a result, a lower mass ratio of n-alkanes per microgram of TSP was recorded. The dry weather persisted through the second day with an ambient temperature hitting 32 ^{o}C at about 2 pm, leading to even lower n-alkanes mass loading as more OC tend to evaporate and remain in the gas-phase.

Table 5-8 n-Alkanes identified and quantified in 24 hours TSP samples collected at Boon Lay bus interchange by Hi-Volume air sampler HVP-3800AFC/230.

n-Alkanes (ngm^{-3})	11Dec03 [a]	12Dec03 [b]	9Jan04	10Jan04	Mean	σ
C15	0.13	0.05	0.06	0.02	0.07	0.05
C16	1.50	0.00	0.14	0.04	0.42	0.72
C17	0.36	0.30	0.26	0.03	0.24	0.15
pristane	0.39	0.34	0.13	ND	0.29	0.14
C18	1.24	0.16	0.48	0.01	0.47	0.55
phytane	0.35	0.26	0.30	0.02	0.23	0.15
C19	0.53	0.40	0.52	0.02	0.37	0.24
C20	0.87	0.30	0.48	0.01	0.41	0.36
C21	0.93	0.44	0.78	0.20	0.59	0.33
C22	2.03	0.68	1.38	0.55	1.16	0.68
C23	3.99	0.93	2.79	1.23	2.24	1.43
C24	7.47	1.52	4.88	2.14	4.00	2.73
C25	10.67	2.08	6.53	2.95	5.56	3.92
C26	11.97	3.03	6.75	3.27	6.26	4.17
C27	11.81	2.92	6.86	3.35	6.23	4.11
C28	10.51	2.28	4.79	2.56	5.03	3.82
C29	6.61	1.80	3.86	2.08	3.59	2.21
C30	3.38	1.09	1.95	1.18	1.90	1.06
C31	4.05	1.54	2.78	1.43	2.45	1.23
C32	1.56	0.77	0.96	0.64	0.98	0.41
C33	2.07	0.83	1.10	0.75	1.19	0.61
C34	0.93	0.20	0.40	0.17	0.43	0.35
C35	1.19	0.28	0.45	0.19	0.53	0.46
Σ *n-Alkanes* (ngm^{-3})	84.53	22.19	48.64	22.85	44.55	29.36
CPI [c]	1.02	1.16	1.17	1.16	1.13	0.07
TSP (μgm^{-3})	34.5	21.9	35.4	34.9	31.7	6.5
n-alkanes/TSP	0.25%	0.10%	0.14%	0.07%	0.14%	0.08%

σ = standard deviation;
[a] sunny in the day but rained after 4pm, lowering ambient temperature;
[b] strong wind dispersion, with minor rain in late afternoon at lower ambient temperature;
[c] CPI: Carbon Preference Index of whole range n-alkanes, $CPI=\Sigma(C_{15}\sim C_{35})/\Sigma(C_{16}\sim C_{34})$ (Bi et al., 2002).

Trace amounts of pristane and phytane were detected, indicating the input of petroleum fuel at the site (Simoneit, 1984). From the bus interchange data, it is evident that the most abundant congeners fall within the C_{24}–C_{31} range, different from the C_{21}–C_{25} category that was observed from a gasoline car exhaust (Yassaa et al., 2001b). On the other hand, the *Carbon Preference Index* (CPI) values of the whole range n-alkanes detected at the bus interchange ranged from 1.02 to 1.17, indicating that diesel residues and fossil fuel combustion were the significant source of n-alkanes at the majority diesel exhaust emission hot-spot (Simoneit et al., 1991; Zheng et al., 2000). The CPI of n-alkane fractions is usually calculated with the objective of discriminating between biogenic (CPI values greater than 3) and fossil fuel combustion (CPI values near unity) contributions (Simoneit et al., 1991; Bi et al., 2002; Rogge et al., 1993b; Fang et al., 1999; Zheng et al., 2000).

PAHs

The evaluation of PAHs in airborne respirable particles is important due to its potential health risk associated with carcinogenic and mutagenic effects (Chuang et al., 1995; Offenberg and Baker, 1999; Yassaa et al., 2001a, 2001b). Most of the PAHs are the product of anthropogenic combustion in relation to motor vehicles, with traffic contributing an estimated 80% of ambient concentrations (Nielsen, 1996). Thirteen species of PAHs and two species of nitro-PAHs were evaluated from the samples collected at the Boon Lay bus interchange. For each collected sample, the sum of the concentration of each PAH species was regarded as the total PAHs concentration, as shown in Table 5-9.

Atmospheric PAHs are volatile and semi-volatile species which may be incorporated in airborne particulate or exist in gas phase (Bidleman et al., 1986; Pankow, 1987; Masclet, et al., 1987). The distribution of PAHs between the two phases depends on ambient temperature, humidity, species of PAHs, concentration of PAHs and PM availability in the atmosphere as well as their residence time in the air (Garg, 2000). Temperature is the most influential factor (Pankow, 1987) as higher ambient temperature induces more volatilisation of PAHs from particulate to gas phase. A study in Hong Kong also revealed that more semi-volatile PAHs were in vapour phase during in the summer due to higher ambient temperature (Zheng et al., 2000; Zheng and Fang, 2000). Garg (2000) reported an average concentration of the total particulate phase and vapour phase PAHs ranged from 1.1 to 6.9 ng/m^3 (mean: 2.83 ng/m^3) and 5.2 to 24.6 ng/m^3 (mean: 12.19 ng/m^3) respectively. Singapore is a tropical country with a daily average ambient temperature of around 30 ^{o}C, and this atmospheric condition may explain the higher concentration of PAHs in vapour phase. Garg (2000) also reported that low molecular weight PAHs tend to be more concentrated in vapour phase while higher molecular weight ones are found to be particulate-bound (Zheng et al., 2000).

Mean concentrations of total particulate-bound PAHs (ΣPAHs+Σnitro-PAHs) detected at the bus interchange were 5.17 ng/m^3 about 2 times higher than what Garg (2000) had measured at the FoE Air Quality Monitoring Station. The most abundant species among the 15 PAHs species measured here in the bus interchange were chrysene, benzo(e)pyrene, indene(1,2,3-CD)pyrene and benzo(g,h,i)perylene with mean concentration of 0.71 ng/m^3, 0.75 ng/m^3, 1.01 ng/m^3 and 0.97 ng/m^3, respectively. The association of benzo(g.h.i)perylene with vehicle exhaust has long been established

(Baek et al., 1991) and a reasonably strong correlation of benzo(g.h.i)perylene with total PAH concentration was established in this study as illustrated in Figure 5.10. This correlation suggests that diesel bus emission is the dominant source of the particulate–bound PAHs measured in the bus interchange.

Table 5-9 PAHs and nitro-PAHs mass concentration in 24 hours TSP samples collected at Boon Lay bus interchange by Hi-Volume air sampler HVP-3800AFC/230.

PAHs (ngm^{-3})	MW [a]	11Dec03	12Dec03	9Jan04	10Jan04	Mean	σ
Phenanthrene	178	0.04	0.03	0.06	0.01	0.03	0.02
Anthracene	178	0.00	0.00	0.06	0.00	0.02	0.03
Fluoranthene	202	0.14	0.07	0.09	0.02	0.08	0.05
Pyrene	202	0.27	0.18	0.37	0.14	0.24	0.11
Benzo(a)anthracene	228	0.66	0.41	0.50	0.06	0.41	0.25
Chrysene	228	1.01	1.06	0.65	0.11	0.71	0.44
Benzo(j)fluoranthene	252	0.40	0.23	0.22	0.14	0.25	0.11
Benzo(k)fluoranthene	252	0.22	0.15	0.29	0.11	0.19	0.08
Benzo(e) pyrene	252	1.42	0.65	0.62	0.29	0.75	0.48
Benzo(a) pyrene	252	0.83	0.63	0.31	0.17	0.49	0.30
Indene(1,2,3-CD) pyrene	276	1.88	1.32	0.56	0.27	1.01	0.73
Dibenzo(a,h)anthracene	278	0.00	0.00	0.00	0.00	0.00	0.00
Benzo(g,h,i)perylene	276	2.05	0.95	0.56	0.33	0.97	0.76
Σ PAHs		8.92	5.68	4.30	1.65	5.15	3.03
Nitro-PAHs (ngm^{-3})	MW [b]	11Dec03	12Dec03	9Jan04	10Jan04	Mean	σ
3-nitrofluoranthene	247	0.03	ND	0.01	0.01	0.02	0.01
1-nitropyrene	247	0.03	ND	ND	0.01	0.02	0.01
Σ nitro-PAHs		0.06	ND	0.01	0.02	0.04	0.02
Total PAHs		8.98	5.68	4.31	1.67	5.19	3.05

ND = Not Detectable;
σ = standard deviation;
[a] Source: Garg (2000);
[b] Source: http://www.irmm.jrc.be/rm/sds/sds-bcr-305.pdf [last accessed: 8th August 2004];

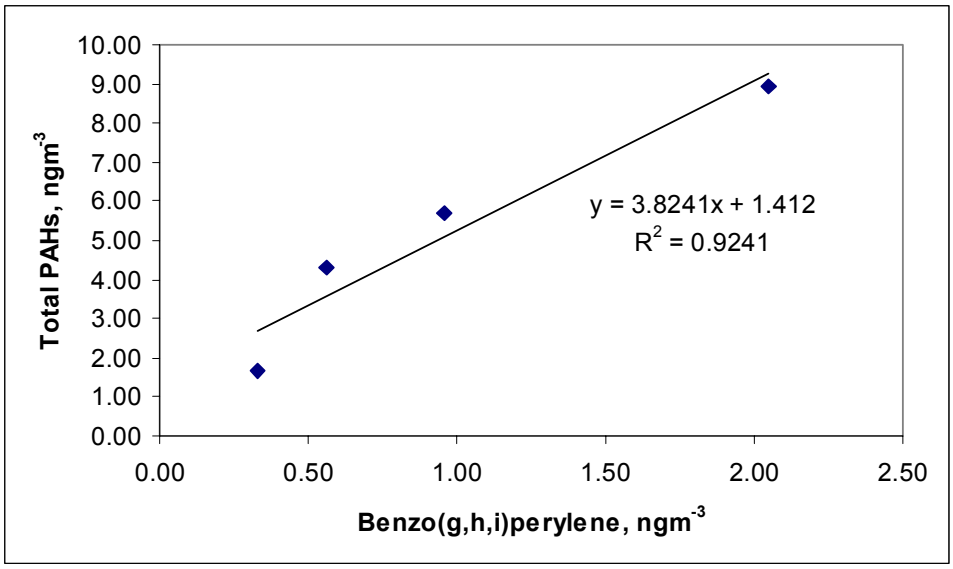

Figure 5.10 Correlation between total PAHs and Benzo(g,h,i)perylene.

From previous study in NUS FoE Air Quality Monitoring Station conducted by Garg (2000), particulate-bound benzo(a)pyrene mean concentration was 0.08 ng/m^3, about one sixth of the value (0.49 ng/m^3) detected at the Boon Lay bus interchange. A strong correlation of benzo(a)pyrene concentration with the total PAHs concentration at the bus interchange (see Figure 5.11) reveals that the diesel bus emission is the key source of benzo(a)pyrene at the site. Benzo(a)pyrene is the most extensively measured PAHs which has the *Toxic Equivalency Factor* (TEF) of 1. TEF is a parameter used in risk assessment on exposure to PAHs (Nisbet and LaGoy, 1992). The risk associated with the inhalation of carcinogenic PAHs is estimated by comparing the carcinogenicity of each PAH species to that of benzo(a)pyrene. The TEF established by Nisbet and LaGoy (1992) was used in this study to determine the carcinogenic potential of the PAH congeners in the bus interchange. Comparative figures of PAHs potential risk level were established between the figures determined by Garg (2000) at NUS and that of this study at Boon Lay bus interchange. As shown in Table 5-10, the toxicity exposure risk at the bus interchange was nearly 4 times higher than that evaluated at the

University although the absolute mean concentration of total PAHs at the bus interchange was only 2.2 times of that in the University. Higher risk of toxicity exposure observed at the bus interchange was mainly due to the increase of higher molecular weight PAHs in the TSP samples at the bus interchange, particularly the concentration of B(a)P which was 6 times larger than that observed in the University campus. As a result, B(a)P is considered the most important surrogate compound of PAHs mixture in the ambient air at the bus interchange with highest carcinogenicity. Although benzo(g,h,i)perylene was a significant fraction of the total PAHs absolute concentration, but its role in the carcinogenicity of the PAHs mixture was less due to its low TEF value. In contrast, dibenzo(a,h)anthracene may appear in minor fraction of the total PAHs mixture, but its TEF is high hence is considered as an important component in determining the PAH's carcinogenicity.

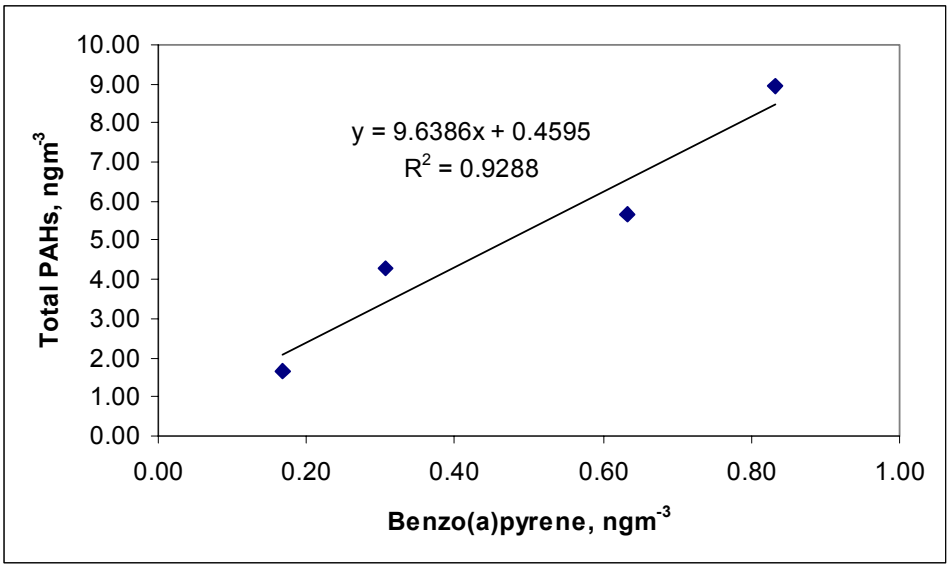

Figure 5.11 Correlation between total PAH and Benzo(a)pyrene.

Table 5-10 B(a)P equivalent concentrations of individual PAHs concentrations: risk assessment for PAHs exposure at NUS and Boon Lay bus interchange.

PAHs	TEF[a]	Mean Concentration ng/m^3		ng B(a)P$_{eq}$/m^3	
		NUS[d]	Boon Lay Bus Interchange	NUS[d]	Boon Lay Bus Interchange
Phenanthrene	0.001	0.14	0.03	0.00014	0.00003
Anthracene	0.01	0.02	0.02	0.0002	0.0002
Fluoranthene	0.001	0.16	0.08	0.00016	0.00008
Pyrene	0.001	0.16	0.24	0.00016	0.00024
Benzo(a)anthracene	0.1	0.08	0.41	0.008	0.041
Chrysene	0.01	0.22	0.71	0.0022	0.0071
Benzo(j)fluoranthene	0.1[b]	-	0.25	-	0.025
Benzo(k)fluoranthene	0.1	0.19	0.19	0.019	0.019
Benzo(e)pyrene	0.01[b]	-	0.75	-	0.0075
Benzo(a)pyrene	1	0.08	0.49	0.08	0.49
Indene(1,2,3-CD) pyrene	0.1	0.52	1.01	0.052	0.101
Dibenzo(a,h)anthracene	1	0.01	0.00	0.01	0
Benzo(g,h,i)perylene	0.01	0.78	0.97	0.0078	0.0097
3-nitrofluoranthene	-[c]	-	0.02	-	-
1-nitropyrene	0.1[b]	-	0.02	-	0.002
Total		2.36	5.19	0.17966	0.70285

[a] Nisbet and LaGoy, 1992;
[b] Source: http://www.city.toronto.on.ca/health/pdf/cr_appendix_b_pah.pdf [accessed 9 August 2004];
[c] No TEF has been suggested;
[d] Garg, 2000.

A mean concentration of 0.04 ng/m^3 of total nitro-PAHs (3-nitrofluoranthene and 1-nitropyrene) was detected at the Boon Lay bus interchange. Nitrated polycyclic aromatic hydrocarbons (nitro-PAHs) are the chemical class of organic compounds with potent mutagenic properties. These species are emitted from a wide range of combustion sources. Some compounds can be formed photochemically via reactions of their parents PAH with OH or NO_3 radicals (in the presence of NO_2) in the gas phase as well as N_2O_5 or HNO_3 when parent PAH is associated with aerosols (Mabilia et al.,

2003). These atmospheric nitro-PAHs may increase the overall environmental health risk associated with PAHs (Yaffe et al., 2001).

In summary, the major chemical components composition of $PM_{2.5}$ collected at the three different locations are illustrated in the pie charts in Figure 5.12. It is obvious that BC content of particles is highly variable among the three locations. BC contributed about 12 $\mu g/m^3$ or approximately 25% of the $PM_{2.5}$ total mass loading which signify the impact of the submicron BC emissions from diesel buses on the air quality in the bus interchange. Sulphate appears to be a major component of $PM_{2.5}$ at all locations. However, it appears that sulphate was not found to be extremely high in the $PM_{2.5}$ composition at the bus interchange although the SO_2 emission was presumably high at the diesel emission hot spot. This is mainly due to the low-oxidation rate of SO_2 to SO_4^{2-} as discussed in the earlier section.

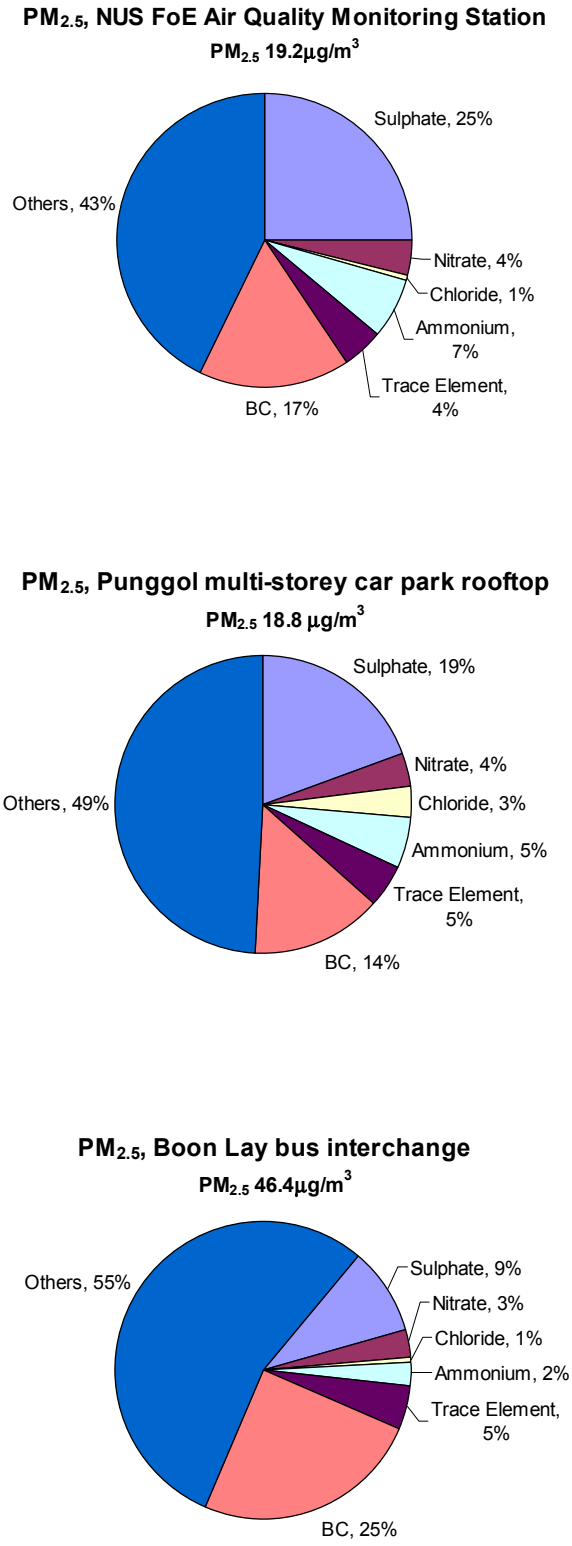

Figure 5.12 Major chemical components of $PM_{2.5}$ sampled at the NUS FoE air quality monitoring station, Punggol multi-storey car park rooftop and Boon Lay bus interchange.

5.3.3 Mass Size Distribution of Ions and Trace Elements

In the previous sections, the identification and evaluation of several major chemical constituents found in $PM_{2.5}$ and TSP collected from the NUS FoE Air Quality Monitoring Station and the Boon Lay bus interchange were discussed. However, little is known about the chemical constituent size distribution pattern from their probable sources. In order to determine mass size distribution of major ionic constituents and metal trace elements with the intention to identify the mode of particle size that contain highest concentration of each major constituent, including sulphate, nitrate, chloride, ammonium, copper, zinc, iron, aluminium, manganese and titanium, and their inter-relationship, size fractionated samples were collected on PTFE filters using MOUDI^{TM}.

Sulphate Size Distribution

Sulphate is the most abundant ionic species available in the $PM_{2.5}$ samples collected at the University and at the bus interchange as illustrated in Table 5-6. As discussed before, sulphate is mainly produced through nucleation when SO_2 is photochemically oxidized forming non-volatile sulphuric acid, which is immediately incorporated into airborne particles (Harrison and Yin, 2000) or agglomerate to form large numbers of sulphuric droplets in the nuclei mode (Kittelson, 1998). The mass concentration size distribution of particulate-bound sulphate shown in Figure 5.14 clearly demonstrates that most of the sulphate was detected in the condensation mode of 0.2 – 2.0 μm size range, with smaller fractions distributed in coarse mode (5 – 6 μm) and in the 0.09 – 0.1 μm modal diameter. The distribution mode established from both sampling sites was identical but varied in magnitude. The sulphate loading at the bus interchange was lower than that observed in the University possibly due to:

1) Higher SO_2 gas concentration in the air of the bus interchange than that in the campus (see Figure 5.13), which indicates that the freshly emitted SO_2 gas mostly remained in the gas phase in the atmosphere at the bus interchange. Unlike nitrogen dioxide, SO_2 is oxidized at a slower pace to form SO_4^{2-} hence less sulphate is formed and incorporated into the airborne particulates although the PM number is high in the bus interchange.

2) Industrial source SO_2 emitted from the distant refinery hub undergoes nucleation and oxidation processes forming SO_4^{2-} during the transport as the wind carries the pollutants to the university. During the transport process, excessive sulphuric acid droplets may have agglomerated to form particles, especially when the ambient humidity is high, resulting in larger surface area that absorb more sulphate in the process.

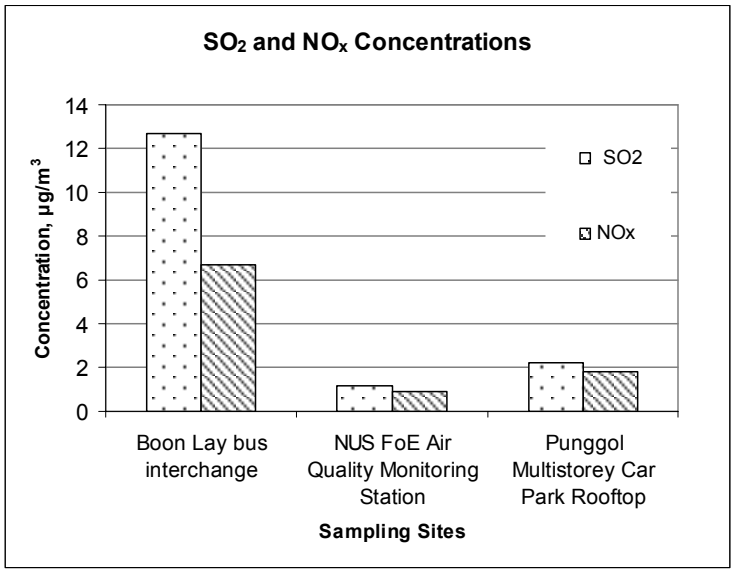

Figure 5.13 Concentration of SO_2 and NO_x (NO & NO_2) at the each sampling sites measured by Annular Denuder System (ADS).

The detection of the coarse mode sulphate as shown in Figure 5.14 might be simply due to the incorporation of sulphate into the agglomerated carbonaceous particles. Zhang (2001) suggested that the possible formation mechanism of the coarse mode sulphate was growth of the condensation mode particles. Meng and Seinfeld (1994) suggested that the coarse mode sulphate was formed by the activation of the condensation mode particles to form fog or cloud droplets, followed by aqueous phase chemistry and fog evaporation.

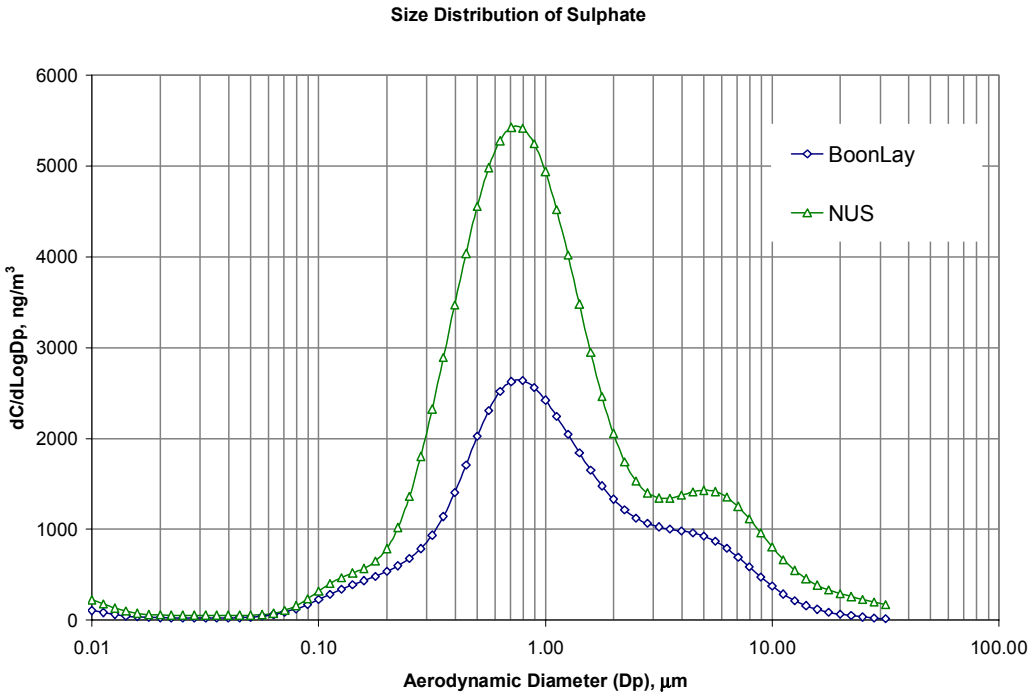

Figure 5.14 Comparison of sulphate mass concentration size distribution at Boon Lay bus interchange and NUS FoE air quality monitoring station.

Nitrate Size Distribution

The mass size distribution of nitrate at the bus interchange differs significantly from that at the university. A mono-modal size distribution was observed at the University as shown in Figure 5.15. Nitrate was predominantly distributed in the coarse mode (3 – 10 µm) with traces of nitrate found distributed in the fine mode without obvious trend.

In contrast, a bimodal size distribution of nitrate was observed at the bus interchange, ranging from 0.3 μm to 1.0 μm in the fine mode followed by the coarse modal diameter ranging from 3 μm to 10 μm.

Nitrate is formed mainly from the oxidation of atmospheric nitrogen dioxide. Fine mode nitrate is formed through the homogeneous gas-phase transformation of NO_x to HNO_3, followed by a reaction either with ammonia gas to form ammonium nitrate (Harrison and Msibi, 1994) or incorporated with pre-existing fine particles. However, in certain environments, sodium nitrate predominates (Harrison and Yin, 2000). As nitrogen dioxide oxidizes appreciably more rapidly than sulphur dioxide and due to the sensitivity of ammonium nitrate to ambient ammonia concentration, which affect the dissociation of ammonium nitrate, the spatial patterns of nitrate are expected to be less uniform than those of sulphate (Harrison and Yin, 2000).

The concentration of NO_x (NO and NO_2), which are the main ammonium nitrate precursors, in the bus interchange remained high throughout the day with a concentration of about 6.7 $\mu g/m^3$ as shown in Figure 5.13 due to a continuous emission of NO_x from the diesel buses. A significant part of the NO_x gas is oxidized fairly quickly into gaseous nitrous acid and the nitric acid, which then reacts with ammonia resulting in higher uptake of ammonium nitrate. The nitric acid in excess is expected to be associated with pre-existing fine particles. However, the concentration of ambient ammonia is rather low in Singapore (Zhang, 2001). In addition, the ambient temperature in Singapore is relatively hot accompanied by high humidity. Hence, the association of nitric acid into pre-existing fine PM seems to dominate over the

formation of ammonium nitrate, as ammonium nitrate is volatile and sensitive to ambient temperature.

Coarse mode nitrate is formed through the reaction of gaseous nitric acid with sodium chloride to form sodium nitrate ($NaNO_3$) (Zhang, 2001), which is relatively more stable and less sensitive to ambient temperature (Yoshizumi and Hoshi, 1985). This reaction is most likely to take place when maritime air masses mix with polluted continental air masses (Harrison and Pio, 1983). Another possible source of coarse mode nitrate is believed to result from the reaction of gaseous nitric acid with calcium carbonate from coarse soil particles to form calcium nitrate ($Ca(NO_3)_2$) (Harrison and Kitto, 1992). However, the observation of chloride and sodium mass size distribution as shown in Figure 5.16 and Figure 5.17 seems to be supportive of Zhang's (2001) hypothesis about the existence of coarse mode nitrate measured at both sites. Nevertheless, resuspension of road dust that may contain calcium carbonate is believed to have contributed to higher nitrate concentration in coarse mode at the bus interchange.

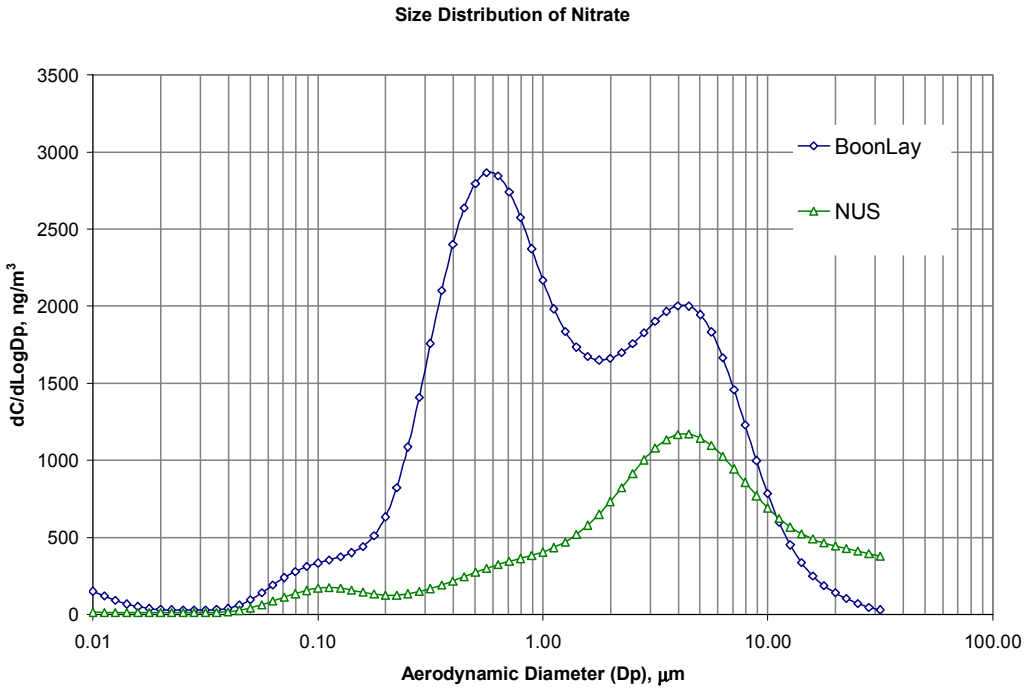

Figure 5.15 Comparison of nitrate mass concentration size distribution at Boon Lay bus interchange and NUS FoE air quality monitoring station.

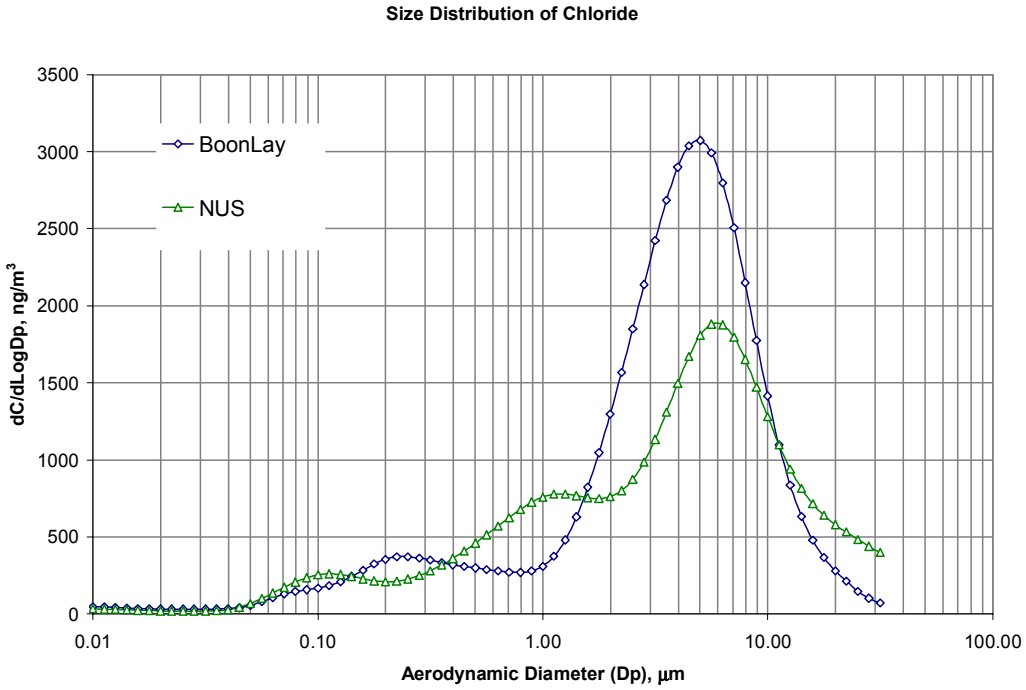

Figure 5.16 Comparison of chloride mass concentration size distribution at Boon Lay bus interchange and NUS FoE air quality monitoring station.

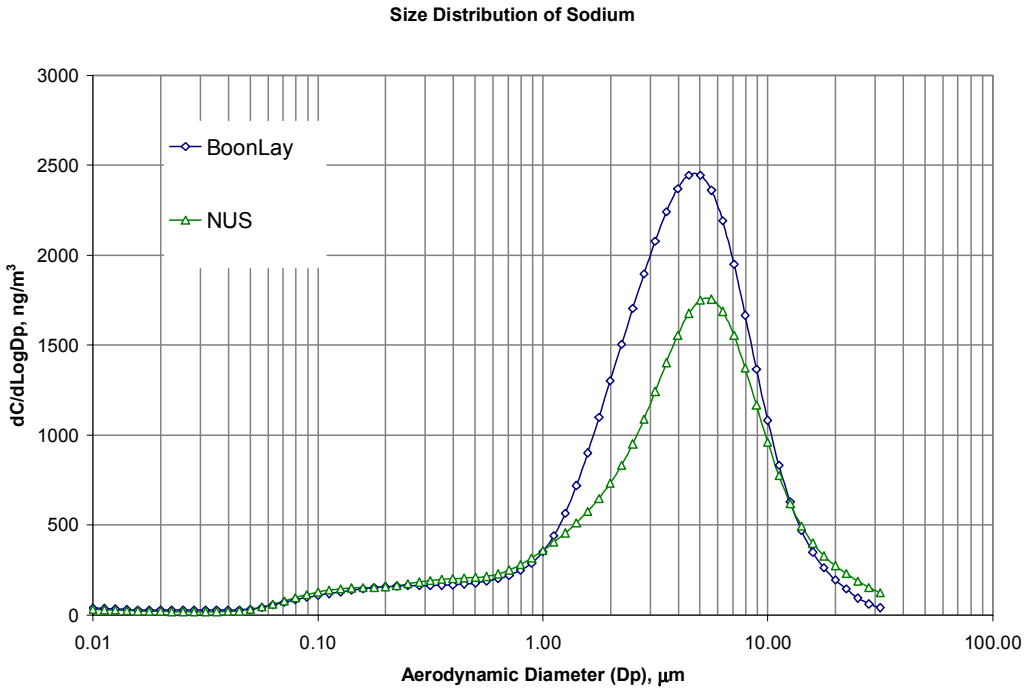

Figure 5.17 Comparison of sodium mass concentration size distribution at Boon Lay bus interchange and NUS FoE air quality monitoring station.

Ammonium Size Distribution

Ammonium is the most abundant cation detected in the $PM_{2.5}$ aerosol samples. The size distribution of ammonium at the University is clearly mono-modal, peaking with a fine modal diameter ranging from 0.3 µm to 2 µm that is consistent with that of sulphate. The modal diameter range of the ammonium detected at the bus interchange was extended to 0.1 µm that peaked within the 0.6 – 0.7 µm modal diameter range. Fraction of ammonium was also found in the coarse mode at the bus interchange (3 – 5 µm) and also at the University (>10 µm).

As seen in Figure 5.18, more than 90% of the ammonium was detected in the fine size range (0.1 – 2.0 µm). Fine particulate ammonium originated from vapour-phase ammonia. Ammonia may condense onto and neutralize an acidic particulate of an

anthropogenic origin and can thus accumulate within the fine mode particles. Alternatively, ammonia may react with acidic gases such as H_2SO_4, HNO_3 and HCl to form $(NH_4)_2SO_4$, NH_4NO_3 and NH_4Cl respectively, contributing to fine mode particles in the atmosphere. Among the ammonium salt, ammonium sulphate is the most stable salt whilst ammonium chloride may sublime over the time (Perry et al., 1997), indicating that a very high possibility that the majority of the ammonium detected in the aerosol samples are ammonium sulphate with strong correlation to traffic emission.

The detection of coarse mode ammonium at NUS and Boon Lay bus interchange in this study is believed to have been contributed from the agglomeration of fine mode ammonium with the coarse particles if excessive ammonia is available in the atmosphere at the sampling sites (Wall et al., 1988; Savoie and Prospero, 1982). In the University, it is speculated that the coarse mode ammonium (>10 μm) was probably derived from the absorption of ammonia gas by acidic contents of re-suspended coarse particles as the University was undergoing major makeover and renovation.

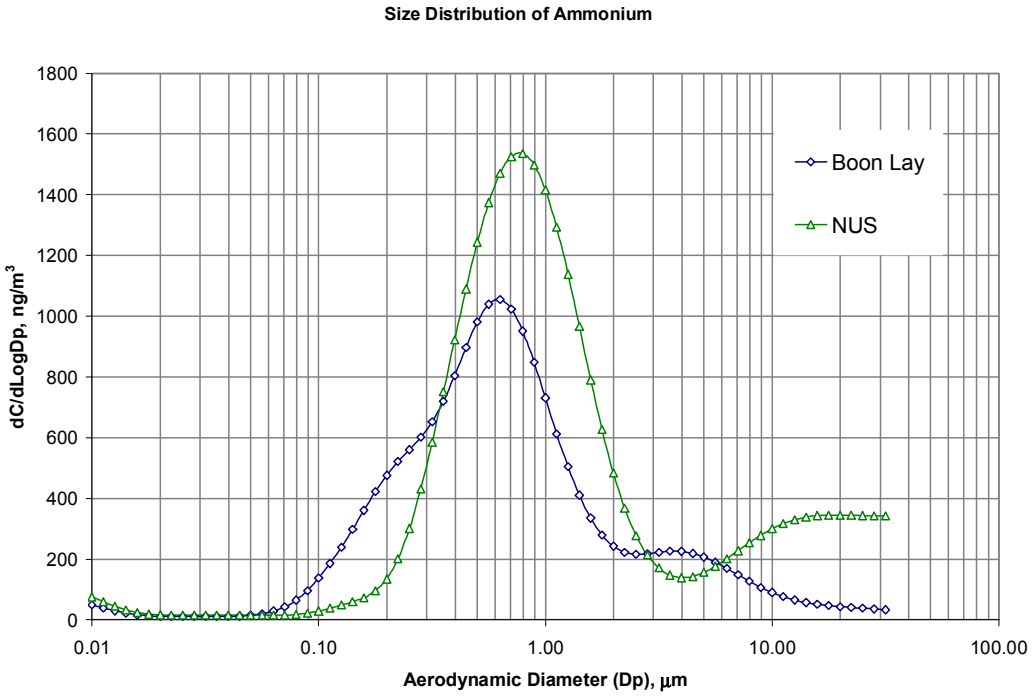

Figure 5.18 Comparison of ammonium mass concentration size distribution at Boon Lay bus interchange and NUS FoE air quality monitoring station.

Trace Element Size Distribution at Boon Lay bus interchange and NUS

Mean concentrations of trace elements analysed from $PM_{2.5}$ aerosol samples collected from NUS, Punggol and Boon Lay bus interchange through the sampling period are presented in Table 5-7. As mentioned in an earlier section, the mass concentrations of Al, Cu, Fe, Mn, Pb, Zn, Ti and V were significantly higher at the bus interchange, illustrating the probable strong correlation with anthropogenic origin and resuspension of road dust. Their mass concentration measured in the $PM_{2.5}$ aerosol samples at the bus interchange appeared to be at least 1.5 times higher than that measured in the University campus. For instance, the mass loading of Al at the bus interchange was about 3.6 times higher than that in the University campus. The size-distribution analysis also showed that for the elements occurring predominantly in the coarse particles such as Cu and Fe the mass loading at the bus interchange was about 3.2 and

1.9 times of that in NUS respectively. Mass concentration of Pb, Mn, Zn and V, which are conventionally recognized as the predominant elements from a combustion source, were higher at the bus interchange than that at the university by a factor of 2.2, 5.5, 9.3 and 1.7 respectively.

The size distributions of the various trace elements at the Boon Lay bus interchange and NUS FoE Air Quality Monitoring Station are illustrated in Figure 5.19 and Figure 5.20 respectively, in which the concentrations are presented in ng/m^3. Concentrations of some low loading elements such as Mn, Pb and V were amplified to reveal their mode of distribution in the figures.

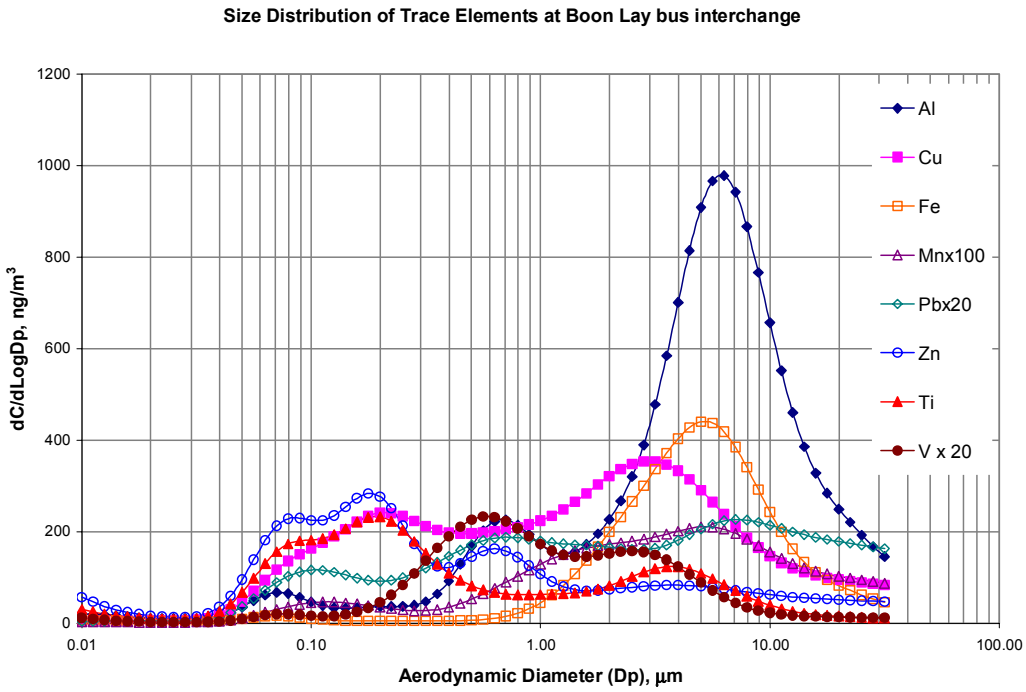

Figure 5.19 Size distribution of Al, Cu, Fe, Mn, Pb, Zn, Ti and V at Boon Lay bus interchange.

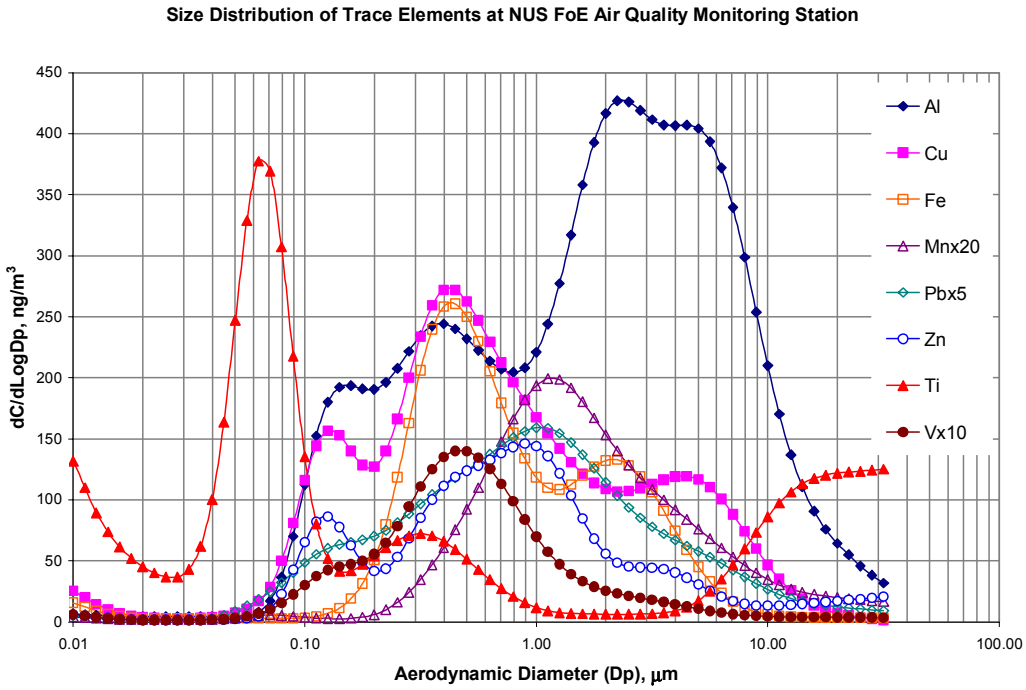

Figure 5.20 Size distribution of Al, Cu, Fe, Mn, Pb, Zn, Ti and V at NUS FoE air quality monitoring station.

In the bus interchange, elements occurring predominantly in coarse mode (2 – 10 µm aerodynamic diameters) are Al, Fe, Cu and Mn. Al and Fe appear to represent a classic size distribution for a component of crustal origin, which shows greater proportion in the coarse (>2.5 µm) particles size range. As illustrated in Figure 5.19, it is obvious that Al and Mn largely originated from road dust resuspension. However a portion of Al, Cu and Mn was observed in fine mode size distribution in the traffic-influenced bus interchange, which is suggestive of Al, Cu and Mn having both crustal and anthropogenic origins. Allen et al. (2000) and Harrison et al. (2003) both verified before that Mn have both crustal and anthropogenic origins. In contrast, Zn, Ti and V were occurring in the fine mode distribution ranging from 0.06 µm to 2 µm modal diameters. Zn was largely distributed in the size range of less than 1 µm in aerodynamic diameter with highest concentration observed between 0.07 µm and 0.3 µm, a clear indication of traffic origin. In comparison to Zn, V was distributed in larger

particle size range from 0.3 μm to 2 μm. Titanium is conventionally associated with coarse particles (Harrison et al., 2003), but was not the case in this study. Significant concentration of Ti is distributed at the particle size range of 0.07 μm and 0.3 μm, indicating that anthropogenic Ti could have been emitted locally or from a distant source. Despite leaded fuel was phased out in Singapore in 1998 (NEA, 2003), Pb was observed at the bus interchange with no specific trend of modal distribution. It is suggestive that Pb could have been emitted from distant industrial source such as incineration or smelting plants.

In summary, the sum of mean mass concentration of trace element species detected at the University sampling site was approximately 37% of that in the bus interchange. A number of elements such as Al, Cu, Fe, Ti and Mn were found bi-modally distributed in the University. Among them, Al was distributed largely in the coarse mode, with a fraction distributed at the modal diameter ranging between 0.1 μm and 1 μm. Fe and Cu were the other two elements found in particle size larger than 2.5 μm. Aside from those detected in the coarse mode, Fe and Cu were also found accumulated in the 0.3 – 0.6 μm size range. Ti shows a heavy abundance in the 0.04 – 0.1 μm and >10 μm size fraction indicating a likely multiplicity of sources contributing to the two polarized diameters. Renovation and demolition works which involved welding and cutting of metallic construction materials and paint works are the most likely sources of both fine and coarse mode Al, Fe, Cu, Ti and Mn. Potentially toxic metals Pb and V were predominantly partitioned in the sub-micron particle size range with peak concentration detected at modal diameters of 1 μm and 0.5 μm, respectively. Traffic associated Zn was clearly fractionated bi-modally at 0.1 μm and 1 μm modal diameters in the

University as shown in Figure 5.20, which can be traced to vehicular emissions and tyre rubber abrasion (Allen et al., 2001; Pacyna, 1986)

The most interesting outcome in this study in regard to the trace element concentration and apportionment is the detection of Ti in the fine mode size fraction even at the sampling site within the University, which is not close to a traffic source. Titanium can be originated from various sources from cosmetic to construction materials such as cement and paints. Renovation works that involved painting and demolition work are suspected to be the primary source of Ti at the University. Clearly, the resuspension of road dust by moving vehicles within the bus interchange is believed to have contributed to the coarse fraction Ti in the bus interchange. However, no specific source has been identified to be responsible for the existence of fine mode Ti at the site. One possibility is that the fine mode Ti might have been emitted from the heavy duty diesel buses at the bus interchange. Alternatively, the distant incineration plants located at the western region of Singapore could be the other likely source for fine mode Ti detected at the bus interchange.

Chapter 6 Conclusions

This study is the first of its kind being conducted in a bus interchange to characterize and assess the level of diesel emitted PM that the general public is exposed to in their daily routine life. The commuters transiting at the Boon Lay bus interchange are exposed to higher concentration of traffic pollution than the residents in Punggol new town and the occupants at the university. Respirable $PM_{2.5}$ average spatial mass concentration at the bus interchange was 46.4 $\mu g/m^3$, over 3 times above the NAAQS regulatory limit of 15 $\mu g/m^3$ (NEA, 2003). Mass concentration size distribution studies reveal that a significant mass of PM was distributed in the fine mode ranging from 0.15 to 0.7 μm at the bus interchange. However, the mass measuring instruments do not sufficiently reflect the existence of ultrafine particles at the site. This is because the PM mass concentration is principally determined by particles greater than 1 micrometer in size. It has been hypothesized that ultrafine particles, which comprise the largest number of particles, can cause more severe health effects than the larger ones. This means that the mass of particles to which an individual is exposed to is of less relevance compared to other particle properties such as particle size, number concentration and chemical composition.

As the buses begin their operation in the morning, ELPI measured a 24-hour average of 69,900 particles suspended in every cm^3 of fumy air within the bus interchange, which differed by a factor of 10 compared to that measured at the University campus. Over 90% of the particles counted at the bus interchange were smaller than 100 nm according to the results obtained from ELPI and SMPS.

Freshly emitted BC overshadowed other chemical constituents by taking up nearly 25% of the $PM_{2.5}$ total mass measured at the bus interchange, whereas only 17% and 14% of the total mass of $PM_{2.5}$ was BC at NUS and Punggol. This observation is indicative of diesel emission intensity and significance at the respective sites. Higher concentrations of ionic species such as nitrate and trace metals including Zn, Cu, Fe, Mn, Pb and Ti were observed at the diesel emission hot spot. However, the concentrations of sulphate and ammonium were not too much different compared to the background measurements. Although conventionally found only in coarse particles, a significant amount of Ti was unexpectedly detected in the fine mode particle size range at both bus interchange and at the University. More study should be conducted if a correlation between Ti and diesel emission or other unidentified anthropogenic activities that are peculiar to the sites is to be established.

This study agrees with the conclusion made by Bi et al. (2002) that the concentrations of particulate matter do not show significant effects on the level of n-alkanes and PAHs in the particles. However, ambient temperature, wind speed and humidity have shown strong influences to the concentrations of particulate-bound aliphatic hydrocarbons and PAHs. Cooler ambient temperature with stagnant air and low UV penetration will lower the loss of lower MW organic compounds via evaporation or sublimation. The cluster of n-alkanes between C_{15} and C_{35} with pristane and phytane represents the direct input of unburned fuel residue at the bus interchange, with most of the mass distributed between C_{22} and C_{33}, despite the lean-burn characteristic that a diesel engine is known for (Cragg, 1992). The CPI values of the whole-range n-alkanes varied from 1.02 to 1.17, indicating the importance of diesel and oil residues contribution at the site. The detection of nitro-PAHs and the increase of higher molecular weight PAHs

concentrations at the bus interchange, particularly the concentration of B(a)P which was 6 times larger than that observed in the University, have induced higher risk of exposure of commuters at the bus interchange to toxicity and carcinogenicity.

Such high particulate counts of ultrafine particles at the bus interchange indicate a high possibility that gas-to-particle conversion could have been taking place. More detailed and long-term studies should be performed including the measurement of gaseous pollutants such as O_3, SO_2, NO_x, NH_3 and VOCs, as well as the observation on meteorological conditions which are influential to airborne pollutants transport phenomena if the mechanisms of particles formation, evolution and removal of condensed materials are to be fully understood at this diesel exhaust emission hot-spot. Studies of gaseous or particulate-bound toxic, mutagenic and carcinogenic substances such as mercury (Hg), cadmium (Cd), and polychlorinated biphenyls (PCB), dioxin, are equally important particularly at public places in close proximity to traffic emission sources although these substances generally occur in low concentrations and are not of any significance for the balance of the major atmospheric components.

By identifying the problems, the best solution in terms of technology and economic feasibility can be sought. Unfortunately, in the context of traffic pollution control and reduction, no single solution could solve the decade's long problems. However, the impacts of the "problems" are likely to be minimized, if vehicles equipped with latest engine technology are well maintained and higher quality fuel such as the OK Petroleum's ProMil City Diesel (0.001% Sulphur content) (Cragg, 1992) is used. Involvement and close co-operation of the policy makers (government), the technology

developer (auto manufacturers) and the fuel suppliers (refineries) is essential in shaping up an environmental sustainable transportation needs for current and future generations.

Appendix A

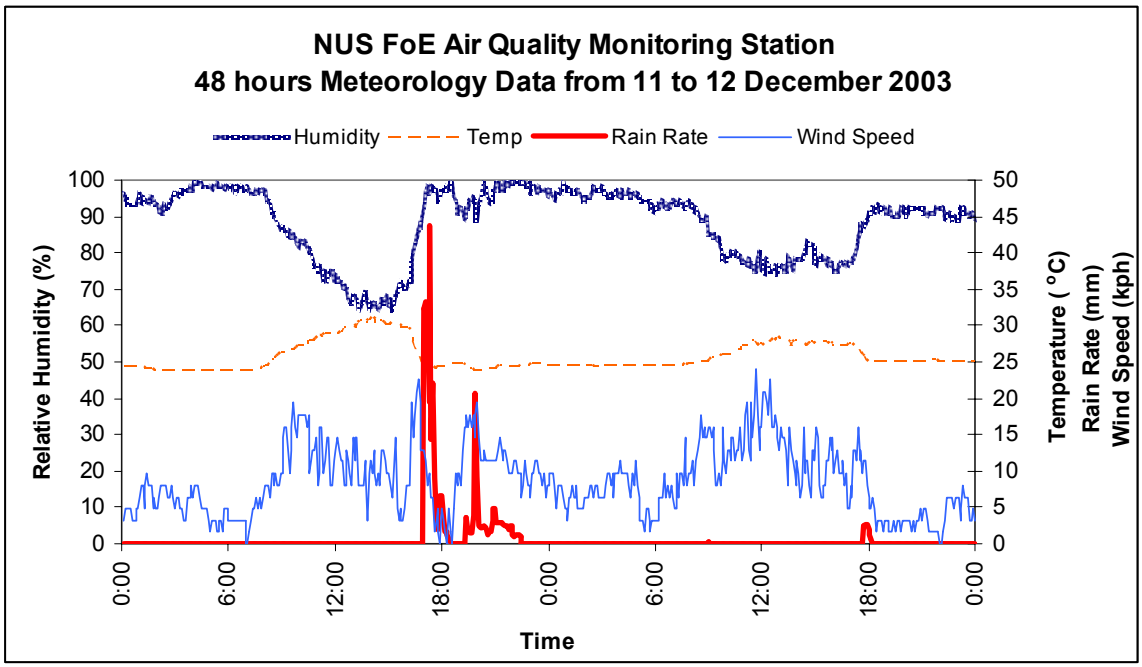

Figure A.1 48-hours Weatherlink® meteorology data from 11 to 12 December 2003 recorded at NUS FoE Air Quality Monitoring Station.

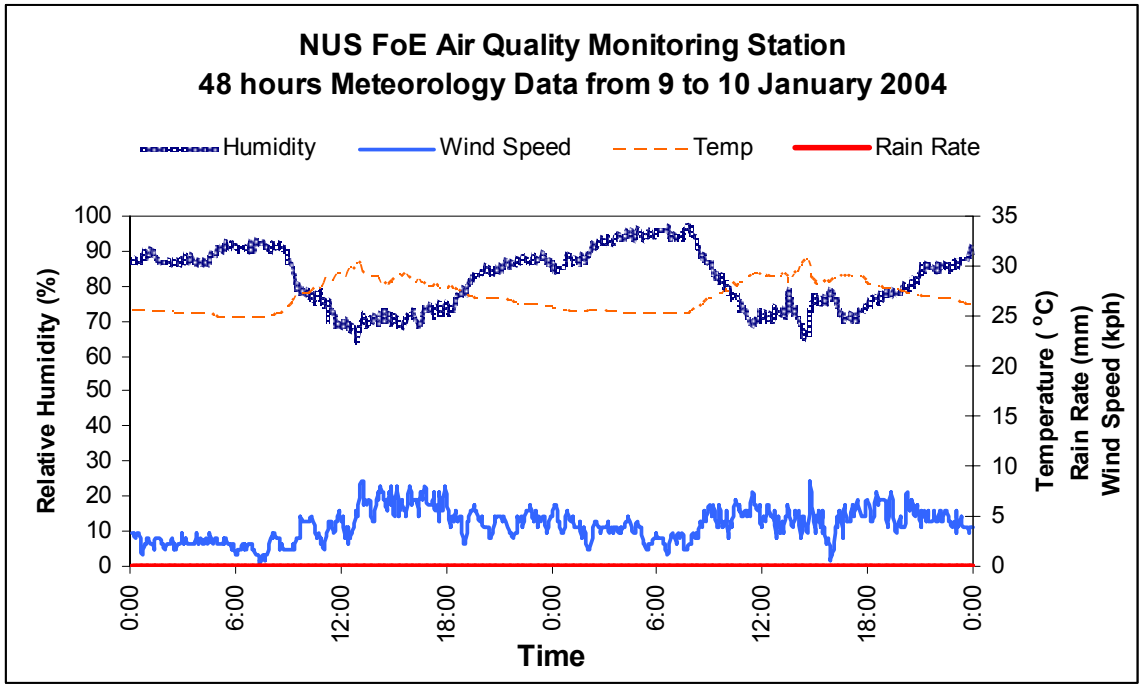

Figure A.2 48-hours Weatherlink® meteorology data from 9 to 10 January 2004 recorded at NUS FoE Air Quality Monitoring Station.

Appendix B

Calculation of gaseous aerosols from the Annular Denuders System (ADS):

Assumptions:

1. NaCl coated denuder (AD1) collects 100% of sampled HNO_3 as nitrate (the diffusivity of HNO_3 is high, diffusion to the wall is assumed fast).
2. $NaCO_3$ coated denuder (AD2) collects 100% of sampled HONO as nitrite, which can be oxidized to nitrate.
3. NaCl & $NaCO_3$ coated denuders together collect 100% of the SO_2 as sulphite, which can be completely oxidized to sulphate.

These assumptions lead to the formulas to compute atmospheric concentration from annular denuder measurement as stated below:

$$C_{HNO3},\ \mu g/m^3 = 1.016*[\ NO_3^-\ ]_{AD1} / V$$

$$C_{HONO},\ \mu g/m^3 = 1.022*[\ NO_2^-\ ]_{AD2} / V + 0.758*[\ NO_3^-\ ]_{AD2} / V$$

$$C_{SO2},\ \mu g/m^3 = 0.667*\{[\ SO_4^{2-}\ ]_{AD1}+[\ SO_4^{2-}\ ]_{AD2}\} / V$$

Where, V = volume of air sampled, m^3

$[X]$ = concentration of the ions, µg/mL

Factor 1.016 = the ratio of molecular weights of HNO_3 & NO_3

Factor 1.022 = ratio to convert NO_2^- to equivalent amounts of HONO

Factor 0.758 = ratio to convert NO_3^- to equivalent amounts of HONO

Factor 0.667 = the ratio of molecular weights of SO_2 & SO_4

Appendix C

Salford FTN77 Inversion Program for MOUDI™ data processing.

```
ccccccccccccccccccccccccccccccccccccccccccccccccccccccccccccccccccccccccccccc
c
c     Program to calculate ambient aerosol mass composition
c     distributions from chemical composition data obtained by chemical
c     analysis of MOUDI impactor collections.
c     based on
c       IMPINV1.FOR     very first inversion program - inlet losses not
c                       considered
c
c     modified on 10/12/98 for tapering.
c
c
ccccccccccccccccccccccccccccccccccccccccccccccccccccccccccccccccccccccccccccc
        program impinvrt
        character specname*15
        common/one/ ndiam, nstages, d(500), dlog(500), fkern(13,500),
     &    numstage(13), dbin, fguess(500), sumout, totalion
        common/three/ nspecies, specname(80), data(80,80), iddata
        common/six/save1(80,500),save2(80,4)

c
c       the call to system routine UNDFL(IFLAG) is necessary for
c       Lahey FORTRAN version 4.0 to handle numeric underflows
c       i.e. when a number is calculated to be smaller than
c       the minimum size this version can handle
c
        call MASK_UNDERFLOWS@
c
        write(*,*)
        write(*,*)' Program : IMPINVRT'
        write(*,*)
        write(*,*)' Usage : inverts MOUDI data -> smooth distribution'
        write(*,*)' Input files : user-specified datafile; free format'
        write(*,*)' Output files : user-specified; must be *.CSV'
        write(*,*)
        write(*,*)' Input file format : '
        write(*,*)' line 1 : sample name, max 20 characters'
        write(*,*)' line 2 : number of ionic species (I3)'
c        PRINT*, " line 3 : species names, space delimited, max 15 chrs"
c        PRINT*, " lines 4-15 : 12 lines, space-delimited, species data"
c        PRINT*, " ### note that all 12 stages must have valid data ###"
        write(*,*)
c
        nstages = 13        ! number of real+ ficticious MOUDI stages
        do i=1, nstages
           numstage(i) = i-2  ! give stages correct MOUDI numbers
        enddo
        decades = 3.6        ! number of decades in particle radius > 0.01 æm
        dbin = 0.05         ! width of size bins wanted, log radius units
        ndiam = int(decades/dbin)
        do i = 1,ndiam
        d(i) = 1.0*10.0**(-2.0 + dbin*(i-1))
        dlog(i) = alog10(d(i))
        enddo
c
        call kernel
c
        call readdata
c
        do i=1, nspecies
c
c     set up initial guess distribution
c
            totalion = 0.0
                 do j = 1, nstages
                    totalion = totalion + data(j,i)
                 enddo
            iddata = i
c
            call initdist
c
            call integ1
```

```
           scalefac = totalion/sumout
           do j = 1,ndiam
                fguess(j) = fguess(j)*scalefac
           enddo
           call iterate
        enddo
           write(6,1000)(save2(k,1),k=1,iddata)
           write(6,2000)(save2(k,2),k=1,iddata)
           write(6,3000)(save2(k,3),k=1,iddata)
           write(6,4000)(save2(k,4),k=1,iddata)
 1000    format('obs. total',',',80(f9.3,','))
 2000    format('inv. total',',',80(f9.3,','))
 3000    format('# of itrns',',',80(f7.3,','))
 4000    format('%rmsresidl',',',80(f7.3,','))
           do k=1,ndiam
                write(6,5000) d(k),(save1(l,k),l=1,nspecies)
c
c If RADIUS is to be written out, must divide d(k) here by 2!
c If you change this here you must also change it at line 190
c
 5000        format(80(1pe12.5,','))
           enddo
        close(6)
        end
ccccccccccccccccccccccccccccccccccccccccccccccccccccccccccccccccccccccccc
c
c     subroutine readdata
c     reads in MOUDI data
c
ccccccccccccccccccccccccccccccccccccccccccccccccccccccccccccccccccccccccc
        subroutine readdata
        character fnamein*12, fnameout*12, sampname*20, specname*15
        common/one/ ndiam, nstages, d(500), dlog(500), fkern(13,500),
     &    numstage(13), dbin, fguess(500), sumout, totalion
        common/three/ nspecies, specname(80), data(80,80), iddata
        write(*,*)' Type in input filename : '
        read(*,*)fnamein
        open(5, file = fnamein)
        write(*,*)' Type in output filename : '
        read(*,*)fnameout
        open(6, file = fnameout, status = 'new')
        open(5, file = fnamein)
        read(5,1000) sampname
 1000 format(a12)
        read(5,2000) nspecies
 2000 format(i2)
        do j=1,1
            read(5,*)(specname(i), i=1, nspecies)
        enddo
        do i=1,nstages-1
            read(5,*)(data(13-i,j), j=1,nspecies)
        enddo
        do j = 1,nspecies
            data(13,j) = data(12,j)*0.10
        enddo
        close(5)
        write(6,1000) sampname
        write(6,3000)'species',(specname(i), i=1,nspecies)
 3000 format(80(a15,','))
        return
        end
ccccccccccccccccccccccccccccccccccccccccccccccccccccccccccccccccccccccccc
c
c     subroutine kernel - calculates stage kernel functions for
c     MOUDI impactor.  Uses function functn.
c
ccccccccccccccccccccccccccccccccccccccccccccccccccccccccccccccccccccccccc
        subroutine kernel
        common/one/ ndiam, nstages, d(500), dlog(500), fkern(13,500),
     &    numstage(13), dbin, fguess(500), sumout, totalion
        common/five/ fkernmax(13)
        dimension t(15, 500)
        do i = 1,nstages
        do j = 1,ndiam
        t(i,j) = 1 - functn(i,d(j))
        enddo
        enddo
c
        do j = 1, ndiam
        fkern(1,j) = functn(1,d(j))*(1.0-functn(0,d(j)))
```

```
         fkern(2,j) = functn(2,d(j))*t(1,j)
         fkern(3,j) = functn(3,d(j))*t(1,j)*t(2,j)
         fkern(4,j) = functn(4,d(j))*t(1,j)*t(2,j)*t(3,j)
         fkern(5,j) = functn(5,d(j))*t(1,j)*t(2,j)*t(3,j)*t(4,j)
         fkern(6,j) = functn(6,d(j))*t(1,j)*t(2,j)*t(3,j)*t(4,j)*t(5,j)
         fkern(7,j) = functn(7,d(j))*t(1,j)*t(2,j)*t(3,j)*t(4,j)*t(5,j)
     &    *t(6,j)
         fkern(8,j) = functn(8,d(j))*t(1,j)*t(2,j)*t(3,j)*t(4,j)*t(5,j)
     &    *t(4,j)*t(7,j)
         fkern(9,j) = functn(9,d(j))*t(1,j)*t(2,j)*t(3,j)*t(4,j)*t(5,j)
     &    *t(6,j)*t(7,j)*t(8,j)
         fkern(10,j) = functn(10,d(j))*t(1,j)*t(2,j)*t(3,j)*t(4,j)*t(5,j)
     &    *t(6,j)*t(7,j)*t(8,j)*t(9,j)
         fkern(11,j) = functn(11,d(j))*t(1,j)*t(2,j)*t(3,j)*t(4,j)*t(5,j)
     &    *t(6,j)*t(7,j)*t(8,j)*t(9,j)*t(10,j)
         fkern(12,j) = functn(12,d(j))*t(1,j)*t(2,j)*t(3,j)*t(4,j)*t(5,j)
     &    *t(6,j)*t(7,j)*t(8,j)*t(9,j)*t(10,j)*t(11,j)
         fkern(13,j) = functn(13,d(j))*t(1,j)*t(2,j)*t(3,j)*t(4,j)*t(5,j)
     &    *t(6,j)*t(7,j)*t(8,j)*t(9,j)*t(10,j)*t(11,j)*t(12,j)
         enddo
c
         do i=1,nstages
             thing=0.0
             do j=1, ndiam
                   thing=amax1(thing,fkern(i,j))
             enddo
             fkernmax(i)=thing
         enddo
ccccccccccccccccccccccccccccccccccccccccccccccccccccccccccccccccccccccccc
c
c    next section is only used if kernel functions are to be written out
c
ccccccccccccccccccccccccccccccccccccccccccccccccccccccccccccccccccccccccc

c      open (5, file = 'imptest.dat', status = 'new')
c      do i = 1, nstages
c      do j = 1, ndiam
c      write(5,*) i, d(j), fkern(i,j)
c      write(*,*) i, d(j), fkern(i,j)
c      enddo
c      enddo
c      close(5)

ccccccccccccccccccccccccccccccccccccccccccccccccccccccccccccccccccccccccc
       return
        end
ccccccccccccccccccccccccccccccccccccccccccccccccccccccccccccccccccccccccc
c
c     function function - calculates MOUDI stage collection functions
c     according to the Winklmayr et al. anaytical function
c
c     stage cut-points are given for particle density of 2.0 g/cm3
c
c    stage 1 is ficticious
c
c    stage 13 is the final filter; it has a ficticious lower cut-off
c
ccccccccccccccccccccccccccccccccccccccccccccccccccccccccccccccccccccccccc
        function functn(nstage,d)
        common/two/ d50(13), s(13)
        d50(1) = 100.0000
        d50(2) = 18.0000
        d50(3) = 10.0000
        d50(4) = 5.6000
        d50(5) = 3.2000
        d50(6) = 1.8000
        d50(7) = 1.0000
        d50(8) = 0.5200
        d50(9) = 0.2950
        d50(10) = 0.1660
        d50(11) = 0.0940
        d50(12) = 0.0530
        d50(13) = 0.0200
        s(1) = 10.0000
        s(2) = 9.8128
        s(3) = 20.7851
        s(4) = 7.4232
        s(5) = 5.6099
        s(6) = 10.2459
        s(7) = 11.5074
```

```
        s(8) = 5.5326
        s(9) = 4.7948
        s(10) = 4.2440
        s(11) = 3.9850
        s(12) = 2.5821
        s(13) = 2.0000
        if(nstage.ne.0)then
            functn = 1/(1 + (d50(nstage)/d)**(2.0*s(nstage)))
        else
            functn = 1/(1 + (2.0*d50(1)/d)**(2.0*s(1)))
        endif
        return
        end
ccccccccccccccccccccccccccccccccccccccccccccccccccccccccccccccccccccccc
c
c     subroutine initdist
c     produces an initial guess distribution from the raw MOUDI data
c
ccccccccccccccccccccccccccccccccccccccccccccccccccccccccccccccccccccccc
        subroutine initdist
        character specname*15
        common/one/ ndiam, nstages, d(500), dlog(500), fkern(13,500),
     &    numstage(13), dbin, fguess(500), sumout, totalion
        common/two/ d50(13), s(13)
        common/three/ nspecies, specname(80), data(80,80), iddata
c
        a1=0.0
        do i=1,nstages
            if(data(i,iddata).gt.a1)then
                  a1=data(i,iddata)
                  a3=d50(i)
            endif
        enddo
        a2=2.0
        do j=1,ndiam
            fguess(j) = funcdist(d(j),a1,a2,a3)
        enddo
        return
        end
ccccccccccccccccccccccccccccccccccccccccccccccccccccccccccccccccccccccc
c
c     subroutine integ1
c     determines integral of fguess over all diameter values

c
ccccccccccccccccccccccccccccccccccccccccccccccccccccccccccccccccccccccc
        subroutine integ1
        common/one/ ndiam, nstages, d(500), dlog(500), fkern(13,500),
     &    numstage(13), dbin, fguess(500), sumout, totalion
        sum = 0.0
        do i=1,ndiam
           sum = sum + fguess(i)
        enddo
        sumout = sum*dbin
        return
        end
ccccccccccccccccccccccccccccccccccccccccccccccccccccccccccccccccccccccc
c
c     subroutine iterate
c     carries out iterative inversion
c
ccccccccccccccccccccccccccccccccccccccccccccccccccccccccccccccccccccccc
        subroutine iterate
        character specname*15
        common/one/ ndiam, nstages, d(500), dlog(500), fkern(13,500),
     &    numstage(13), dbin, fguess(500), sumout, totalion
        common/three/ nspecies, specname(80), data(80,80), iddata
        common/four/idstage, amount, ratio
        common/six/save1(80,500),save2(80,4)
c
        nrep = 10                ! number of iterations
        sumer=0.0
        rms=0.0
        rmsold=1.e3
        do iter=1,nrep
            if(rms.gt.0.)rmsold=rms
            sumer=0.0
c          ermax=0.0
        do j=2,nstages
            idstage=j
```

```
            call integ
            ratio=data(j,iddata)/amount
c           sumer=sumer+(ratio-1.0)**2
c           ermax=amax1(ermax,abs(ratio-1.0))
            sumer=sumer+(data(j,iddata)-amount)**2
            call alter
            thing=0.0
            do i=1,ndiam
                  thing=amax1(thing,fguess(i))
            enddo
            do i=1,ndiam
                  fguess(i)=amax1(thing*1.e-2,fguess(i))
            enddo
            do i=3,ndiam-3
                fguess(i) = (fguess(i-2)*0.1111+fguess(i-1)*0.3333
     &                   + fguess(i)
     &                   + fguess(i+1)*0.1111+fguess(i+2)*0.3333)/1.888
c
c the original smoothing weights used by Jill were 0.25,0.5,1,0.5,0.25
c
            enddo
            fguess(2)=(0.333*fguess(1)+fguess(2)+0.333*fguess(3))/1.667
            fguess(ndiam-2)=fguess(ndiam-3)-
     &                      (fguess(ndiam-4)-fguess(ndiam-3))
            this=fguess(ndiam-2)/fguess(ndiam-3)
            fguess(ndiam-1)=fguess(ndiam-2)-
     &                      this*(fguess(ndiam-3)-fguess(ndiam-2))
            this=fguess(ndiam-1)/fguess(ndiam-2)
            fguess(ndiam)=fguess(ndiam-1)-
     &                      this*(fguess(ndiam-2)-fguess(ndiam-1))
            call integ1

            totalmas=sumout
          do ij= 1,ndiam
          fguess(ij)=fguess(ij)*totalion/sumout
          enddo
        enddo
           rms=sqrt(sumer/nstages)
           rms=100.*rms/totalion
           if(abs(rms-rmsold)/rmsold.lt.0.001.or.iter.eq.nrep)then
                 do i=1,ndiam
                        save1(iddata,i)=fguess(i)
                 enddo
                 save2(iddata,1)=totalion
                 save2(iddata,2)=totalmas
                 save2(iddata,3)=real(iter)
                 save2(iddata,4)=rms
                 return
           endif
        enddo
        return
        end
ccccccccccccccccccccccccccccccccccccccccccccccccccccccccccccccccccccccccccc
c
c     subroutine integ
c
ccccccccccccccccccccccccccccccccccccccccccccccccccccccccccccccccccccccccccc
        subroutine integ
        character specname*15
        common/one/ ndiam, nstages, d(500), dlog(500), fkern(13,500),
     &    numstage(13), dbin, fguess(500), sumout, totalion
        common/three/ nspecies, specname(80), data(80,80), iddata
        common/four/idstage, amount, ratio
        sum=0.
        do i=1,ndiam
            sum=sum+fguess(i)*fkern(idstage,i)
        enddo
        amount=sum*dbin
        return
        end
ccccccccccccccccccccccccccccccccccccccccccccccccccccccccccccccccccccccccccc
c
c     subroutine alter
c
ccccccccccccccccccccccccccccccccccccccccccccccccccccccccccccccccccccccccccc
        subroutine alter
        common/one/ ndiam, nstages, d(500), dlog(500), fkern(13,500),
     &    numstage(13), dbin, fguess(500), sumout, totalion
        common/four/idstage, amount, ratio
        common/five/ fkernmax(13)
```

```
        do i=1,ndiam
            if(fkern(idstage,i).gt.0.0001)then
                fguess(i)=fguess(i)*(1.0+(ratio-1.0)
     &       *(fkern(idstage,i)/fkernmax(idstage))**1.0)
            endif
        enddo
        return
        end
CCCCCCCCCCCCCCCCCCCCCCCCCCCCCCCCCCCCCCCCCCCCCCCCCCCCCCCCCCCCCCCCCCCCCCCCCCCCCCC
C                                                                              C
C     FUNCTION funcdist(XI,A)                                                  C
C                                                                              C
C   Purpose  : The function is for the log-normal distribution                 C
C              specified as                                                    C
C                                                                              C
C                                                 __                       __ C
C           dN           A(1).ln(10)             |   -sqr[ln{r/A(3)}]     | C
C          ----  = ------------------- * exp| ---------------------  | C
C         dlog r   sqrt[2*PI] * A(2)           |    2 * sqr[ A(2) ]     | C
C                                              --                       -- C
CCCCCCCCCCCCCCCCCCCCCCCCCCCCCCCCCCCCCCCCCCCCCCCCCCCCCCCCCCCCCCCCCCCCCCCCCCCCCCC
        FUNCTION funcdist(XI,a1,a2,a3)
C
        PI=3.141592654
        TWO_PI = SQRT(2.0 * PI)
        DLOG_1  = ALOG(XI/A3) ** 2
        VALUE_1 = -DLOG_1 / (2.0 * (A2 ** 2))
        IF (VALUE_1 .LT. -700.0) VALUE_1 = -700.0
C
        func =  A1 /( TWO_PI * A2 ) * EXP(VALUE_1)
        funcdist = func
        if(funcdist.lt.1.e-5)funcdist=1.e-5
        RETURN
        END
```

References

Abu-Allaban, M., Rogers, C. F., Gertler, A. W. (2004), A Quantitative Description of Vehicle Exhaust Particle Size Distributions in a Highway Tunnel, Journal of Air and Waste Management Association, Vol. 54, pp. 360-366.

Adamson, I. Y. R., Prieditis, H., Vincent, R. (1999), Pulmonary Toxicity of an Atmospheric Particulate Sample is Due to the Soluble Fraction, Toxicology and Applied Pharmacology, Vol. 157, pp. 43-50.

Airborne Particles Expert Group (APEG) (1999), Source Apportionment of Airborne Particulate Matter in the United Kingdom, Report of the Airborne Particles Expert Group, Department of the Environment, Transport and the Regions, UK.

Allen, A. G., Nemitz, E., Shi, J. P., Harrison, R. M., Greenwood, J. C. (2001), Size Distributions of Trace Metals in Atmospheric Aerosols in the United Kingdom, Atmospheric Environment, Vol. 35, pp. 4581-4591.

Allen, J. O., Hughes, L. S., Salmon, L. G., Mayo, P. R., Johnson, R. J., Cass, G. R. (2000), Characterization and Evolution of Primary and Secondary Aerosols During $PM_{2.5}$ and PM_{10} Episodes in the South Coast Air Basin, Environmental Engineering and Science Department, California Institute of Technology. Available: http://www.public.asu.edu/~jallen1/scos97/A22_final.pdf [accessed 3 July 2004].

Allison, A. C., Harington, J. S. and Birbeck, M. (1966), An Examination of the Cytotoxic Effects of Silica on Macrophages, Journal of Experimental Medicine, Vol. 124, pp. 141-153.

Amann, C. A. and Siegla, D. C. (1982), Diesel Particulates – What They Are and Why, Aerosol Science Technology, Vol. 1, pp. 73-101.

American Cancer Society, (2003), Cancer Facts & Figures 2003. Available: http://www.cancer.org/docroot/STT/stt_0_2003.asp?sitearea=STT&level=1 [accessed 12 August 2004].

Anderson, H. R. (1999), Health effects of air pollution episodes. In: Holgate, S. T., Samet, T. M., Koren, H. S., Maynard, R. L. (Eds.), Air Pollution and Health, Academic Press, New York, pp. 461-482.

Andreae, M.O., Andreae, T.W., Ferek, R.J., and Raemdonck, H. (1984), Long-range Transport of Soot Carbon in the Marine Atmosphere, The Science of the Total Environment, Vol. 36, pp. 73-80.

Ashmore, M. (2001), Personal Exposure to Air Pollution – the Role of Transport. Proceedings of the 3rd International Conference on Health Effects of Vehicle Emissions, Birmingham, UK.

Baek, S. O., Field, R. A., Goldstone, M. E., Kirk, P. W., Lester, J. N., Perry, R. (1991), A Review of Atmospheric Polycyclic Aromatic Hydrocarbons: Sources, Fate and Behaviour, Water, Air and Soil Pollution, Vol. 60, pp. 279-300.

Baik, N. J., Kim, Y. P., Moon, K. C. (1996), Visibility Study in Seoul, 1993, Atmospheric Environment, Vol. 30 (13), pp. 2319-2328.

Bermudez, E., Mangum, J. B., Asgharian, B., Wong, B. A., Reverdy, E. E., Janszen, D. B., Hext, P. M., Warheit, D. B., Everitt, J. I. (2002), Long-term Pulmonary Responses of Three Laboratory Rodent Species to Sub Chronic Inhalation of Pigmentary Titanium Dioxide Particles, Toxicology Science, Vol. 70(1), pp. 86-97.

Bi, X. H., Sheng, G. Y., Peng, A. P., Zhang, Z. Q., Fu, J. M. (2002), Extractable Organic Matter in PM_{10} from LiWan District of Guangzhou City, PR China, The Science of The Total Environment, Vol. 300, pp. 213-228.

Bidleman, T. F., Billings, W. N., Foreman, W. T. (1986), Vapour Particle Partitioning of Semivolatile Organic Compounds – Estimates from Field Collections, Environmental Science and Technology, Vol. 20, pp. 1038-1043.

Brasseur, G. P., Prinn, R. G., Pszenny, A. A. P. (ed) (2003), Atmospheric Chemistry in a Changing World: An Integration and Synthesis of a Decade of Tropospheric Chemistry Research, pp. 138-139, Berlin: Springer-Verlag.

Cadle, S.H. and Mulawa, P.A. (1990), Atmospheric Carbonaceous Species Measurement Methods Comparison Study: General Motors Results, Aerosol Science Technology. Vol. 12, pp. 128-141.

Chalupa, D. C., Morrow, P. E., Oberdörster, G., Utell, M. J., Frampton, M. W. (2004), Ultrafine Particle Deposition in Subjects with Asthma, Environmental Health Perspectives, Vol. 112 (No. 8), pp. 879-882.

Cheng, Z. L., Lam, K. S., Chan, L. Y., Wang, T., Cheng, K. K. (1999), Chemical Characteristics of Aerosols at Coastal Station in Hong Kong. I. Seasonal Variation of Major Ions, Halogens and Mineral Dusts between 1995 and 1996, Atmospheric Environment, Vol. 34, pp. 2771-2783.

Chin, A. T. H. (1996), Containing Air Pollution and Traffic Congestion: Transport Policy and the Environment in Singapore, Atmospheric Environment, Vol. 30 (5), pp. 787-801.

Chow, J. C., Watson, J. G., Lowenthal, D. H., Countess, R. J. (1996), Sources and Chemistry of PM_{10} Aerosol in Santa Barbara County, CA, Atmospheric Environment, Vol. 30, pp. 1489-1499.

Chuang, J. C., Callahan, P. J., Menton, R. G., Gordon, S. M., Lewis, R. G., Wilson, N. K. (1995), Monitoring Methods for Polycyclic Aromatic Hydrocarbons and Their Distribution in House and Track-in Soil, Environmental Science and Technology, Vol. 29, pp. 494-500.

Ciccioli, P., Cecinato, A., Brancaleoni, E., Frattoni, M., Zacchei, P., Miguel, A. H., Vasconcellos, P. C. (1996), Formation and Transport of 2-Nitrofluoranthene and 2-Nitropyrene of Photochemical Origin in the Troposphere, Journal of Geophysical Research, Vol. 101 (D14), pp. 19567-19581.

Clarke, A. G., Azadi-Boogar, G. A., Andrews, G. E. (1999), Particle Size and Chemical Composition of Urban Aerosols, The Science of the Total Environment, Vol. 235, pp. 15-24.

Colvile, R. N., Hutchison, E. J., Mindell, J. S., Warren, R. F. (2001), The Transport Sector as a Source of Air Pollution, Atmospheric Environment, Vol. 35, pp. 1537-1565.

Cragg, C. (1992), Cleaning Up Motor Car Pollution: New Fuels and Technology, Financial Times Management Report, Financial Times Business Information, London.

Dentener, F. J. and Crutzen, P. J. (1998), Reaction of N_2O_5 on Tropospheric Aerosols: Impact on the Global Distribution of NO_x, O_3 and OH, Journal of Geophysical Research, pp. 7149-7163.

Department of Health (1995), Committee on the Medical Effects of Air Pollution. Non-biological Particles and Health, London, HMSO.

Dockery, D. W., Pope, C. A., Xu, X., Spengler, J. D., Ware, J. H., Fay, M. E., Ferris, B. G., Speizer, F. E. (1993), An Association between Air Pollution and Mortality in Six US cities, Northern England Journal of Medicine, Vol. 329, pp. 1753-1759.

Donaldson, K., Brown, G. M., Brown, D. M., Bolton, R. E. and Davis, J. M. G. (1989), The Inflammation Generating Potential of Long and Short Fibre Amosite Asbestos Samples, British Journal of Industrial Medicine, Vol. 46, pp. 271-276.

Donaldson, K., Li, X. Y., MacNee, W. (1998), Ultrafine (Nanometre) Particle Mediated Lung Injury, Journal of Aerosol Science, Vol. 29, pp 553-560.

Donaldson, K., Stone, V., Clouter, A., Renwick, L., MacNee, W. (2001), Ultrafine Particles, Occupational and Environmental Medicine, Vol. 58 (3), pp. 211-216.

Driscoll, K. E., Higgins, J. M., Leytart, M. J. and Crosby, L. L. (1990), Differential Effects of Mineral Dusts on the In Vitro Activation of Alveolar Macrophage Eicosanoid and Cytokine Release, Toxicology in Vitro, Vol. 4, pp. 284-288.

ESPERE, Environmental Science Published for Everybody Round the Earth, Cloud and Particles, (2004). Available: http://www.atmosphere.mpg.de/enid/a9ee1be69b1f9bdf702685ea7e50260c,0/tk.html [accessed 10 July 2004].

Fang, M., Zheng, M., Wang, F., To, K. L., Jaafar, A. B., Jia, R. F., Fan, S. F., Peng, P. A. (1999), The Solvent-extractable Organic Compounds in the Indonesia Biomass Burning Aerosols – Characterization Studies, Atmospheric Environment, Vol. 33, pp. 783-795.

Ferin, J., Oberdorster, G. and Penney, D. P. (1992), Pulmonary Retention of Ultrafine and Fine Particles in Rats, American Journal of Respiratory Cell and Molecular Biology, Vol. 6, pp. 535-542.

Fubini, B., Mollo, L., Giamello, E. (1995), Free Radical Generation at the Solid/Liquid Interface of Iron-containing Minerals, Free Radical Research, Vol. 23, pp. 593-614.

Gaggeler, H. W., Baltensperger, U., Emmenegger, M., Jost, D. T., Schmidt, O. H., Haller, P., Hofmann, M. (1989), The Epiphaniometer, A New Device For Continuous Aerosol Monitoring, Journal of Aerosol Science, Vol. 20, pp. 557-564.

Garg, N. (2000), Field Investigation of Black Carbon and Polycyclic Aromatic Hydrocarbons in the Ambient Air, M. Eng Thesis, Department of Chemical and Environmental Engineering, National University of Singapore.

Ghio, A. J. and Huang, Y. C. T. (2004), Exposure to Concentrated Ambient Particles (CAPs): A Review, Inhalation Toxicology, Vol. 16 (1), pp. 53-59.

Gilmour, P. S., Brown, D. M., Lindsay, T. G., Beswick, P. H., MacNee, W., Donaldson, K. (1996), Adverse Health Effects of PM_{10} Particles: Involvement of Iron in Generation of Hydroxyl Radical, Occupational Environmental Medicine, Vol. 53, pp. 817-822.

Gonzalez Gomez, M. E., Howard-Hildige, R., Leahy, J. J., O'Reilly, T., Supple, B. and Malone, M. (2000), Emission and Performance Characteristics of a 2 Litre Toyota Diesel Van Operating on Esterified Waste Cooking Oil and Mineral Diesel Fuel, Environmental Monitoring and Assessment, Vol. 65, pp. 13-20.

Gouriou, F., Morin, J. P., Weill, M. E. (2004), On-road Measurements of Particle Number Concentrations and Size Distributions in Urban and Tunnel Environments, Atmospheric Environment, Vol. 38, pp. 2831-2840.

Goyer, R. A. and Cherian, M. G. (1995), Handbook of Experimental Pharmacology, Springer-Verlag, New York.

Hall, D.E., Stradling, R. J., Rickeard, D. J., Martini, G., Morato-Meco, A., Hagemann, R., Scendefi, J., Rantanen, L., Zemroch, P. J. (2001), Measurement of the Number and Mass Weighted Size Distributions of Exhaust Particles Emitted from European Heavy Duty Engines, CONCAWE Report 01/51, January 2001. Available: http://www.concawe.be/Content/Default.asp?PageID=62 [accessed 2 July 2004].

Hall, J. V. (1996), Assessing Health Effects of Air Pollution, Atmospheric Environment, Vol. 30 (5), pp. 743-746.

Hansen, A.D.A., Bodhaine, B.A., Dutton, E.G., and Schnell, R.C. (1988), Aerosol Black Carbon Measurements at the South Pole: Initial Results, 1986-1987, Geophys. Res. Lett. Vol. 15, pp. 1193-1196.

Hansen, A.D.A., Rosen, H., and Novakov, T. (1984), The Aethalometer – An Instrument for the Real-time Measurement of Optical Absorption by Aerosol Particles, The Science and the Total Environment, Vol. 36, pp.191-196.

Harrison, R. M. and Allen, G. (1990), Measurements of Atmospheric HNO_3, HCl and Associated Species on a Small Network in Eastern England, Atmospheric Environment, Vol. 24A, pp. 369-376.

Harrison, R. M. and Grieken R. V. (Ed) (1998), Atmospheric Particles, Wiley, Sussex, England.

Harrison, R. M. and Kitto, A. M. N. (1992), Estimation of the Rate Constant for the Reaction of Acid Sulphate Aerosol with NH_3 Gas from Atmospheric Measurements, Journal of Atmospheric Chemistry, Vol. 15, pp. 133-143.

Harrison, R. M. and Msibi, I. M. (1994), Validation of Techniques for Fast Response Measurement of HNO_3 and NH_3 and Determination of the $[NH_3]$ $[HNO_3]$ Concentration Product, Atmospheric Environment, Vol. 28, pp. 247-255.

Harrison, R. M. and Pio, C. A. (1983), Size Differentiated Composition of Inorganic Atmospheric Aerosol of both Marine and Polluted Continental Origin, Atmospheric Environment, Vol. 17, pp. 1733-1738.

Harrison, R. M. and Yin, J. X. (2000), Particulate Matter in the Atmosphere: which Particle Properties are Important for its Effects on Health, The Science of the Total Environment, Vol. 249, pp. 85-101.

Harrison, R. M., Shi, J. P., Xi, S. H., Khan, A., Mark, D., Kinnersley, R., Yin, J. X. (2000), Measurement of Number, Mass and Size Distribution of Particles in the Atmosphere, The Royal Society, Vol. 358, pp. 2567-2580.

Harrison, R. M., Tilling, R., Romero, M. S. C., Harrad, S., Jarvis, K. (2003), A study of Trace Metals and Polycyclic Aromatic Hydrocarbons in the Roadside Environment, Atmospheric Environment, Vol. 37, pp. 2391-2402.

Harrison, R. M., Yin, J., Mark, D., Stedman, J., Appleby, R. S., Booker, J., Moorcroft, S. (2001), Studies of the Coarse Particle (2.5 – 10 μm) Component in UK Urban Atmospheres, Atmospheric Environment, Vol. 35, pp. 3667-3679.

HECS (Healthy Environments and Consumer Safety), Canada, (2003), National Ambient Air Quality Objectives for Particulate Matter – Executive Summary. Available: http://www.hc-sc.gc.ca/hecs-sesc/air_quality/publications/particulate_matter_exec_summary/impacts.htm [accessed 10 July 2004]

Hitchins, J., Morawska, L., Wolff, R., Gilbert, D. (2000), Concentrations of Submicrometer Particles from Vehicle Emissions near a Major Road, Atmospheric Environment, Vol. 34, pp. 51-59.

Horvath, H., Kasahara, M., Pesava, P. (1996), The Size Distribution and Composition of the Atmospheric Aerosol at a Rural and Urban Location, Journal of Aerosol Science, Vol. 27 (3), pp. 417-435.

Housing Development Board (HDB), Statistics and Charts 2003, Singapore (2003). Available: http://www.hdb.gov.sg/isoa031p.nsf/ImageView/0102AR/$file/p073-086%20StatisticsCharts.pdf [accessed 7 July 2004].

Keskinen, J., Pietarinen, K., Lehtimäki, M. (1992), Electrical Low Pressure Impactor, Journal of Aerosol Science, Vol. 23, No. 4, pp. 353-360.

Kittelson, D. B. (1998), Engine and Nanoparticles: a Review, Journal of Aerosol Science, Vol. 29, pp. 575-588.

Kittelson, D. B., Watts, W. F. Johnson, J. (2002a), Diesel Aerosol Sampling Methodology CRC E-43: Final Report, University of Minnesota, Report for the Coordinating Research Council. Available: http://www.crcao.com/reports/recentstudies00-02/UMN%20Final%20E-43%20Report.pdf [accessed 26 June 2004].

Kittelson, D. B., Watts, W., Johnson, J. (2002b), Particle Measurement Methodology: E-43 Overview and Postmortem, CRC Real-World Group Meeting, Arizona. Available: http://www.crcao.com/reports/recentstudies2003/e-43pm.pdf [accessed 28 June 2004].

Koe, L. C. C., Arellano Jr., A. F., McGregor, J. L. (2001), Investigation the Haze Transport from 1997 Biomass Burning in Southeast Asia: Its Impact Upon Singapore, Atmospheric Environment, Vol. 35, pp. 2723-2734.

Kumazawa, R., Watari, F., Takashi, Y., Uo, M., Totsku, Y. (2002), Effects of Ti Ions and Particles on Neutrophil Function and Morphology, Biomaterials, Vol. 23(17), pp. 3757-3764.

Künzli, N., Kaiser, R., Medina, S., Studnicka, M., Chanel, O., Fillinger, P., Herry, M., Horak, F. Jr., Puybonnieux-Texier, V., Quenel, P., Schneider, J., Seethaler, R., Vergnaud, J-C., Sommer, H. (September 2000), Public-health Impact of Outdoor and Traffic-related Air Pollution: a European Assessment, The Lancet, Vol. 356.

Lee, C. T., Lin, N. H., Hsu, W. C., Chang, Y. L., Chang, S. Y. (1999), Local Circulation and Aerosol Water-soluble Ions – A Case Study in Taiwan During Mei-Yu Season, Chemosphere, Vol. 38 (2), pp. 425-443.

Lee, S. C., Li, W. M., Chan, L. Y. (2001), Indoor Air Quality at Restaurants with Different Styles of Cooking in Metropolitan Hong Kong, The Science of the Total Environment, Vol. 279, pp. 181-193.

Lloyd, A. C. and Cackette, T. A. (2001), Diesel Engines: Environmental Impact and Control, Journal of Air and Waste Management Association, Vol. 51, pp. 809-847.

Mabilia, R., Cecinato, A., Tomasi Sciano, M. C., Vasconcellos, P., Carvalho, L., Mattos, L., Franco, A. (2003), Nitro-PAH Compounds in the Atmosphere of São Paulo, Brazil, Geophysical Research Abstracts, Vol. 5, 09322. Available: http://www.cosis.net/abstracts/EAE03/09322/EAE03-J-09322.pdf [accessed 9 August 2004].

Marple, V. A., Rubow, K. L., Behm, S. M. (1991), A Microorifice Uniform Deposit Impactor (MOUDI): Description, Calibration, and Use, Aerosol Science and Technology, Vol. 14, pp. 434-446.

Masclet, P., Bresson, M. A., Mouvier, G. (1987), Polycyclic Aromatic Hydrocarbons Emitted by Power Stations and Influence of Conditions Parameters, Fuel, Vol. 66, pp. 556-566.

MedlinePlus (2004), A Service of National Institutes of Health, USA. Available: http://www.nlm.nih.gov/medlineplus/ency/article/003471.htm [accessed 17 August 04]

Meng, Z. and Seinfeld, J. H. (1994), On the Source of the Submicrometer Droplet Mode of Urban and Regional Aerosols, Aerosol Science and Technology, Vol. 20, pp. 253-265.

Miyamoto, N., Ogawa, H., Iemura, A. (1997), Cycle-to-Cycle Transient Characteristics of Exhaust Gas Emissions from a Diesel Engine with Different Increasing and Decreasing Load Patterns, Society of Automotive Engineers, Diesel Engine Combustion Processes and Emission Control Technologies SP-1246, pp. 1-10.

Molnár, P., Janhäll, S., Hallquist, M. (2002), Roadside Measurements of Fine and Ultra Fine Particles at a Major Road North of Gothenburg, Atmospheric Environment, Vol. 36, pp. 4115-4123.

Morawska, L., He, C. R., Hitchins, J., Mengersen, K., Gilbert, D. (2003), Characteristics of Particle Number and Mass Concentrations in Residential Houses in Brisbane, Australia, Atmospheric Environment, Vol. 37, pp. 4195-4203.

Morawska, L. and Thomas, S. (2000), Modality of Ambient Particle Distributions as a Basis for Developing Air Quality Regulations, Proc. 15th Clean Air & Environment Conference, Sydney.

Morrow, P. E. (1988), Possible Mechanism to Explain Dust Overloading of the Lungs, Fund. Appl. Toxicol., Vol. 10, pp. 369-384.

Nanzetta, M. K. and Holmén, B. A. (2004), Roadside Particle Number Distributions and Relationships between Number Concentrations, Meteorology, and Traffic Along a Northern California Freeway, Journal of Air and Water Management Association, Vol. 54, pp. 540-554.

National Environmental Agency of Singapore (NEA), 2003, NEA Annual Report 2002-2003. Available: http://app.nea.gov.sg/cms/htdocs/category_sub.asp?cid=230 [accessed 15 June 2004].

Nemery, B., Hoet, P. H., Nemmar, A. (2001), The Meuse Valley Fog of 1930: An Air Pollution Disaster, The Lanset, Vol. 357, pp. 704-708.

Nemmar, A., Hoet, P. H., Vanquickenborne, B., Dinsdale, D., Thomeer, M., Hoylaerts, M. F., Vanbilloen, H., Mortelmans, L., Nemery, B. (2002), Passage of Inhaled Particles Into the Blood Circulation in Humans, Circulation 105, pp. 411-414.

Nemmar, A., Hoylaerts, M. F., Hoet, P. H. M., Nemery, B. (2004), Possible Mechanisms of the Cardiovascular Effects of Inhaled Particles: Systemic Translocation and Prothrombotic Effecs, Toxicology Letters, Vol. 149, pp. 243-253.

Nielsen, T. (1996), Traffic Contribution of Polycyclic Aromatic Hydrocarbons in the Centre of a Large City, Atmospheric Environment, Vol. 30, pp. 3481-3490.

Nisbet, C. and LaGoy, P. (1992), Toxic Equivalency Factors (TEFs) for Polycyclic Aromatic Hydrocarbons, Regional Toxicology Pharmacology, Vol. 16, pp. 290-300.

Oberdörster, G. (1996), Significance of Particle Parameters in the Evaluation of Exposure-Dose-Response Relationships of Inhaled Particles, Particulate Science and Technology, Vol. 14 (2), pp. 135-151.

Oberdörster, G. (2001), Pulmonary Effects of Inhaled Ultrafine Particles, International Archives of Occupational and Environmental Health, Vol. 74 (1), pp. 1-8.

Oberdörster, G., Sharp, Z., Atudorei, V., Elder, A., Gelein, R., Lunts, A., Kreyling, W., Cox, C. (2002), Extrapulmonary Translocation of Ultrafine Carbon Particles following Whole-body Inhalation Exposure of Rats, J. Tox. & Environ. Health, Vol. 65 (20), pp. 1531-1543.

Oberdörster, G., Sharp, Z., Atudorei, V., Elder, A., Gelein, R., Kreyling, W., Cox, C. (2004), Translocation of Inhaled Ultrafine Particles to the Brain, Inhalation Toxicology, Vol. 16 (6-7), pp. 437-445.

Offenberg, J. H. and Baker, J. E. (1999), Aerosol Size Distributions of Polycyclic Aromatic Hydrocarbons in Urban and Over-water Atmospheres, Environmental Science and Technology, Vol. 33, pp. 3324-3331.

Pacyna, J. M., Nriagu, J. O., Davidson, C. I. (Eds) (1986), Toxic Metals in the Atmosphere, Wiley, New York.

Pankow, J. F. (1987), Review and Comparatives Analysis of the Theories on Partitioning between the Gas and Aerosol Particulate Phases in the Atmosphere, Atmospheric Environment, Vol. 22, pp. 2275-2283.

Park, K., Cao, F., Kittelson, D.B., McMurry, P.H. (2003), Relationship between Particle Mass and Mobility for Diesel Exhaust Particles, Environmental Science & Technology Vol. 37(3), pp. 577–583.

Perry, R. H., Green, D. W., Maloney, J. O. (1997), Perry's Chemical Engineers' Handbook (7^{th} ed.), New York: McGraw Hill.

Pope, C. A., Dockery, D. W., Schwartz, J. (1995), Review of Epidemiological Evidence of Health Effects of Particulate Air Pollution, Inhalation Toxicology, Vol. 7, pp. 1-18.

Rehn, B., Seiler, F., Rehn, S., Brunch, J., Maier, M. (2003), Investigation on the Inflammatory and Genotoxic Lung Effects of Two Types of Titanium Dioxide: Untreated and Surface Treated, Toxicol. Appl. Pharmacol., Vol. 189 (2), pp. 84-95.

Rogge, W. F., Hildemann, L., Mazurek, M. A., Cass, G. R., Simoneit, B. R. T. (1993a), Sources of Fine Organic Aerosol: 3. Road Dust, Tire Debris and Organometallic Brake Lining Dust: Roads as Sources and Sinks, Environmental Science and Technology, Vol. 27, pp. 1892-1904.

Rogge, W. F., Hildemann, L., Mazurek, M. A., Cass, G. R., Simoneit, B. R. T. (1993b), Sources of Fine Organic Aerosol: 2. Non-catalyst and Catalyst-equipped Automobiles and Heavy Duty Diesel Trucks, Environmental Science and Technology, Vol. 27, pp. 636-651.

Rogge, W. F., Hildemann, L., Mazurek, M. A., Cass, G. R., Simoneit, B. R. T. (1998), Source of Fine Organic Aerosol: 9. Pine, Oak, and Synthetic Log Combustion in Residential Fireplaces, Environmental Science and Technology, Vol. 32, pp. 13-22.

Sakurai, H., Park, K., McMurry, P.H. (2003), Size-dependent Mixing Characteristics of Volatile and Nonvolatile Components in Diesel Exhaust Aerosols, Environmental Science & Technology, Vol. 37(24), pp. 5487–5495.

Samet, J. M., Dominici, F., Curriero, F. C., Coursac, I., Zeger, S. L. (2000), Fine Particulate Air Pollution and Mortality in 20 US Cities, 1987-1994, New England Journal of Medicine, Vol. 343, pp. 1742-1749.

Sato, M., Hansen, J., Koch, D., Lacis, A., Ruedy, R., Dubovik, O., Holben, B., Chin, M. and Novakov, T. (2003), Global Atmospheric Black Carbon Inferred from AERONET, Proceedings of the National Academy of Sciences, Vol. 100 (11), pp. 6319-6324. Available: http://pubs.giss.nasa.gov/docs/2003/2003_ SatoHansen.pdf [accessed 13 July 2004].

Savoie, D. L. and Prospero, J. M. (1982), Particle Size Distribution of Nitrate and Sulphate in the Marine Atmosphere, Geophysical Research Letters, Vol. 9, pp. 1207-1210.

SBS Transit, Operational Information-Average Daily Ridership, 2004a. Available: http://www.sbstransit.com.sg/about_opinfo.asp [accessed 30 June 2004].

SBS Transit, Bus Interchanges in Singapore, 2004b. Available: http://www.sbstransit.com.sg/geninfo_businterchanges.asp [accessed 14 July 2004]

Schwartz, J. (1994), What Are People Dying of on High Air Pollution Days, Environmental Research, Vol. 64, pp. 26-35.

Schwela, D. and Zali, O. (ed). (1999). Urban Traffic Pollution, pp. 3-4, 219-220. London: E & FN Spon.

Seinfeld, J. H. (2004), Air Pollution: A Half Century of Progress, AIChE Journal, Vol. 50 (6), pp. 1096-1108.

Seinfeld, J. H. and Pankow, J. N. (2003), Organic Atmospheric Particulate Material, Annual Review of Physical Chemistry, Vol. 54, pp. 121-140.

Shi, J. P., Harrison, R. M., Evans, D. (2001), Comparison of Ambient Particle Surface Area Measurement by Epiphaniometer and SMPS/APS, Atmospheric Environment, Vol. 35, pp. 6193–6200.

Shi, J. P., Khan, A.A., Harrison, R.M. (1999), Measurements of Ultrafine Particle Concentration and Size Distribution in the Urban Atmosphere, The Science of the Total Environment Vol. 235, pp. 51–64.

Simoneit, B. R. T. (1984), Organic Matter of the Troposphere-III Characterization and Sources of Petroleum and Pyrogenic Residues in Aerosols over the Western United States, Atmospheric Environment, Vol. 18, pp. 51-67.

Simoneit, B. R. T., Sheng, G. Y., Chen, X. J., Fu, J. M., Zhang, J., Xu, Y. P. (1991), Molecular Marker Study of Extractable Organic Matter in Aerosols from Urban Areas of China, Atmospheric Environment, Vol. 25A (10), pp. 2111-2129.

Stolzenburg, M. R. and McMurry, P. H. (1991), An Ultrafine Aerosol Condensation Nucleus Counter, Aerosol Science and Technology, Vol. 14, pp. 48-65.

Swami, K., Judd, C. O., Orsini, J., Yang, K. X, Husain, L. (2001), Microwave Assisted Digestion of Atmospheric Aerosol Samples Followed by Inductively Coupled Plasma Mass Spectrometry Determination of Trace Elements, Fresenius' Journal of Analytical Chemistry, Vol. 369, pp. 63-70.

Tanaka, S. and Shimizu, T. (1999), A Study of Composition and Size Distribution of Particulate Matter from DI Diesel Engine, Diesel Engines Combustion and Emissions, Society of Automotive Engineers Inc., SP1484, pp. 1-9.

ten Brink, H. (2003), Aerosol: Composition and Size Evolution of the Secondary Aerosol–Overview of Subproject Aerosol, Energy Research Foundation (ECN), Petten, Netherlands. Available: http://aerosol.web.psi.ch/Final_reports/004%20%20Overview.pdf [accessed 8 July 2004].

Twomey, S. A. and Zalabsky, R. A. (1981), Multifilter Technique for Examination of the Size Distribution of the Natural Aerosol in the Submicrometer Size Range, Environmental Science and Technology, Vol. 15 (2), pp. 177-184.

U.S. Environmental Protection Agency (USEPA) (1997), Health and Environmental Effects of Particulate Matter Fact Sheet, July 17, 1997.

U.S. Environmental Protection Agency (USEPA) (2002), Health Assessment Document for Diesel Engine Exhaust, EPA/600/8-90/057F, Office of Research and Development, National Centre for Environmental Assessment, Washington D. C.

Unal, A., Frey, H. C., Rouphail, N. M. (2004), Quantification of Highway Vehicle Emissions Hot Spots Based upon On-Board Measurements, Journal of Air and Waste Management Association, Vol. 54, pp. 130-140.

Vasconcellos, P. C., Zacarias, D., Pires, M. A. F., Pool, C. S., Carvalho, L. R. F. (2003), Measurements of Polycyclic Aromatic Hydrocarbons in Airborne Particles from the Metropolitan Area of São Paulo City, Brazil, Atmospheric Environment, Vol. 37, pp. 3009-3018.

Vesilind, P. A., Peirce, J. J., Weiner, R. F. (1994), Environmental Engineering 3rd edition, Boston: Butterworth-Heinemann.

Vignati, E., Berkowicz, R., Palmgren, F., Lyck, E., Hummelshøj, P. (1999), Transformation of Size Distributions of Emitted Particles in Streets, The Science of the Total Environment, Vol. 235, pp. 37-49.

Wåhlin, P., Palmgren, F., Van Dingenen, R. (2001), Experimental Studies of Ultrafine Particles in Streets and the Relationship to Traffic, Atmospheric Environment, Vol. 35 (supp. 1), pp. S63-S69.

Wall, S. M., John, W., Ondo, J. L. (1988), Measurement of Aerosol Size Distribution for Nitrate and Major Ionic Species, Atmospheric Environment, Vol. 22, pp. 1649-1656.

Wallace, L. A., Emmerich, S. J., Howard-Reed, C. (2004), Source Strengths of Ultrafine and Fine Particles Due to Cooking with a Gas Stove, Environmental Science and Technology, Vol. 38, pp. 2304-2311.

Wang, M. L., Tuli, R., Manner, P.A., Sharkey, P.F., Hall, D.J., Tuan, R.S. (2003), Direct and Indirect Induction of Apoptosis in Human Mesenchymal Stem Cells in Response to Titanium Particles, Journal of Orthopaedic Research, Vol.4. pp. 697-707.

Wantanabe, M., Okada, M., Kudo, Y., Tonori, Y., Niitsuya, M., Sato, T., Aizawa, Y., Kotani, M. (2002), Differences in the Effects of Fibrous and Particulate Titanium Dioxide on Alveolar Macrophages of Fischer 344 rats. Journal of Toxicology and Environmental Health (A), Vol. 65 (15), pp. 1047-1060.

Wehner, B., Birmili, W., Gnauk, T., Wiedensohler, A. (2002), Particle Number Size Distributions in a Street Canyon and Their Transformation into the Urban-Air Background Measurements and a Simple Model Study, Atmospheric Environment, Vol. 36, pp. 2215-2223.

Weijers, E. P., Khlystov, A. Y., Kos, G. P. A., Erisman, J. W. (2004), Variability of Particulate Matter Concentrations Along Roads and Motorways Determined by a Moving Measurement Unit, Atmospheric Environment, Vol. 38, pp. 2293-3002.

Yaffe, D., Cohen, Y., Arey, J., Grosovsky, A. J. (2001), Multimedia Analysis of PAHs and Nitro-PAHs Daughter Products in the Los Angeles Basin, Risk Analysis, Vol. 21 (2), pp. 275-294.

Yang, K. X., Swami, K., Husain, L. (2002), Determination of Trace Metals in Atmospheric Aerosols with a Heavy Matrix of Cellulose by Microwave Digestion-Inductively Coupled Plasma Mass Spectroscopy, Spetrochimica Acta Part B, Vol. 57, pp. 73-84.

Yassaa, N., Meklati, B. Y., Cecinato, A., Marino, F. (2001a), Organic Aerosols in Urban and Waste Landfill of Algiers Metropolitan Area: Occurrence and Sources, Environmental Science and Technology, Vol. 35, pp.306-311.

Yassaa, N., Meklati, B. Y., Cecinato, A., Marino, F. (2001b), Particulate N-Alkanes, N-Alkanoic Acids and Polycyclic Aromatic Hydrocarbons in the Atmosphere of Algiers City Area, Atmospheric Environment, Vol. 35, pp. 1843-1851.

Yoshizumi, K. and Hoshi, A. (1985), Size Distribution of Ammonium Nitrate and Sodium Nitrate in Atmospheric Aerosol, Environmental Science and Technology, Vol. 19, pp. 258-261.

Zhang, C. L. (2001), Physical and Chemical Characteristics of Ambient Aerosols in Singapore, M. Eng Thesis, Department of Chemical and Environmental Engineering, National University of Singapore.

Zhang, D. Z., Shi, G. Y., Iwasaka, Y., Hu, M. (2000), Mixture of Sulphate and Nitrate in Coastal Atmospheric Aerosols: Individual Particle Studies in Qingdao (36^{o}04'N, 120^{o}21'E), China, Atmospheric Environment, Vol. 34, pp. 2669-2679.

Zheng, M. and Fang, M. (2000), Particle-associated Polycyclic Aromatic Hydrocarbons in the Atmosphere of Hong Kong, Water, Air and Soil Pollution, Vol. 117, pp. 175-189.

Zheng, M., Fang, M., Wang, F., To, K. L. (2000), Characterization of the Solvent Extractable Organic Compounds in $PM_{2.5}$ Aerosols in Hong Kong, Atmospheric Environment, Vol. 34, pp. 2691-2702.

Zheng, M., Wan, T. S. M., Fang, M., Wang, F. (1997), Characterization of the Non-Volatile Organic Compounds in the Aerosols of Hong Kong-Identification, Abundance and Origin, Atmospheric Environment, Vol. 31, pp. 227-237.

Zhu, Y., Hinds, W. C., Kim, S., Shen, S., Sioutas, C. (2002), Study of Ultrafine Particles near a Major Highway with Heady-Duty Diesel Traffic, Atmospheric Environment, Vol. 36, pp. 4323-4335.

Zou, L. Y. and Hooper M. A. (1997), Size-resolved Airborne Particles and Their Morphology in Central Jakarta, Atmospheric Environment, Vol. 31 (8), pp. 1167-1172.

- End -